Universidade de Brasília – UnB
Instituto de Geociências

PETROGÊNESE E ANÁLISE ESTRUTURAL DA SUÍTE CARACOL: IMPLICAÇÕES PARA A EVOLUÇÃO GEODINÂMICA DO BLOCO RIO APA - SUL DO CRÁTON AMAZÔNICO

Dalila Pexe Plens

Tese de Doutorado

Brasília

Agosto de 2018

Universidade de Brasília – UnB
Instituto de Geociências

PETROGÊNESE E ANÁLISE ESTRUTURAL DA SUÍTE CARACOL: IMPLICAÇÕES PARA A EVOLUÇÃO GEODINÂMICA DO BLOCO RIO APA - SUL DO CRÁTON AMAZÔNICO

Dalila Pexe Plens

Tese de Doutorado

Orientador: Prof. Dr. Márcio Martins Pimentel;
Co-orientador: Prof. Dr. Amarildo Salina Ruiz.

Banca Examinadora:
Prof. Dr. Márcio Martins Pimentel (Orientador);
Prof. Dr. Reinhardt Adolfo Fuck (UnB);
Prof[a]. Dr[a]. Maria Emília Della Giustina (UnB);
Prof. Dr. Moacir José Buenano Macambira (UFPA);
Prof. Dr. Colombo Celso Gaeta Tassinari (USP)

Brasília, DF, Agosto de 2018

AGRADECIMENTOS

Ao Criador pela proteção e inspiração.

Ao meu marido Leandro, por ser a luz da minha vida. E à nossa prenda amada, Clara.

À minha família, pelo aconchego e carinho.

Ao meu orientador Dr. Márcio Pimentel (*in memoriam*), envio toda a gratidão por me aceitar enquanto aluna, por me atender e ensinar sempre com entusiasmo e pela dedicação a esta tese. Foi uma honrra trabalhar com o senhor!

Ao meu co-oreintador Dr. Amarildo Ruiz, pelo cuidado e dedicação com nosso trabalho.

Às professoras Drª Zélia e Mª Elisa pelo carinho e disponibilidade em ajudar.

Aos membros do comitê de acompanhamento da tese, professores Dr. Reinhardt Fuck e Dr. Elton Dantas por terem feito colocações necessárias nas etapas finais do trabalho.

Às amigas que o doutorado na UnB me trouxe para perto: Fernanda, Letícia e Luana.

Às meninas da pós-graduação UFMT pelo companheirismo nos últimos dois anos.

Ao Programa de Pós Graduação em Geologia da UnB, do qual me encho de orgulho por dele fazer parte neste período de doutoramento.

À FAGEO - UFMT por me acolher, disponibilizar estrutura física e calor humano.

À professora Drª. Débora Faria da FAGEO por me emprestar um cantinho da sua sala onde coubéssemos eu e minhas tantas amostras. E a todos os alunos da graduação FAGEO que de alguma maneira me ajudaram.

Ao IENG-UFMT por me liberar das atribuições acadêmicas durante o afastamento.

Aos professores do curso de Engenharia de Minas-UFMT por cobrirem minhas atribuições acadêmicas durante o precioso tempo de afastamento.

A todos os integrantes do Laboratório de Geocronologia UnB que de alguma forma me ajudaram.

À aluna de doutorado Juliana Rezende por me ajudar com os dados finais.

Ao Grupo de Pesquisa em Evolução Crustal e Tectônica Guaporé, do qual participo desde a graduação.

Ao Instituto Nacional de Ciências e Tecnologia de Geociências da Amazônia (GEOCIAM) pela disponibilização do carro para campo.

À Coordenação de Aperfeiçoamento de Pessoal do Nível Superior (Capes) e à Fundação de Amparo à Pesquisa do Estado de Mato Grosso (FAPEMAT), pelo apoio finaceiro.

Finalmente, a todos que direta e indiretamente contribuíram para o desenvolvimento desta tese.

À minha Clara.

RESUMO

Dalila Pexe Plens. 2018. *Petrogênese a análise estrutural da Suíte Caracol e encaixantes: implicações para a evolução geodinâmica do Bloco Rio Apa, sul do Cráton Amazônico*. Tese de doutorado, Universidade de Brasília, Instituto de Geociências, Brasília, 132 p.

O Bloco Rio Apa, exposto no sudoeste de Mato Grosso do Sul, abrangendo também a porção nordeste do Paraguai, é compartimentado em dois terrenos tectônicos justapostos – ocidental e oriental - com características distintas. Esta tese de doutoramento apresenta o terreno oriental do Bloco Rio Apa com base em mapeamento geológico que gerou novos dados petrográficos, geocronológicos e isotópicos, além de buscar estabelecer abordagem descritiva e cinemática dos diferentes episódios deformacionais e metamórficos que afetam a região. A área estudada é representada pelo Ortognaisse Lau de Já (embasamento), pelas rochas granito-gnaissicas da Suíte Caracol e pelas rochas metavulcanossedimentares do Grupo Alto Tererê. O embasamento apresenta a idade mais antiga da área (1822 ± 6 Ma; U-Pb, LA-ICPMS, zircão) e ε_{Nd} positivo (0,69), sugerindo pouca ou nenhuma participação de crosta antiga em sua formação, com idade modelo Sm-Nd T_{DM} de 2.03 Ga. A Suíte Caracol abrange rochas plutônicas de composição cálcio-alcalina de alto-K representadas pelas fácies: (i) granito-gnaisse hololeucocrático rosa, (ii) biotita granito-gnaisse rosa, (iii) granito-gnaisse porfirítico rosa, (iv) anfibólio granito-gnaisse rosa, (v) anfibólio biotita granito-gnaisse cinza e (vi) anfibólio tonalito cinza. A suíte apresenta idade de cristalização entre 1776±13 e 1748 ±19 Ma (U-Pb, LA-ICPMS, zircão); Os dados de ε_{Nd} são positivos a levemente negativos, entre 3.25 e -1.75 e os de ε_{Hf} são negativos a positivos, oscilando entre -4.64 e 5.32, o que sugere assimilação de crosta mais antiga pelo magma mantélico parental. Mostram idades modelos T_{DM} Lu-Hf entre 1.92 e 2.30 Ga, e Sm-Nd entre 1.82 e 2.25 Ga. O Grupo Alto Tererê exposto na área estudada é representado por silimanita-quartzo xistos, cujos grãos detríticos de zircão indicam provável proveniência a partir da Suíte Caracol, sugerindo deposição em bacia do tipo *back-arc* desenvolvida no terreno oriental, antes da justaposição com a parte ocidental do Bloco Rio Apa. As rochas sedimentares apresentaram valores de ε_{Nd} positivos entre 1.03 e 2.00, o que sugere não participação de crosta mais antiga no magma parental fonte dos sedimentos. Mostram idades modelo T_{DM} Sm-Nd entre 1.90 e 2.01 Ga, coerentes com as rochas do terreno oriental. Foram constatadas três fases deformacionais compressivas (F_1, F_2 e F_3), além

de evento rúptil. F_1 inicialmente ocorre restrita ao embasamento e é responsável pela foliação de bandamento composicional metamórfico. Posteriormente, em processo de deformação progressiva, as rochas gnáissicas são dobradas, gerando foliação espaçada de clivagem de crenulação. Na Suíte Caracol a fase deformacional F_1 é responsável por foliação penetrativa do tipo xistosidade. A segunda fase de deformação (F_2) é o evento mais expressivo, sendo responsável pelo dobramento da foliação S_1 na Suíte Caracol, gerando dobras, foliação do tipo clivagem de crenulação e xistosidade (S_2). A xistosidade é observada também nas rochas metassedimentares do Grupo Alto Tererê. Os processos de deformação progressiva são identificados nesta fase, uma vez que a xistosidade, comumente orientada para NWW com mergulhos em ângulos baixos, nas porções norte e extremo oeste assume alterações em sua trajetória. São sugeridos três domínios estruturais para esta mesma a fase deformacional F_2: (i) domínio estrutural 1- porção central a sul com orientação predominante SE-NW, e ângulos de mergulho horizontalizados; (ii) domínio estrutural 2 - extremo leste do terreno oriental, com estruturas preferencialmente orientadas para N-S; (iii) domínio estrutural 3 - porção norte da área com a deformação compressiva mais intensa. O principal evento de deformação (F_2) está associado a metamorfismo de aproximadamente 1300 Ma, relacionado à justaposição dos terrenos oriental e ocidental, via cavalgamento de topo para NW e mergulhos de baixo ângulo. A fase F_3 mostra-se dúctil-rúptil na forma de dobras, clivagem de crenulação e lineação de intersecção entre as foliações S_1 e S_2. Tentativamente, é sugerido que as rochas estudadas sejam correlacionadas com os granitos e gnaisses do Complexo Chiquitania , Terreno Paraguá, no sudoeste do Cráton Amazônico.

Palavras Chave: Bloco Rio Apa, terreno oriental, Suíte Caracol, geocronologia, deformação progressiva.

ABSTRACT

Dalila Pexe Plens. 2018. *Petrogênese a análise estrutural da Suíte Caracol e Encaixantes: implicações para a evolução geodinâmica do Bloco Rio Apa, sul do Cráton Amazônico.* Tese de doutorado, Universidade de Brasília, Instituto de Geociências, Brasília, 132 p.

The Rio Apa Block is exposed in the southwest of Mato Grosso do Sul, Brazil, and extends southwards into Paraguay. It comprises two juxtaposed terranes – the western and eastern terranes. This work presents the eastern part of the Rio Apa Block based on geological mapping that generated new petrographic, geochronologic and isotopic data, as well as a descriptive and kinematic approach to the different deformational and metamorphic episodes recorded in the region. The studied area is represented by the Lau de Já Orthogneiss (basement), by the granite-gneiss of the Caracol Suite and by volcano-sedimentary rocks of the Alto Tererê Group. The basement presents the oldest age in the area (1822 ± 6 Ma, U-Pb, LA-ICPMS, zircon) and positive ε_{Nd} (0,69), suggesting little or no participation of old crust in its formation, Sm-Nd T_{DM} model age of 2.03 Ga. The Caracol Suite includes high-K calc-alkaline granite-gneiss rocks represented by the following facies: (i) pink hololeucocratic granite, (ii) pink biotite granite, (iii) pink porphyritic granite, (iv) pink amphibole granite, (v) gray amphibole biotite granite, (vi) gray amphibole tonalite. The suite presents crystallization ages between 1776±13 and 1748±19 Ma (U-Pb, LA-ICPMS, zircon). The ε_{Nd} values are positive to slightly negative varying from 3,25 to -1.75 while ε_{Hf} values are negative to positive, ranging from -4.64 to 5.32 and suggesting assimilation of older crust by the parental magma. They show Lu-Hf T_{DM} model ages between 1.92 and 2.30 Ga, and Sm-Nd T_{DM} model ages between 1.82 and 2.25 Ga. The Alto Tererê Group, exposed in the studied area, is represented by silimanite-quartz schist, for which detrital zircon ages probably indicate provenance from rocks of the Caracol Suite, suggesting deposition in a back-arc basin developed in the eastern terrane, before collision with the western part of the Rio Apa Block. The sedimentary rocks show positive ε_{Nd} values between 1.03 and 2.00, which suggests juvenile sources. They show Sm-Nd T_{DM} model ages between 1.90 and 2.01 Ga, consistent with the eastern terrain rocks. As for tectonic-structural features, three compressive deformational phases (D_1, D_2, and D_3) and a ruptile event were recorded. D_1 was initially restricted to the basement and was responsible for the foliation of the metamorphic compositional banding. In a later progressive deformation process,

the gneissic rocks were folded, generating a spaced crenulation cleavage. In the Caracol Suite, deformation phase D_1 was responsible for a schistosity-type penetrative foliation. The second deformation phase (D_2) was the most significant event. It is responsible for folding S_1 foliation in the Caracol Suite, generating folds, crenulation cleavage and schistosity (S2). The schistosity is also present in the metasedimentary rocks of the Alto Tererê Group. Progressive deformation processes were also identified in this deformation phase because the schistosity, which is commonly oriented NWW with low-angle dips, changes orientation in the northern and extreme western portions of the study region. Three structural domains were recognized for the D_2 deformational phase: (i) structural domain 1 – the center to southern portion of the study area with dominantly SE-NW oriented structures with near horizontalized dips; (ii) structural domain 2 - extreme eastern part of the eastern terrane with dominantly N-S-oriented structures; and (iii) structural domain 3 - northern portion of the area with the most intense compressive deformation. The main deformation event (D_2) is associated with the metamorphism that occurred at approximately 1300 Ma, which has been described in the literature and was related to the juxtaposition of the eastern and western terranes by low-angle thrusting to the NW. The D_3 phase appears to be ductile-brittle with folds, crenulation cleavage and intersection lineations between the S_1 and S_2 foliations. Tentatively, it is suggested that the rocks investigated here may be correlated with the granites and gneisses of the Chiquitania Complex, Paraguá Terrane, in the southwestern Amazonian Craton.

Key Words: Rio Apa Block, oriental terrane, Caracol Suite, geochronology, Progressive deformation.

SUMÁRIO

Lista de Figuras

CAPÍTULO 3 - GEOLOGY AND GEOCHRONOLOGY (U-Pb, Sm-Nd and Lu-Hf) OF THE CARACOL SUITE AND COUNTRY ROCKS: IMPLICATIONS OF MAGMATIC EVOLUTION AND TECTONICS IN THE RIO APA BLOCK - SOUTH AMAZONIAN CRATON

Lista de Tabelas

Capítulo 1 – INTRODUÇÃO

1.1.ESTRUTURA DA TESE

A tese está constituída por cinco capítulos. O primeiro, trata dos tópicos introdutórios, da apresentação e objetivos a respeito do tema estudado, metodologia e contexto geológico regional. Os dois capítulos posteriores abordam os resultados obtidos durante o desenvolvimento deste doutoramento, em forma de artigos submetidos a periódicos de circulação internacional *Journal Brazilian of Gelogy* e *Journal of South American Earth Sciences.*

O artigo referente ao capítulo 2 tem como título "*Lithostructural framework of the eastern terrane of the Rio Apa Block - Southern Amazonian Craton*" e traz uma abordagem descritiva e cinemática dos diferentes episódios deformacionais e metamórficos que afetam o terreno oriental do Bloco Rio Apa.

O capítulo 3 se refere ao artigo intitulado "*Geology and geochronology (U-Pb, Sm-Nd and Lu-Hf) of the Caracol Suite and country rocks: implications to the magmatic and tectonic evolution of the Rio Apa Block - south of Amazonian Craton*" e discute os dados petrográficos e geocronológicos obtidos para as principais rochas aflorantes no terreno oriental.

O quarto capítulo traz um apanhado geral dos resultados apresentados nos dois capítulos anteriores, a fim de discutir e concluir a presente tese.

O quinto e último capítulo apresenta breves recomendações para possíveis trabalhos futuros na área. Toda a literatura consultada é listada em subitem subsequente.

1.2.APRESENTAÇÃO DO TEMA

Os blocos e terrenos paleoproterozóicos descendentes da composição e aglutinação do Supercontinente Rodínia, que constituem o embasamento do continente sul-americano são observados amplamente e registram eventos de formação de rochas, bem como variados conjuntos de orogenias.

O Bloco Rio Apa está posicionado no sudoeste de Mato Grosso do Sul, estendendo-se para o Paraguai. Compreende um conjunto de unidades litoestratigráficas que registram segmentos infra- e supracustais, cuja evolução tectônica dá-se, em grande parte, nos períodos Orosiano e Estateriano, representando, assim importante papel na consolidação do Supercontinente Rodínia.

Ruiz (2005) e Cordani *et al.* (2010), resgatando a concepção de Almeida (1965), com base em interpretações geológicas/geocronológicas, consideram o Bloco Rio Apa como parte integrante do Cráton Amazônico (Fig. 1.1). Baseados em isótopos de Nd, Cordani *et al.* (2010) defendem a existência de dois diferentes compartimentos tectônicos justapostos no Bloco Rio Apa, divididos em terrenos ocidental e oriental.

As rochas objeto deste trabalho encontram-se inseridas na porção oriental do Bloco Rio Apa, apresentando como embasamento o Ortognaisse Lau de Já, a Suíte Caracol, constituida por rochas granito-gnaissicas de composição cálcio-alcalina de alto-K, bem como uma porção metavulcanossedimentar do Grupo Alto Tererê.

As rochas do embasamento são individualizadas pela primeira vez, assim como a porção efusiva, que aflora na porção leste da área. A Suíte Caracol, sob a denominação de Gnaisse Caracol, é descrita por Cordani *et al.* (2010), como composta por ortognaisses, levemente a moderadamente foliados, cinza a rosa, granulação média a grossa, de textura granoblástica, com idades de cristalização pelo método U-Pb (SHRIMP) de 1721±25 Ma. Já o Grupo Alto Tererê é representado por uma sequência metavulcano-sedimentar paleoproterozóica, dobrada e metamorfisada na fácies anfibolito, com retrometamorfismo na fácies xisto verde (Godoi *et al.*, 1999; Lacerda Filho *et al*., 2006; 2016; Godoy *et al.*, 2009).

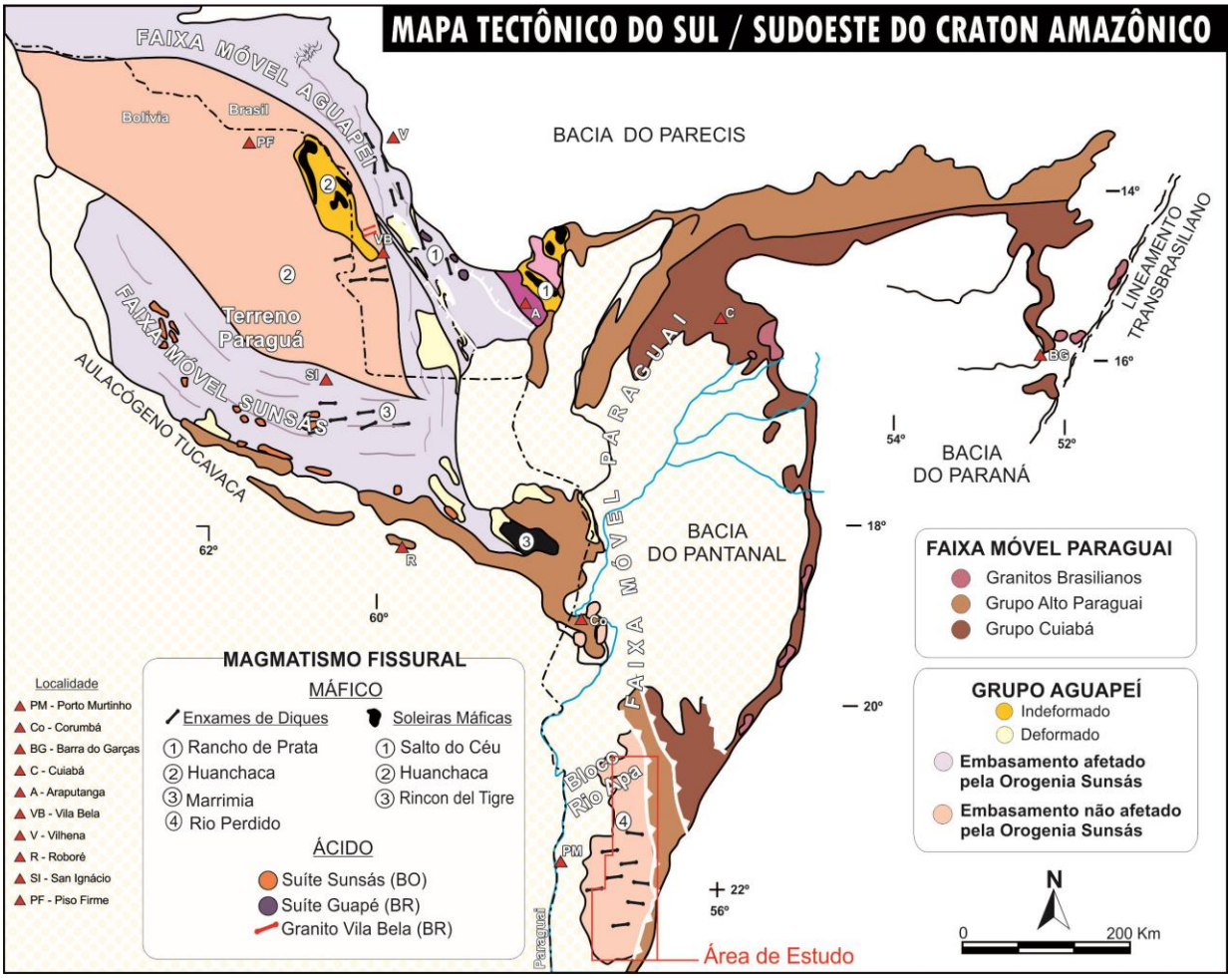

Fig. 1.1. Mapa tectônico do Sul/Sudoeste do Cráton Amazônico (Extraído e modificado de Ruiz *et al.*, 2010a; *in* Lima, 2016).

Quanto ao quadro tectono-estrutural, o terreno oriental é constituído por um conjunto de rochas polideformadas onde são descritos três eventos deformacionais compressivos, dois deles mostram-se dúcteis e um dúctil-rúpitil, além de um último distensivo rúptil.

Apesar de recentes estudos petrogenéticos e geocronológicos terem trazido novas informações sobre a evolução crustal do Bloco Rio Apa (Cordani *et al.*, 2010; Brittes *et al.*, 2013; Plens *et al.*, 2013; Redes *et al.*, 2015; Faleiros *et al.*, 2015; Lacerda Filho *et al.*, 2016), vastas são as questões relacionadas à cronologia dos eventos magmáticos que afetaram o terreno oriental do Bloco Rio Apa. Raros também são os trabalhos que tragam uma abordagem descritiva e cinemática do arcabouço tectono-estrutural do terreno oriental, bem como do Rio Apa como um todo.

1.3.OBJETIVOS

O propósito desta pesquisa de doutoramento é caracterizar a natureza e evolução geológico-tectônica do terreno oriental do Bloco Rio Apa, enfatizando as rochas graníticas da Suíte Caracol e suas encaixantes.

O trabalho se deu partir de mapeamento geológico em escala de reconhecimento (1:250.000) e, posteriormente de detalhe de áreas chaves (1:10.000), da caracterização petrográfica, e do emprego de análises geocronológicas e isotópicas, bem como da classificação dos apectos deformacionais observados. Tem os seguintes objetivos específicos:

i. Descrição e delimitação das unidades correspondentes ao terreno oriental do Bloco Rio Apa aflorantes na área de estudo, sendo o Ortognaisse Lau de Já, a Suíte Caracol (granito-gnaisses) e a porção metassedimentar do Grupo Alto Tererê, além das rochas vulcânicas;
ii. Caracterização da faciologia petrográfica dos granito-gnaisses da Suíte Caracol;
iii. Caracterização dos diferentes episódios deformacionais que afetam o terreno oriental e correlação, quando possível, com as condições de metamorfismo;
iv. Análise estrutural de detalhe, buscando estabelecer a cronologia e o significado tectônico das estruturas e microestruturas;
v. Elaboração da cronologia dos eventos magmáticos geradores do Ortognaisse Lau de Já e dos granito-gnaisses da Suíte Caracol, com o emprego do método radiométrico U-Pb em zircão;
vi. Análise dos episódios de acresção e processos de retrabalhamento crustal através dos métodos Lu-Hf em zircão e Sm-Nd em rocha total;
vii. Investigação das possíveis correlações entre magmatismo e metamorfismo que afetaram o terreno oriental do Bloco Rio Apa com as orogenias que marcam os granitos e gnaisses aflorantes no SW do Cráton Amazônico.

Este estudo acarretará no enrriquecimento do banco de dados da Suíte Caracol, bem como em um avanço para a compreensão da história magmática e deformacional do Bloco Rio Apa.

1.4.MATERIAIS E MÉTODOS

1.4.1. MAPEAMENTO GEOLÓGICO E ANÁLISE ESTRUTURAL

Antes do mapeamento geológico foi realizada a interpretação de de imagens de satélite LANDSAT e Geocover, além de imagens SRTM (*Shuttle Radar Topography Mission*). Foram observadas também imagens dos levantamentos aero-geofísicos disponíveis para a região (imagem ternária e imagem de amplitude do sinal analítico). Além de que, foi realizada a integração dos dados geológicos obtidos na área estudada por Lacerda Filho *et al.* (2006 e 2016), Cordani *et al.* (2010), Brittes *et al.* (2013), Plens *et al*. (2013), Redes *et al*. (2015), Faleiros *et al.* (2015), Lacerda Filho (2015).

Foram realizadas várias etapas de mapeamento geológico, o primeiro em escala de reconhecimento de 1:250.000 para coleta de amostras, dados estruturais, distinção e delimitação das unidades litológicas. A partir de então, áreas chaves foram estabelecidas e novas etapas de campo foram feitas em escala de detalhe (1:10.000), buscando esclarecer dúvidas a cerca dos tipos litológicos cartografados, além de estabelecer a cronologia e o significado das estruturas tectônicas registradas.

As amostras coletadas foram descritas macroscopicamente considerando os aspectos texturais, composicionais e estruturais. Foram selecionados exemplares para confecção de seções delgadas, realizada nos Laboratórios de Laminação da Universidade Federal de Mato Grosso e Universidade de Brasília. As análises em micro-escala tiveram por fim estabelecer as variações faciológicas e, no caso da abordagem estrutural, determinar (quando possível) os mecanismos de deformação intracristalina referentes a cada fase deformacional e correlacioná-los com as condições de metamorfismo que afetaram a área. Considerando as amostras mais representativas, sua distribuição na área de estudo, diversidade textural e mineralógica, foram separados também exemplares para análises isotópicas e geocronológicas pelos métodos U-Pb e Lu-Hf em zircão por LA-ICP-MS e Sm-Nd em rocha total.

A definição de diferentes tipos faciológicos nas rochas granito-gnaissicas da Suíte Caracol foi estabelecida a partir de imprescindível mapeamento geológico que, além de ser a chave para a possível delimitação das rochas aflorantes, também as caracteriza quanto ao comportamento estrutural. A partir de análises microscópicas foram identificadas características texturais,

estruturais e mineralógicas específicas, aliadas à estimativa visual da proporção dos minerais componentes das rochas. Foram utilizados os critérios de Ulbrich *et al.* (2001) para a interpretação, classificação e denominação das fácies.

Para facilitar a apresentação dos dados, foram usados os critérios tradicionais de superposição de Ramsay (1967), onde siglas foram utilizadas para descrever os elementos estruturais sendo, Fn (fase de deformação), Dn (dobras), Mn (metamorfismo), Sn (foliações) e Ln (lineações). Quando traduzidas para o inglês, no capítulo 3, *Dn* será usado para *deformation* e *Fn* para *folds*, as demais siglas não requerem alteração do idioma. Definições à respeito de deformação progressiva sugeridas por Fossen *et al*. *(article in press)* também foram exploradas.

A definição e caracterização das estruturas secundárias, bem como de fases deformacionais seguiram os conceitos amplamente aceitos em análise estrutural de terrenos polideformados (Fossen, 2012). Descrição e interpretação dos mecanismos de deformação intracristalina foram baseadas principalmente em Paschier & Trow (2005).

1.4.2. GEOCRONOLOGIA E GEOLOGIA ISOTÓPICA

Cristais de zircão foram utilizados para análises U-Pb e Lu-Hf por La-ICP-MS, seguindo a sistemática de Bühn *et al.* (2009) e Matteini *et al.* (2010), respectivamente. A preparação das amostras foi realizada de acordo com o procedimento convencional com técnicas gravimétricas e magnéticas do Laboratório de Geocronologia da Universidade de Brasília. Após a separação, os cristais de zircão foram selecionados para a montagem dos *mounts*, em resina epóxi, desgastados e polidos para a exposição dos grãos, e a limpeza feita com banho de HNO_3 diluído (2%). Para investigar a estrutura interna dos cristais e obter o melhor posicionamento do *spot*, imagens *Backscatter Electron* foram utilizadas.

As análises por LA-ICP-MS foram realizadas no Laboratório de Geocronologia da Universidade de Brasilia, e o equipamento utilizado foi o *Neptune* (*Thermo-Finnigan*) acoplado a Nd-YAG (λ=213nm) *Laser Ablation System* (*New Wave Research*, USA). Hélio misturado com Argônio foram usados para carregar o gás por meio de fluxo para o interior do equipamento. A frequência no laser é de 10 Hz e a energia de ~100 mJ/cm^2, spot para análises sistemáticas U-Pb de 30μm, e para análises isotópicas de Hf, de 40μm. Foram empregados dois padrões internacionais para as análises U-Pb LA-ICP-MS (GJ-1 e PAD-1). O padrão GJ-1 (Jackson *et al.*,

2004) foi usado como fator de correção, em sequência de sete análises, incluindo uma de branco laboratorial e uma do padrão. O padrão 91500 (Wiedenbeck *et al.*, 1995) é analisado no início e no final de cada sequência, bem como a cada dois ciclos do padrão anterior.

Para as análises isotópicas de Hf foram usados os cristais de zircão anteriormente furados pelo método U-Pb, e selecionados grãos com concordância geralmente de ± 5%. O spot para análise de Hf é localizado ao lado do spot de U-Pb. Antes de iniciar as análises com *laser ablation*, o espectrômetro deve ser calibrado com a solução padrão JMC 475 (Yb/Hf=0.02 e Lu/Hf=0.02), usada no começo de cada seção analítica. Durante as análises, o padrão GJ-1 também foi utilizado para monitorar os valores de $^{176}Hf/^{177}Hf$. Os valores de T_{DM} foram calculados utilizando como comparação de crosta continental, segundo o modelo de Bouvier *et al.* (2008).

Os dados brutos de U-Pb e Hf foram trabalhados e reduzidos no programa ISOPLOT versão 3.0 (Ludwig, 2003) e os erros apresentados são de 1σ para as análises sitemáticas e de 2 σ, para as isotópicas, ambas em porcentagem.

As análises isotópicas Sm-Nd também foram realizadas no Laboratório de Geocronologia da Universidade de Brasília, seguindo o método descrito por Gioia e Pimentel (2000). Aproximadamente 50 mg de amostra pulverizada são misturados a uma solução de ^{149}Sm e ^{150}Nd e dissolvida em cápsulas Savillex® por meio de ataques ácidos com HF, HNO3 e HCl. Os conteúdos de Sm e Nd são extraídos em colunas de troca catiônica, confeccionadas em teflon e depositados em filamentos duplos de rênio com ácido nítrico para evaporação. Leituras das medidas são realizadas em espectrômetro de massa multicoletor *Finnigan* MAT 262 em modo estático. As incertezas para as razões de Sm/Nd e $^{143}Nd/^{144}Nd$ são inferiores a ±0,5% (2σ) e ±0,005% (2σ), respectivamente, baseadas em repetidas análises dos padrões internacionais BHVO-1 e BCR-1. As razões $^{143}Nd/^{144}Nd$ foram normalizadas em função da razão $^{146}Nd/^{144}Nd$ de 0,7219. Os valores de T_{DM} foram calculados usando o modelo de De Paolo (1981).

1.5.CONTEXTO TECTÔNICO REGIONAL

1.5.1. CRÁTON AMAZÔNICO

O Cráton Amazônico, localizado na parte norte da América do Sul, têm como limite oriental os cinturões neoproterozoicos Paraguai e Araguaia, respectivamente a sudeste e leste,

estando os limites norte, sul e oeste, recobertos pelos sedimentos das Bacias Subandinas. Abrange uma área de aproximadamente 4.500.000 km_2, aflorando no Brasil, Bolívia, Colômbia, Guiana, Guiana Francesa e Suriname, e está dividido, pela Sinéclise do Amazonas, em dois escudos: o Escudo Brasil Central e o Escudo das Guianas.

Três principais modelos de compartimentação para o cenário evolutivo do Cráton Amazônico permanecem em debate na literatura recente: Tassinari & Macambira (1999, 2004), Santos *et al.* (2000, 2008) e Ruiz (2005).

Tassinari & Macambira (1999, 2004), compartimentam o cráton em províncias geocronológicas, com sucessivas acresções de crostas juvenis em cinturões móveis proterozóicos (Fig. 1.2) sendo elas: Província Maroni-Itacaíunas (2.2 a 1.9 Ga), Província Ventuari-Tapajós (1.9 a 1.8 Ga), Província Rio Negro-Juruena (1.8 a 1.55 Ga), Província Rondoniano-San Ignácio (1.55 a 1.3 Ga) e Província Sunsás-Aguapeí (1.2 a 0.9 Ga), situadas ao redor de núcleo proto-cratônico arqueano denominada Província Amazônia Central (> 2,3 Ga).

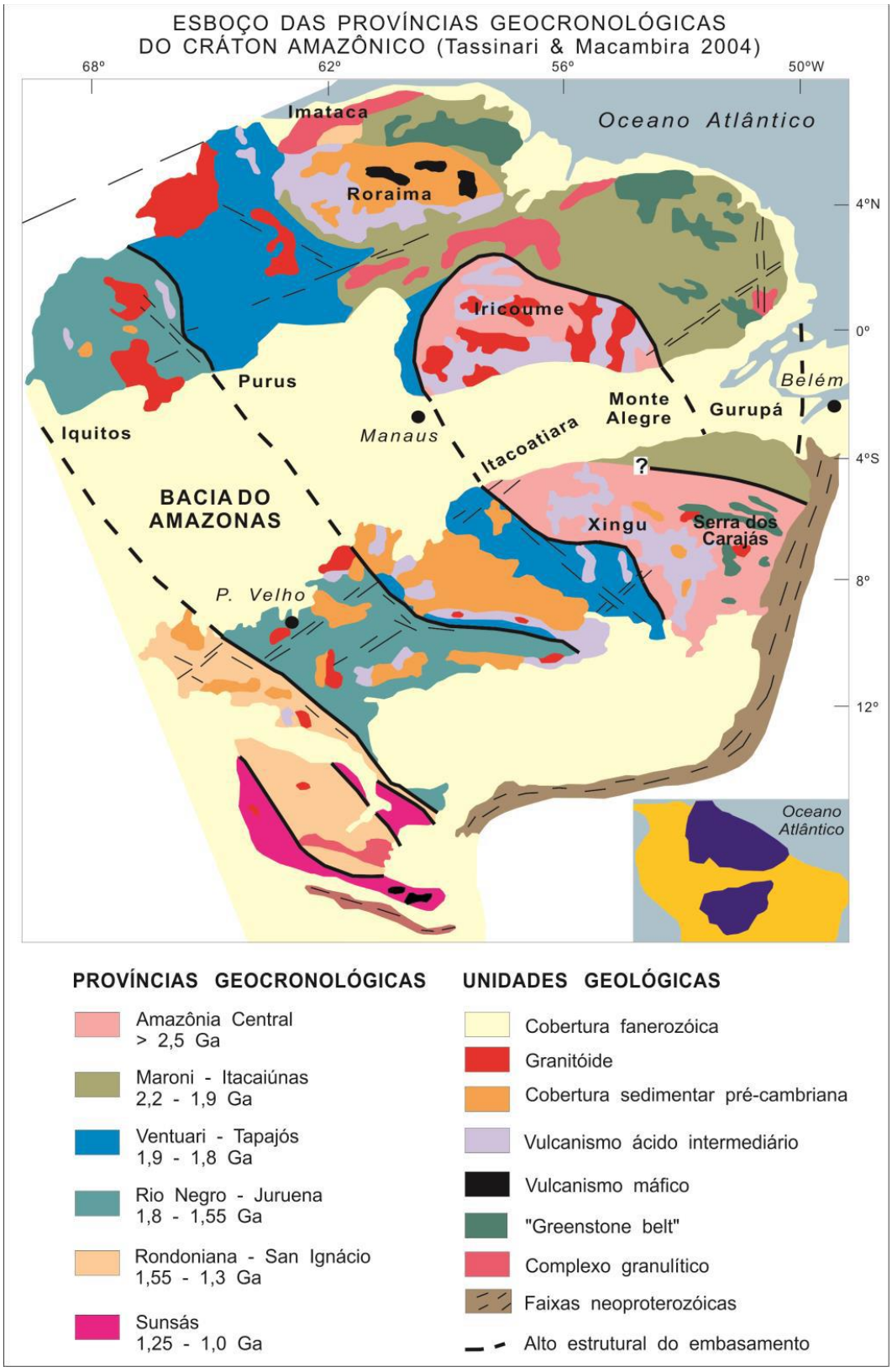

Figura 1.2. Províncias geocronológicas do Cráton Amazônico Extraído de Tassinari & Macambira (1999).

Santos *et al.* (2000, 2008) identificaram oito províncias tectônicas (Fig. 1.3) com base, principalmente, nos dados geocronológicos obtidos pelo método U-Pb SHRIMP. Em sequência cronológica, são: províncias Carajás (3,0-2,5 Ga), Transamazônica (2,26-2,01 Ga), Tapajós-Parima (2.03-1.88 Ga), Amazônia Central (Arqueana?), Rio Negro (1.82-1.52 Ga), Rondônia-Juruena (1.82-1.54 Ga) e Sunsás (1.45-1.10 Ga; Figura 1.3).

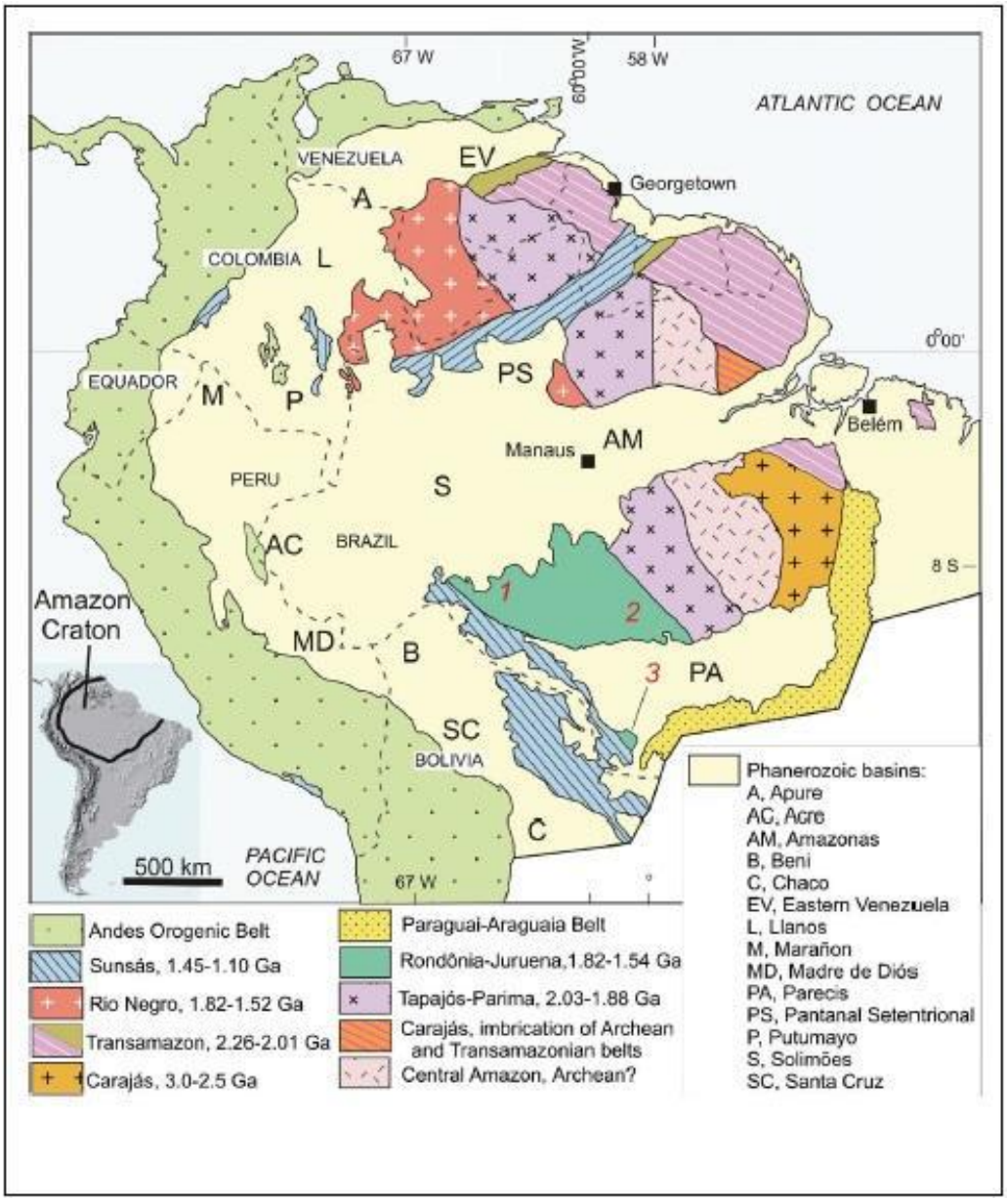

Figura 1.3. Províncias geocronológicas do Cráton Amazônico. Extraído de Santos *et al.* (2008).

A compartimentação de Ruiz (2005), baseando-se em Tassinari & Macambira (2004), vai ao encontro das concepções originalmente propostas por Almeida (1967) e, fundamentado em dados geológicos e geocronológicos, considera o Bloco Rio Apa, como parte integrante do Cráton Amazônico (Fig. 1.4). Na figura o Bloco Rio Apa está representado com a cor da Província San Ignácio, uma vez que a ultima orogenia (Orogenia San Ignácio) é proposta como correlacionável à ultima deformação de mesma idade no Bloco Rio Apa. Nesse trabalho adotou-se a prosposta de compartimentação de Ruiz (2005), uma vez que inclui o Bloco Rio Apa como parte do Cráton.

Entre os argumentos utilizados por Ruiz (2005) podem destacar-se os seguintes:

i. A Suíte Intrusiva Alumiador, que aflora em grande parte do terreno oriental do Boloco Rio Apa é cartografada também na região de Corumbá (MS) e Santo Corazon, na Bolívia, mostrando um prolongamento desta suíte até a porção sudoeste do Cráton Amazônico, em território boliviano;

ii. Ocorrências de enxames de diques e *sills* máficos proterozóicos referentes às suítes intrusivas Rio Perdido e Huncavaca (1.1 Ga; Teixeira *et al.,* 2016), são relatadas no oriente boliviano, em Mato Grosso e em Mato Grosso do Sul;

iii. As rochas carbonáticas da Faixa de Dobramentos Paraguai são observadas recobrindo toda a extensão oeste e sul do Cráton Amazônico, desde a região de Nova Xavantina, em Mato Grosso, até a Serra do Bodoquena, onde afloram rochas do Bloco Rio Apa;

iv. O Aulacógeno Tucavaca (Brasiliano), assenta-se sobre as rochas do Terreno Paraguá/Faixa Sunsás e Bloco Rio Apa (Corumbá e Santo Corazon);

v. A Faixa Paraguai margeia em continuidade física e tectônica o Bloco Rio Apa e os Terrenos Paraguá, Jauru e Rio Alegre, no sudoeste do Cráton Amazônico. Em tais condições, o Cráton Amazônico, incluindo a porção sul, Bloco Rio Apa, teria se comportado como margem continental passiva durante a deposição de parte das unidades da Faixa Paraguai em toda sua extensão.

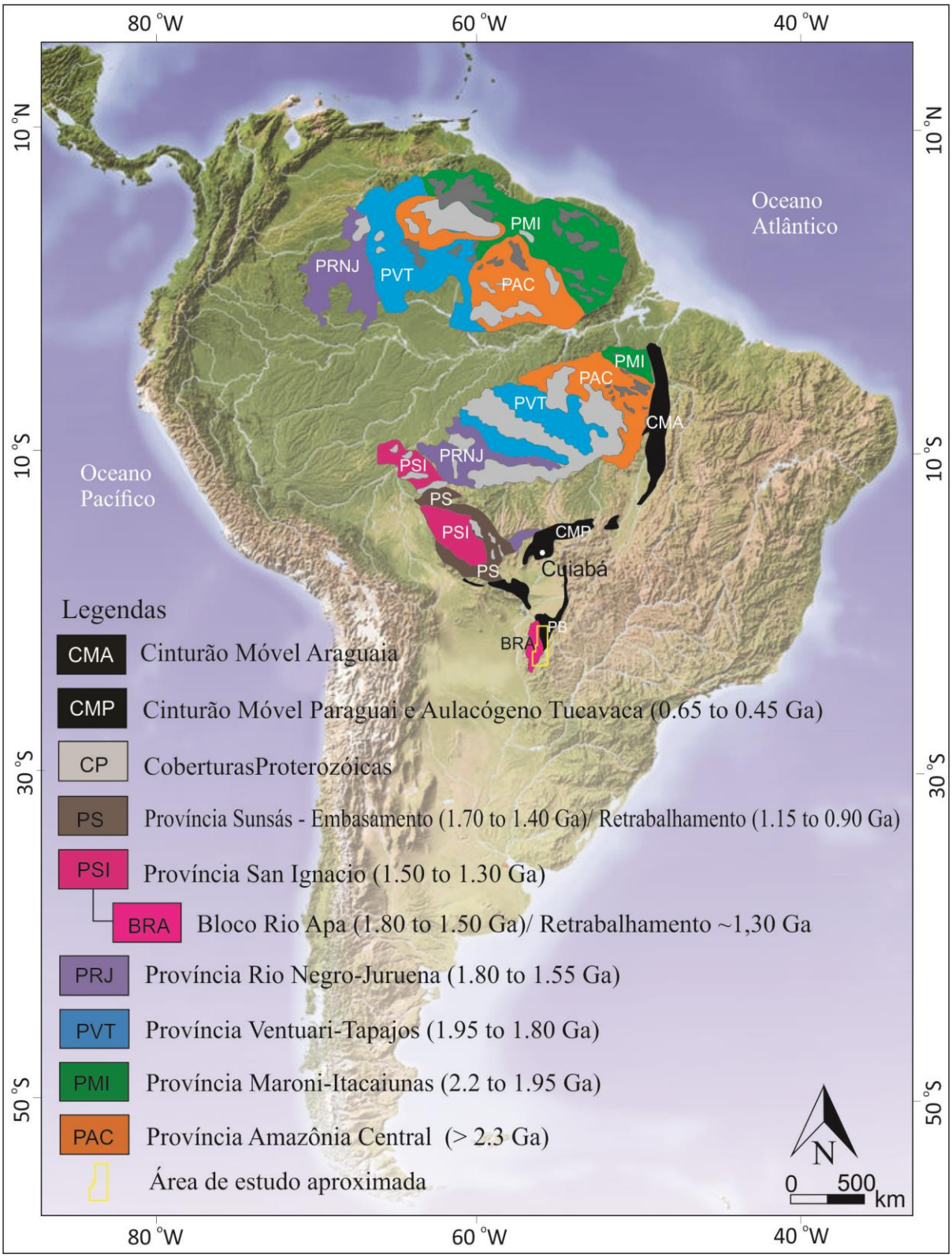

Figura 1.4. Compartimentação geocronológica e tectônica do Cráton Amazônico, considerando o Bloco Rio Apa como parte sul. Extraído e modificado de Tassinari & Macambira (1999) e Ruiz (2005).

1.5.1.1.Bloco Rio Apa

O extremo sul do Cráton Amazônico está representado pelo Bloco Rio Apa, que aflora na porção sudoeste do estado de Mato Grosso do Sul, fronteira com o Paraguai (Ruiz, 2005). O Bloco Rio Apa compreende um segmento crustal dominantemente paleoproterozóico e constitui o embasamento da Faixa Paraguai, na região. Possui cerca de 220 km de comprimento segundo a direção N-S e 60 km de largura média. Limita-se, a leste, por rochas pelítico-carbonáticas do Grupo Corumbá (Serra da Bodoquena) e, a oeste, encontra-se coberto por sedimentos cenozoicos da Bacia do Pantanal (Lacerda Filho *et al.*, 2006).

Quanto à compartimentação geotectônica, quatro principais modelos são propostos, Lacerda Filho *et al.* (2006), Cordani *et al.* (2010), Faleiros *et al.* (2015), e posteriormente, Lacerda Filho (2015) modifica sua proposta inicial.

Lacerda Filho *et al.* (2006) subdividiram o Bloco Rio Apa em três compartimentos geotectônicos distintos: i) Remanescente de Crosta Oceânica, de idade riaciana, representada pelo Complexo Metamórfico Alto Tererê; ii) Arco Magmático Rio Apa, orosiriano, equivalente aos gnaisses do Complexo Rio Apa; e iii) Arco Magmático Amoguijá, estateriano, constituído pela Formação Serra da Bocaina (Brittes *et al.*, 2013) e pelos granitos da Suíte Intrusiva Alumiador. Corpos máficos sob forma de batólitos e diques são agrupados como parte do Magmatismo Máfico Continental de provável idade estateriana ou toniana. Nessa compartimentação a área objeto do presente estudo está inserida no Arco Magmático Rio Apa.

Considerando a distribuição de idades modelo Sm-Nd, Cordani *et al.* (2010) propõem a existência de dois diferentes terrenos tectônicos no Bloco Rio Apa (ocidental e oriental), com histórias evolutivas distintas, limitados por zona de sutura aproximadamente N-S (Fig. 1.5).

A área objeto deste estudo está localizada no terreno oriental, constituído pelo Gnaisse Caracol e Complexo Morraria, Grupo Alto Tererê e Província Paso Bravo, em território paraguaio, (Wiens, 1986). O terreno ocidental é constituído pelo Complexo Rio Apa, Gabro-Anortosito Serra da Alegria (Silva 1998), Supersuíte Amoguijá (Godoi & Martins 1999) – Suíte Intrusiva Alumiador (Araújo *et al.*, 1982) e Formação Serra da Bocaina (Brites *et al.*, 2013); Grupo San Luis (Wiens, 1986) e Suíte Intrusiva Morro do Triunfo (Araujo *et al.*, 1982).

A tabela abaixo reúne os terrenos oriental e ocidental de Cordani *et al.* (2010) com breve descrição litológica de cada unidade retirada do trabalho supra citado, e as idades radiométricas pelos métodos U-Pb e Rb-Sr obtidas até o momento da publicação do trabalho em questão.

Cordani *et al.* (2010) apresentam idades de metamorfismo de aproximadamente 1300 Ma, obtidas pelos métodos K-Ar e Ar-Ar, interpretadas como parte do evento de aquecimento regional que afeta toda a região.

Tabela 1.1. Resumo da compartimentação proposta por Cordani *et al.*, (2010) para o Bloco Rio Apa.
* U-Pb – Lacerda Filho *et al.,* (2006); ** U-Pb Cordani *et al.,* (2010); *** Rb-Sr Araújo et al., (1982). Extraído e modificado de Cordani *et al.,* (2010).

		Unidade Litoestratigráfica	Breve descrição	Idade (Ma)
Terreno Oriental		Grupo Alto Terrrê	Granada-muscovita-biotita xitos e em menor quantidade muscovita-biotita gnaisses com quartzitos intercalados	-
		Gnaisse Caracol	Ortognaisses leucocraticos foliados e pobres em biotita.	1774 ± 26**
				1721 ± 25**
		Complexo Passo Bravo	Hornblenda biotita gnaisse e migmatito intrudido por granitos	1846 ± 47***
Terreno Ocidental	**Supersuíte Amoguijá**	Suíte Intrusiva Alumiador	Sieno a monzo granitos de granulação fina a média, rosa a cinza.	1839 ± 33**
		Formação Serra da Bocaina	Rochas porfiríticas, riolitos, dacitos e brechas vulcânicas	1794*
	Gabro Anortosito Serra da Alegria		Anortositos, leucogabros e melagabros	1791*
	Complexo Porto Murtinho		Gnaisses bandados e migmatitos, anfibolitos em menor quantidade.	-

Além dos terrenos ocidental e oriental, Faleiros *et al.* (2015) individualizaram o terreno sudeste (Fig. 1.5). Os terrenos são limitados por zonas de cisalhamento e sua evolução magmática se deu por meio de eventos acrescionários distintos, refletindo regime tectônico extremamente móvel (Faleiros *et al.,* 2015). O terreno ocidental é formado por rochas do Complexo Porto Murtinho (constituído pelos Gnaisse Córrego Jibóia e Granito Morro da Lenha; Faleiros *et al.,* 2015), Granito Chatelodo (1902 ± 12; U-Pb, SHRIMP, zircão; Faleiros *et al.,* 2015), Supersuíte

Amoguijá e Formação Naitaca (Faleiros *et al.*, 2013). O terreno oriental é constituído pelos gnaisses Morraria e Caracol e pela Suíte Baia das Garças, formada pelo Granito Sanga Bonita (1721 ± 25 Ma; U-Pb, SHRIMP, zircão; Remédio *et al.*, 2013) e ortognaisses Santa Clarinha e Espinilho (Remédio *et al.*, 2013; 1716 ± 11Ma e 1735 ± 12 Ma; U-Pb, SHRIMP, zircão; respectivamente), além do Granito Cerro Porã (1749 ± 45 Ma; U-Pb, SHRIMP, zircão; Plens *et al.*, 2013), até então descrito como pertencente ao terreno ocidental. No terreno sudeste são descritos os gnaisses João Candido e Rio Areia (1820±18 Ma; U-Pb, LA-ICP MS, zircão; Faleiros *et al.*, 2015) e Granito Scardine (1791±19 Ma; U-Pb, LA-ICP MS, zircão; Faleiros *et al.*, 2015). A área estudada localiza-se nos terrenos oriental e sudeste. A tabela abaixo sumariza a compartimentação apresentada por Faleiros *et al.* (2015), mostrando as unidades pertencentes a cada terreno.

Tabela 1.2. Resumo da compartimentação proposta por Faleiros *et al.,* (2015) para o Bloco Rio Apa. As descrições litológicas apresentadas na tabela são do autor acima citado e as idades são de a Faleiros *et al.,* (2015) , b Cordani *et al.* (2010), c Brittes et al., (2013), d Plens *et al.* (2013), e Remédio *et al.* (2013), f Araújo *et al.*, (1984). Os métodos são *U-Pb - SHRIMP, **U-Pb - LA-ICP-MS, ***Rb-Sr.

Unidade Litoestratigráfica			Breve descrição	Idade (Ma)
Terreno Ocidental	Formação Naica		Lapili tufo andesítico;	1813 ± 18a*
	Supersuíte Amoguijá	Suíte Intrusiva Alumiador	Sieno a monzo granitos de granulação fina a média, rosa a cinza;	1839 ± 33b*
		Formação Serra da Bocaina	Rochas porfiríticas, riolitos, dacitos e brechas vulcânicas;	1877 ± 4c*
	Granito Chateolo		Sienogranito granofírico;	1902 ± 12a*
	Complexo Porto Murtinho	Gnaisse Córrego Gibóia	Ortognaisse milonítico cinza;	1947 ± 9a*
		Granito Morro da Lenha	Biotita monzogranito porfirítico;	1989 ± 11a*
Terreno Oriental	Grupo Alto Terrrê		Granada-muscovita-biotita xitos e muscovita-biotita gnaisses com quartzitos intercalados	-
	Granito Cerro Porã		Sieno a monzo granitos de composição calcio-alcalina do tipo A de ambiente pós-colisional	1749 ± 45d *
	Suíte Baía das Gáças	Granito Sanga Bonita	Granitos e gnaisses deformados.	1721 ± 25e*
		Ortognaisse Santa Clarinha		1716 ± 11e*
		Ortognaisse Espinílho		1735 ± 12e*
	Gnaisse Caracol		Ortognaisses leucocráticos rosados foliados.	1774 ± 26a* 1753 ± 13a*
	Gnaisse Morraria		Bandamento composicional característico com lentes intercaladas de anfibolitos.	1950 ± 23b*
	Complexo Passo Bravo		Gnaisses bandados e migmatitos, anfibolitos em menor quantidade.	1846 ± 47f***
Terreno Sudeste	Granito Scardine		Hornblenda-biotita monzogranito;	1791 ± 19a**
	Gnaisse Rio da Areia		Biotita monzogranito bandado com porfiroclástos;	1809 ± 9a**
	Gnaisse João Candido		Biotita gnaisse de composição monzogranítica.	-

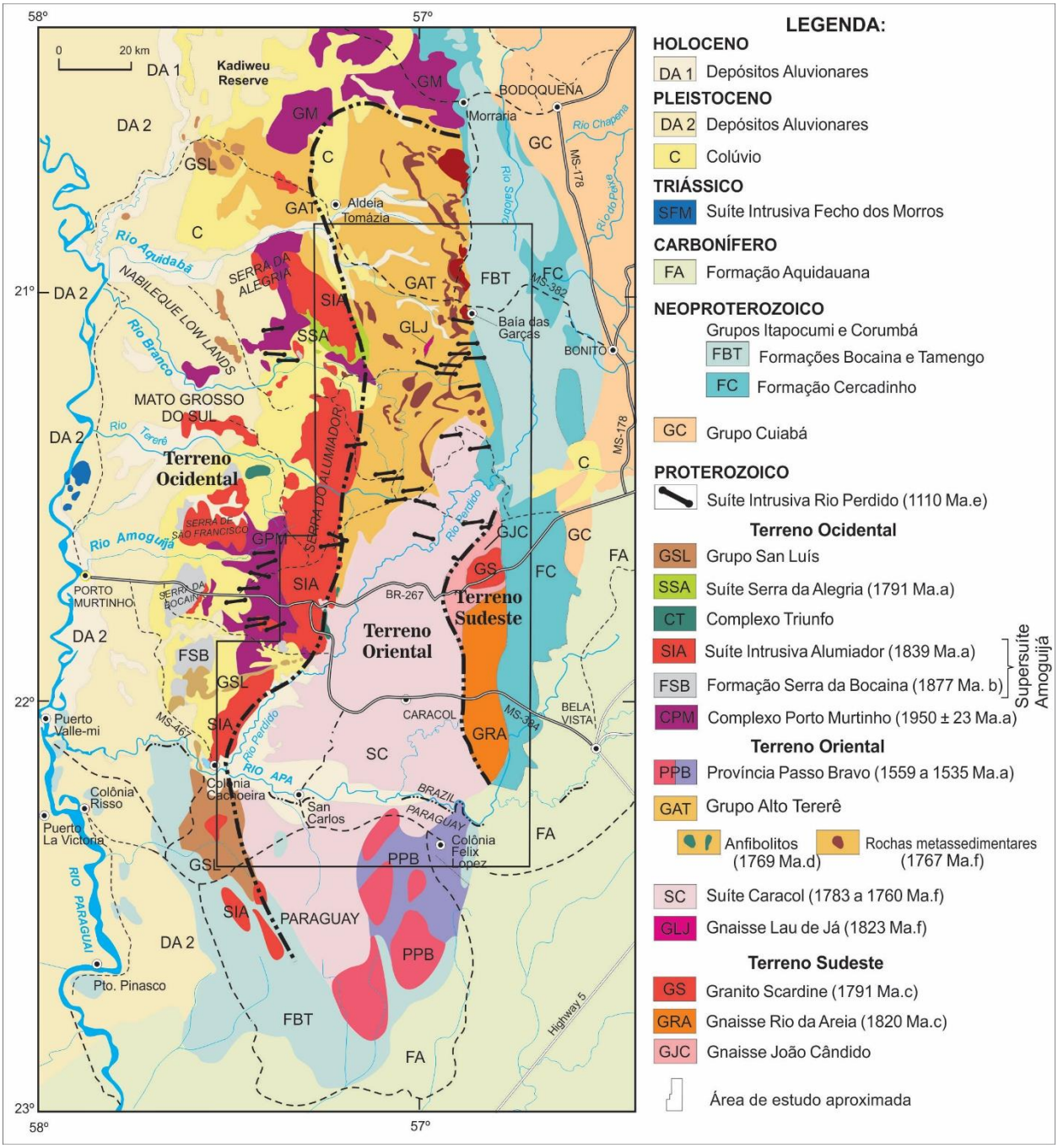

Figura 1.5. Esboço geológico da região do Bloco Rio Apa no sudoeste de Mato Grosso do Sul (Brasil) e noroeste do Paraguai. (Extraído e modificado de Cordani *et al.* 2010). As análises geocronológicas foram obtidas por a (Cordani *et al.*; 2010); b (Brittes *et al.;*2013); c (Faleiros *et al.;* 2015); d (Lacerda Filho; 2015); e (Teixeira *et al.;* 2016); f, (este trabalho).

Lacerda Filho (2015) compartimentam o Bloco Rio Apa em três segmentos (ocidental, central e oriental; fig. 1.5). Os autores sugerem cinco principais eventos magmáticos graníticos (2.07-1.71 Ga) que constituem uma evolução progressiva e representam vários estágios de acresção do Arco

Magmático de Amoguiá. As rochas estudadas estariam nas fases finais desse arco magmático, no período entre 1760 e 1750 Ma, interpretadas como granitos orogênicos tardios do tipo A. O Terreno Oriental é constituído pela associação de rochas já citada nas duas compartimentações acima, com algumas modificações: ao Complexo Porto Murtinho são adicionadas as unidades Gnaisse Piatã, Paragnaisse Tonalítico, Granito Chateolo (1902±11 Ma; U-Pb, SHRIMP, zircão; Faleiros *et al.*, 2015) e Gabro Matão (1969±5 Ma, U-Pb, LA-ICPMS, zircão; Faleiros *et al.*, 2015). Os granitos Córrego Servo e Aquidabã também são acrescentados. Para o terreno central é mantida a denominação Complexo Rio Apa, caracterizado como uma associação de granitos e gnaisses representados pelas unidades recentemente propostas por Cordani *et al.* (2010), Remédio *et al.* (2013), e Faleiros *et al.* (2015), além de terminologias inéditas como Granito Tamanduá (1736±19 Ma; U-Pb, LA-ICPMS, zircão; Lacerda Filho *et al.*, 2016) e Granito Santo Antônio (1794± 14 Ma; U-Pb, LA-ICPMS, zircão; Lacerda Filho, 2015), e incluem também a Província Passo Bravo (Wiens, 1986; 1559±55 Ma; U-Pb, SHRIMP, zircão; Cordani *et al.*, 2010) em território paraguaio. O Complexo Paraíso é constituído pelos gnaisses e granitos descritos no terreno sudeste de Faleiros *et al.* (2015).

Os terrenos central (Complexo Rio Apa e Grupo Alto Tererê) e oriental (Complexo Paraiso) constituem a área estudada, bem como o Grupo Alto Tererê. A tabela 1.3 apresenta os terrenos ocidental, central e oriental sureridos por Lacerda Filho (2015), bem como as unidades litoestratigráficas constituintes de cada um deles.

Tabela 1.3. Resumo da compartimentação proposta por Lacerda Filho (2015) para o Bloco Rio Apa. As descrições litológicas apresentadas na tabela são do autor acima citado e as idades são de a Lacerda Filho (2015); b Faleiros *et al.*, (2015) , c Cordani *et al.* (2010), d Plens *et al.* (2013), e Brittes et al., (2013), f Lacerda Filho *et al.*, (2006), g Pavan *et al.*, (2014). Os métodos são *U-Pb - SHRIMP, **U-Pb - LA-ICP-MS, ***Rb-Sr.

Unidade Litoestratigráfica			Breve descrição	Idade (Ma)
Terreno Ocidental	**Supersuíte Amoguijá**	Formação Serra da Bocaina	Riolitos, pórfiros, riodacitos, dacitos, tufos riolíticos e riodacíticos, tufovítrios, lapilitufos e brechas vulcânicas;	1877 ± 4c*
		Granito Alumiador	Biotita granitos, monzogranitos com autólitos de tonalito, pegmatitos;	1867f*
	Granito Aquidabã		Biotita granitos e sienogranitos;	1830 ± 5*
	Granito Córrego Servo		Biotita gnaisse cinza a leuco gnaisse;	1841 ± 7g*
	Complexo Porto Murtinho	Gnaisse Porto Murtinho	Gnaisses bandados, veios pegmatítcos, subordinadamente anfibolitos e gabros	2074 ± 7a**
		Gnaisse Morraria		1950 ± 23 f*
		Gabro Matão		1969 ± 5a**
		Granito Chateolo		1902 ± 12b*
		Granito Morro da Lenha		1947 ± 9b*
		Gnaisse Córrego Jibóia		1989 ± 11b *
		Paragnaisse Tonalítico		-
		Gnaisse Piatã		1892 ± 31a**
Terreno Central	**Grupo Alto Terrrê**	Metavulcânicas	Unidade metavulcânica básica;	1768 ± 6 a**
		Metassedimentos	Granada-muscovita-quartzo xitos, muscovita-quartzo xistos, granada-silimanita-cianita-estaurolita xisto e quartzitos;	1.70 a 2.12 (Zr detrítico) a**
	Complexo Rio Apa	Granito Baía das Garças	Biotita granito rosa;	1754±42b**
		Granito Cerro Porã	Sieno a monzogranitos calcio-alcalinos.	1749 ± 45d*
		Granito Santa Clarinha	Hornblenda-biotita gnaisse, monzogranito proto a milonítico;	1750±9b*
		Granito Tamanduá	Biotita gnaisse milonítico cinza rosad, mozo a sienogranito;	1736±19 a**
		Granito Sanga Bonita	Biotita-granito a sienogranito rosa;	1721 ±25b**
		Gnaisse Caracol	Ortognaisses protomiloníticos a ultramiloníticos cinza a rosa, magnetita-granada-biotita gnaisse, migmatito, biotita-hornblenda gnaisse, quartzo monzonito e sienogranito foliado.	1774 ± 26b* 1753 ± 13b*
Terreno Oriental	Granito Scardine		Hornblenda-biotita monzogranito;	1791 ± 19b**
	Gnaisse Rio da Areia		Biotita monzogranito bandado com porfiroclástos;	1809 ± 9b**
	Gnaisse João Candido		Biotita gnaisse de composição monzogranítica.	-

Lacerda Filho *et al.* (2016) apresentam extensa discussão sobre o Grupo Alto Tererê e o descrevem como representado por sequência metavulcano-sedimentar. A unidade metassedimentar caracteriza-se por metapelitos aluminosos constituídos por micaxistos granadíferos, cianita-estaurolita xisto, epidoto-clorita-actinolita xistos, granada-cianita-muscovita xisto, muscovita-quartzo xisto, biotita-quartzo xisto, quartzitos e, subordinamente, sillimanita-cianita-estaurolita xisto, com intercalações de anfibolitos. Os dados istópicos apresentados por Lacerda Filho *et al.* (2016) para estas rochas mostraram idades de proveniência obtidas pelo método U-Pb em zircão (LA-ICP-MS), indicando idade máxima de sedimentação em 1728 e 1700 Ma para duas amostras de granada-cianita-muscovita xisto. Os autores descrevem a unidade metavulcânica básica como constituída por anfibolitos, divididos em três fácies: (ii) anfibolitos de granulação média e textura sub-ofítica reliquiar (metagabros); (iii) anfibolitos com textura cumulática reliquiar (metapiroxenitos); e apresentam idades de cristalização de 1769±36 Ma (U-Pb, LA-ICPMS, zircão).

Capítulo 2

LITHOSTRUCTURAL FRAMEWORK OF THE EASTERN TERRANE OF THE RIO APA BLOCK - SOUTHERN AMAZONIAN CRATON

Dalila Pexe Plens
Márcio Martins Pimentel
Amarildo Salina Ruiz
Reinhardt A. Fuck

Submetido: *Brazilian Journal of Geology*

14-Jul-2018

Dear Mrs. Plens:

Your manuscript entitled "LITHOSTRUCTURAL FRAMEWORK OF THE EASTERN TERRANE OF THE RIO APA BLOCK - SOUTHERN AMAZONIAN CRATON" has been received by the Editorial Office of the Brazilian Journal of Geology.

Please note that this message is not a confirmation of submission, which will only be given once your manuscript is considered to be within the scope and of interest to the journal.

Your manuscript ID is BJGEO-2018-0077.

Please mention the above manuscript ID in all future correspondence or when calling the office for questions. If there are any changes in your street address or e-mail address, please log in to ScholarOne Manuscripts at https://mc04.manuscriptcentral.com/bjgeo-scielo and edit your user information as appropriate.

You can also view the status of your manuscript at any time by checking your Author Center after logging in to https://mc04.manuscriptcentral.com/bjgeo-scielo.

Thank you for submitting your manuscript to the Brazilian Journal of Geology.

Sincerely,

Brazilian Journal of Geology Editorial Office.

2. LITHOSTRUCTURAL FRAMEWORK OF THE EASTERN TERRANE OF THE RIO APA BLOCK - SOUTHERN AMAZONIAN CRATON

Dalila Pexe Plens[1,4,5*], Márcio Martins Pimentel[1,2], Amarildo Salina Ruiz[3,4], Reinhadt A. Fuck[1, 2]

[1]Geology Pos-Graduate Program/UnB; [2]Geochronology Laboratory/UnB; [3]College of Geology/UFMT; [4]Mining Engineering Graduate, IENG/UFMT; [5]Crustal and Tectonic Evolution Research Group. *Corresponding author: dalilaplens@ufmt.br.

RESUMO

O Bloco Rio Apa expõe-se no sudoeste de Mato Grosso do Sul e em território paraguaio. É compartimentado em dois terrenos justapostos, ocidental e oriental. Este trabalho enfatiza o terreno oriental com abordagem descritiva e cinemática dos diferentes episódios deformacionais e metamórficos. Foram registradas três fases deformacionais compressivas (D_1, D_2 e D_3). D_1 inicialmente ocorre restrita ao embasamento como bandamento composicional. Em processo de deformação progressiva, as rochas gnáissicas são dobradas, gerando clivagem de crenulação. Na Suíte Caracol D_1 gera xistosidade. A segunda fase (D_2) é o evento mais expressivo que, no embasamento e na Suíte Caracol, redobrou S_1 e gerou dobras, clivagem de crenulação e xistosidade. Processos de deformação progressiva ocorrem em F_2, em que xistosidade, comumente orientada para NWW com mergulhos baixos, assume diferentes trajetórias nas porções norte e oeste da área. D_2 está associado ao metamorfismo de 1300 Ma relacionado à justaposição dos terrenos oriental e ocidental, via cavalgamento de topo para NW. D_3 mostra-se dúctil-rúptil como dobras, clivagem de crenulação e lineação de intersecção. Sugerimos a correlação geotectônica entre o Bloco Rio Apa e o Complexo Chiquitania do Terreno Paraguá no sudoeste do Cráton Amazônico.

Palavras Chaves: Bloco Rio Apa, terreno oriental, Suíte Caracol, deformação progressiva.

ABSTRACT

The Rio Apa Block is exposed in the southwest part of Mato Grosso do Sul and in Paraguay. It is divided into two juxtaposed terranes - the western and eastern terranes. This study focuses on the eastern terrane and provides a description and kinematic analysis of the different deformation and metamorphic events. Three compressive deformation phases were recorded (D_1, D_2, and D_3). D_1 was initially restricted to the basement as compositional banding. During progressive deformation, the gneissic rocks were folded, which generated crenulation cleavage. In the Caracol Suite, D_1 generated schistosity. The second phase (D_2) was the most significant event that, in the basement, refolded S_1 and generated folds, crenulation cleavage, and schistosity. Progressive deformation processes occurred in D_2, in which the schistosity, which is commonly oriented NW with low dips, has different orientations in the northern and western portions of the area. D_2 was associated with metamorphism at 1300 Ma, which was related to the juxtaposition of the eastern and western terranes by thrusting to the NW. D_3 is a ductile-brittle deformation, including folds, crenulation cleavage, and intersection lineation. We suggest a geotectonic correlation between the Rio Apa Block and the Chiquitania Complex of the Paraguá Terrane in the southwestern portion of the Amazonian Craton.

Keywords: Rio Apa Block, eastern terrane, Caracol Suite, progressive deformation.

2.1.INTRODUCTION

The Rio Apa Block is a segment of the Amazonian Craton that is composed of infracrustal and supracrustal lithostratigraphic units whose evolution occurred mainly during the Orosirian and Statherian periods.

According to Plens et al. (submitted b), the eastern terrane of the Rio Apa block is composed of tonalitic to granodioritic orthogneisses (Lau de Já orthogneiss), significant plutonic magmatism of granitic-gneiss composition and rare occurrences of effusive dacitic rocks (Caracol Suite), and a metavolcanosedimentary section (Alto Tererê Group).

The Rio Apa Block has mainly been studied from geological and geochronological points of view (Cordani et al., 2010; Brittes et al., 2013; Plens et al., 2013; Redes et al., 2015; Faleiros et

al., 2015; Lacerda Filho et al., 2016), although a few studies have addressed its orogenic evolution, including the polyphase deformation history and the metamorphic events.

This contribution focuses on the deformational and metamorphic aspects of the eastern terrane of the Rio Apa Block with the goal of defining its tectonic framework to contribute to the understanding of the crustal evolution of the Rio Apa Block.

2.2.MATERIALS AND METHODS

2.2.1. GEOLOGICAL MAPPING AND STRUCTURAL ANALYSIS

Prior to the geological mapping, an initial interpretation of LANDSAT and Geocover satellite images and Shuttle Radar Topography Mission (SRTM) images was performed to identify the main regional structures. Images from aero-geophysical surveys of the region were also reviewed (ternary image and analytic signal amplitude image). Additionally, the geological data obtained in the study area by Lacerda Filho et al. (2006, 2016), Cordani et al. (2010), Brittes et al. (2013), Plens et al. (2013), Redes et al. (2015), Faleiros et al. (2015) and Lacerda Filho (2015) were compiled.

The geological mapping was carried out in several steps. The first mapping step was performed at the 1:250,000 scale for sample collection, obtaining structural data, and delimitation of lithological units. Key areas were then established, and additional fieldwork stages were conducted at a more detailed scale (1:10.000) to clarify the uncertainties with the mapped lithological types and to establish the chronology and significance of the tectonic structures.

The collected samples were macroscopically described, including their textural, compositional and structural aspects. Samples were selected for the preparation of thin sections, which was carried out in the lamination laboratories of the Federal University of Mato Grosso and University of Brasília.

The aim of the microscale analyses was to establish the mechanisms of intracrystalline deformation that occurred in each deformation phase and to correlate them with the metamorphic conditions. The description and interpretation of the intracrystalline deformation mechanisms were based on Passchier & Trouw (2005).

To facilitate the presentation of the data, the superposition criteria of Ramsay (1967) were adopted, in which acronyms were used to describe the structural elements, namely: Dn

(deformation phase), Fn (folds), Mn (metamorphism), Sn (foliations) and Ln (lineations). The definitions of progressive deformation suggested by Fossen et al. (article in press) were also used.

The secondary structures and deformational phases were defined and characterized following widely accepted concepts of structural analysis of polydeformed terranes (Fossen, 2012).

2.3.REGIONAL CONTEXT

The Amazonian Craton is bounded on the east by the Neoproterozoic Paraguay and Araguaia belts, and its northern, southern and western boundaries are covered by the sediments of the sub-Andean basins.

Based on Tassinari & Macambira (1999, 2004) and on geological and geochronological considerations, Ruiz (2005) describes the Rio Apa Block as an extension of the Amazonian Craton (Fig. 2.1).

Several other ideas about the placement of the Rio Apa Block have been proposed. Ramos & Vujovick (1993) assume that the Rio Apa Block is the northwestern portion of the Rio de La Plata Craton, and Ramos et al. (2010) suggest that the Rio Apa Block is located in the eastern portion of the Pampia Craton and borders the northwest portion of the Paranapanema Block. Casquet et al. (2012) suggest that the Rio Apa Block is located in the eastern portion of the Mara Craton, and Dragone et al. (2017), based on a gravity map, suggest that the Rio Apa Block may cover a broader area than that mapped by Cordani et al. (2010), underlying covering the Pantanal basin subsoil and the southern boundary of the Sunsás Province (Tassinari & Macambira, 1999).

Four main classifications have been proposed for the geotectonic division of the Rio Apa Block, including those by Lacerda Filho et al. (2006), Cordani et al. (2010), Faleiros et al. (2015) and Lacerda Filho (2015).

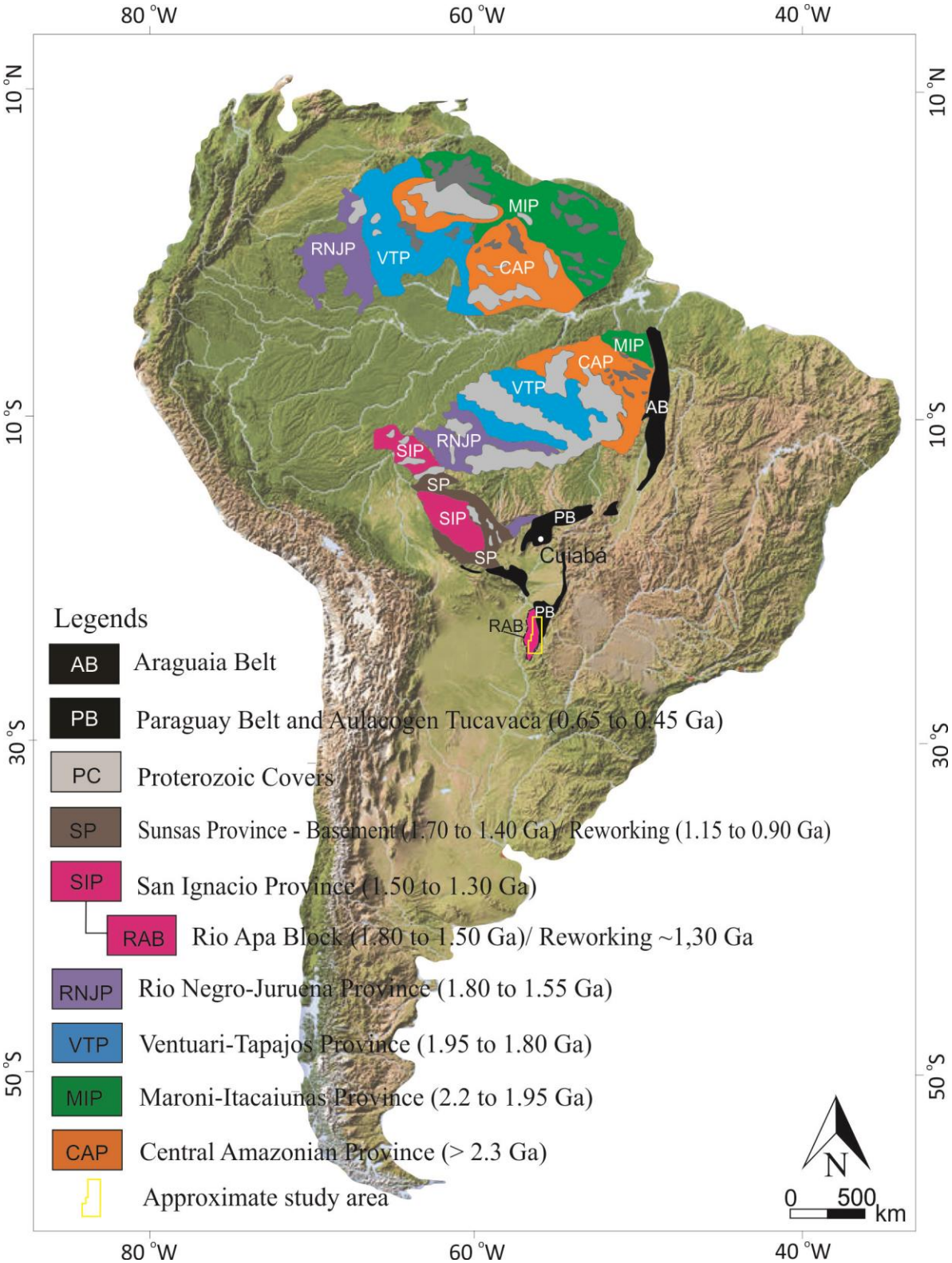

Figure 2.1. Geochronological and tectonic division of the Amazonian Craton, which considers the Rio Apa Block as an integral part of it extracted and modified from Tassinari & Macambira (1999) and Ruiz (2005). Note that the Rio Apa Block is colored as the San Ignacio Province, since the last orogeny (San Ignácio Orogeny) of the province is proposed as correlated to the deformation of the same age in the Rio Apa Block.

Lacerda Filho et al. (2006) subdivided the Rio Apa Block into three distinct geotectonic compartments: (i) remnant oceanic crust of Rhyacian age, which is represented by the Alto Tererê Metamorphic Complex; ii) the Rio Apa Magmatic Arc, which is Orosirian and is equivalent to the gneisses of the Rio Apa Complex; and (iii) the Amoguijá Magmatic Arc, which is Statherian and is composed of the Serra da Bocaina Formation (Brittes et al., 2013) and the granites of the Alumiador Intrusive Suite. Mafic bodies, including batholiths and dikes, are grouped as part of the continental mafic magmatism of likely Statherian or Tonian age.

Based on this subdivision, the study area is included in the Rio Apa Magmatic Arc, which is composed of rocks that were deformed by brittle to brittle-ductile tectonics that are expressed as confined transcurrent zones with predominant NW-SE orientations and sinistral kinematics (Lacerda Filho et al., 2006).

Based on the distribution of Sm-Nd model ages, Cordani et al. (2010) proposed the existence of two tectonic terranes in the Rio Apa Block (western and eastern) with distinct evolutionary histories that are bounded by an approximately N-S-oriented suture zone (Fig. 2.2). The study area is located in the eastern terrane. Cordani et al. (2010) did not use the term Rio Apa Complex and rather proposed the presence of the Caracol Gneiss, the Morraria Complex and the metavolcanosedimentary rocks of the Alto Tererê Group as well as the granites and gneisses of the Paso Bravo Province, which are restricted to Paraguayan territory (Wiens, 1986). Geochronological data obtained using the U-Pb zircon method (SHRIMP) presented by Cordani et al. (2010) indicate an age of 1721 ± 25 Ma for crystallization of the Caracol Gneiss.

Cordani et al. (2010) describe a regional foliation with low-angle dips trending approximately 20° NW that is present especially in the southern part of the study area, which is possibly related to medium grade metamorphism. According to Cordani et al. (2010), penetrative schistosity with occasionally greater dips is present in the northern and central areas, and an older deformation phase is often observed. These authors present K-Ar and Ar-Ar metamorphic ages of approximately 1300 Ma, which are interpreted as part of the regional cooling event that affected the entire region (Cordani et al., 2010).

Faleiros et al. (2015) followed the categorization of Cordani et al. (2010) in the western and eastern terranes; however, they described a third terrane, the southeastern terrane (Fig. 2.2). This terrane is bounded by shear zones, and its magmatic evolution occurred through distinct accretionary events that reflect an extremely mobile tectonic regime (Faleiros et al., 2015). The

eastern terrane consists of the Morraria and Caracol gneisses and the Baia das Garças Suite, which is composed of the Sanga Bonita Granite (1721 ± 25 Ma; U-Pb, SHRIMP, zircon; Remédio et al., 2013) and the Santa Clarinha and Espinilho orthogneisses (Remédio et al., 2013; 1716 ± 11 Ma and 1735 ± 12 Ma; U-Pb, SHRIMP, zircon; respectively) as well as the Cerro Porã granite (1749 ± 45 Ma; U-Pb, SHRIMP, zircon; Plens et al., 2013), which was previously described as belonging to the western terrane. The João Candido and Rio Areia gneisses (1820 ± 18 Ma; U-Pb, LA-ICP MS, zircon; Faleiros et al., 2015) and Scardine Granite (1791 ± 19 Ma; U-Pb, LA-ICP MS, zircon; Faleiros et al., 2015) have been identified in the southeastern terrane. The study area is located in the eastern and southeastern terranes.

Faleiros et al. (2015) describe a intensely deformed zone that separates the eastern and southeastern terranes. Similar to Cordani et al. (2010), Faleiros et al. (2015) also emphasize west-oriented structures in the eastern terrane, describing them as a thrust zone that formed by generalized mylonitic deformation.

Lacerda Filho et al. (2016) divide the Rio Apa Block into three segments (western, central and eastern), each with their own characteristics, that were affected by a succession of tectonically juxtaposed magmatic events (1.87-1.71 Ga). The authors suggest five individual main granitic magmatic events (2.07-1.71 Ga), which comprise a progressive evolution and represent several magmatic stages of the Amoguijá Magmatic Arc. The studied rocks were involved in the final stages of this magmatic arc between 1760 and 1750 Ma, and they are interpreted as A-type post-orogenic granites. The study area encompasses the central (Rio Apa Complex and Alto Tererê Group) and eastern (Paraíso Complex) terranes.

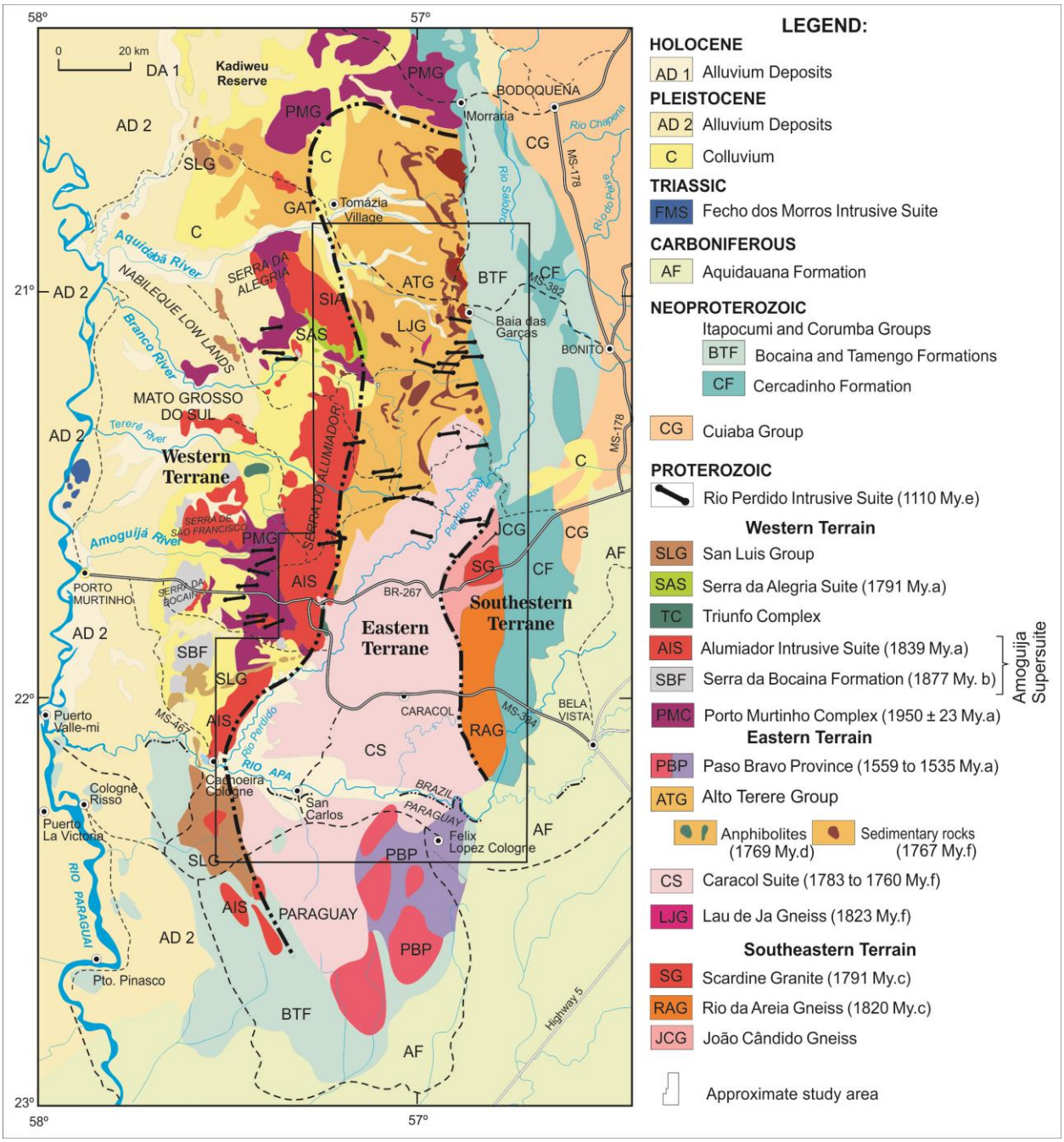

Figure 2.2. Geological sketch of the Rio Apa Block region in southwestern Mato Grosso do Sul (Brazil) and northwestern Paraguay (extracted and modified from Cordani et al., 2010). The geochronological analyses were taken from: a (Cordani et al.; 2010); b (Brittes et al.; 2013); c (Faleiros et al.; 2015); d (Lacerda Filho et al.; 2016); e (Teixeira et al.; 2016); f (Plens et al.; submitted b).

About the Alto Tererê Group, Lacerda Filho et al. (2016) also present a broad discussion and describe it as represented by a metavolcanic-sedimentary sequence. The metasedimentary rocks are composed of garnet-kyanite-muscovite schist, muscovite-quartz schist, garnet-muscovite schist, biotite-quartz schist, chlorite-muscovite-quartz schist, epidote-chlorite-quartz schist and muscovite

quartzite metamorphosed to medium amphibolite facies, with retrometamorphism to greenschist facies, related to the D_2 deformation phase. The isotopic data for these rocks showed ages obtained by the U-Pb method on detrital zircon (LA-ICP-MS), suggesting maximum sedimentation age of 1728 and 1700 Ma for two samples of garnet-kyanite-muscovite schist. The authors describe the mafic metavolcanic unit as consisting of three lithofacies: (i) fine-grained banded amphibolite (metabasalt); (ii) medium-grained amphibolite with relict subophitic texture (metagabbro) and; (iii) amphibolite with relict cumulate texture (metapyroxenite). These authors determined a crystallization age of 1769 ± 36 Ma (U-Pb in zircon; LA-ICP-MS) for one amphibolite sample.

The term Rio Apa Complex is retained by these authors for the central terrane, which is characterized as an association of granites and gneisses that are represented by the units recently proposed by Cordani et al. (2010) and Faleiros et al. (2015) in addition to new units, such as the Tamanduá Granite (1736 ± 19 Ma, U-Pb, LA-ICP MS, zircon; Lacerda Filho et al., 2016), and the Santo Antonio Granite (1794 ± 14 Ma, U-Pb, LA-ICP MS, zircon; Lacerda Filho et al., 2016) as well as the Passo Bravo Province (Wiens, 1986; 1559 ± 55 Ma, U-Pb, SHRIMP, zircon; Cordani et al., 2010) in Paraguay. The Paraíso Complex is composed of the gneisses and granites described in the southeast terrane by Faleiros et al. (2015).

Manzano et al. (2008), Godoy et al. (2009) and Manzano (2013) suggested five phases of deformation (Dn-1, Dn, Dn+1, Dn+2, Dn+3). The first two were attributed to Paleo-Mesoproterozoic events, and the others were attributed to the tectonic-metamorphic formations that are superimposed by the Neoproterozoic Paraguay Belt.

Based on geological mapping and structural data, Lacerda Filho (2015) proposes subdividing the Rio Apa Block into three lithostructural domains (domains 1, 2 and 3) with the eastern terrane located in domain 3. Three progressive phases of deformation (D_1, D_2, and D_3) resulting from a compressive regime are identified. Phase D_1 is represented by foliation of the rocks of the Rio Apa Complex (Caracol Suite) and the Alto Tererê Group. The D_2 phase produced varied textures with a predominance of ductile low-angle deformation and the transposition of the previous foliations. This phase was accommodated by folds and shear zones with the development of thrust ramps, and the M_2 metamorphism is associated with a nappe system that is generally oriented N-S. The D_3 phase is characterized by smooth undulations of the S_2/S_1 foliation and the development of open folds.

2.4.RESULTS

2.4.1. LITHOSTRATIGRAPHIC UNITS

The lithostratigraphic framework of the eastern terrane includes, from the base to the top, the Lau de Já orthogneiss (basement), the Caracol Suite, which is composed of granite-gneisses rocks, and the metavolcanosedimentary rocks of the Alto Tererê Group (Plens et al., submitted b). Although it is part of the eastern terrane, the Paso Bravo Province, which is located in Paraguayan territory, is not present in the study area.

2.4.1.1.Lau de Já orthogneiss

The Lau de Já orthogneiss occurs as a narrow xenolith in the northwestern portion of the Caracol Suite and forms a strip of discontinuous and restricted outcrops (Fig. 2.3). It is gray, medium to fine grained with well-developed gneiss banding, and characterized by felsic bands composed of quartz, plagioclase and feldspar and mafic bands composed of biotite, muscovite, epidote and opaque minerals.

2.4.1.2. Caracol Suite

The Caracol Suite consists of granite-gneiss that underlies much of the eastern terrane and a small volume of dacitic effusive rocks. Its mapped area is approximately 190 km long in the N-S direction and 50 km wide in Brazil, and it extends for approximately 65 km to the south in Paraguay. It is in contact to the west with the rocks of the Alto Tererê Group and to the east with the rocks of the Corumbá Group, and the southwest portion is partially covered by unconsolidated sediments of the Pantanal Formation. It outcrops in the form of slabs, blocks, hills, small hills, and in river beds, and it is composed of foliated rocks that, when deformed by local or regional shear zones, form mylonites and schists. Evidence of secondary hydrothermal processes causing the formation of chlorite and muscovite may be related to greenschist facies metamorphic events.

Six facies were identified in the Caracol Suite based on its field and petrographic characteristics: a pink hololeucocratic facies, pink biotite granite-gneiss facies, pink porphyritic granite-gneiss facies, pink amphibole granite-gneiss facies, gray amphibole biotite granite-gneiss facies and gray amphibole tonalite facies in addition to rocks associated with shear zones.

2.4.1.3. Alto Tererê Group

The Alto Tererê Group consists of a narrow strip oriented N-S at the boundary between the eastern and western terranes of the Rio Apa Block, which consists of metavolcanosedimentary rocks. It is in contact with the rocks of the Alumiador Intrusive Suite (western terrane) to the west and with the Caracol Suite to the east.

The metasedimentary rocks are represented by sillimanite-quartz schists. They occur in small slabs and pits in the western portion of the study area. They are beige and orange, and the weathered part shows the formation of rounded fragments with sizes of 0.5 to 4 cm, which are oriented and stretched preferentially to the west.

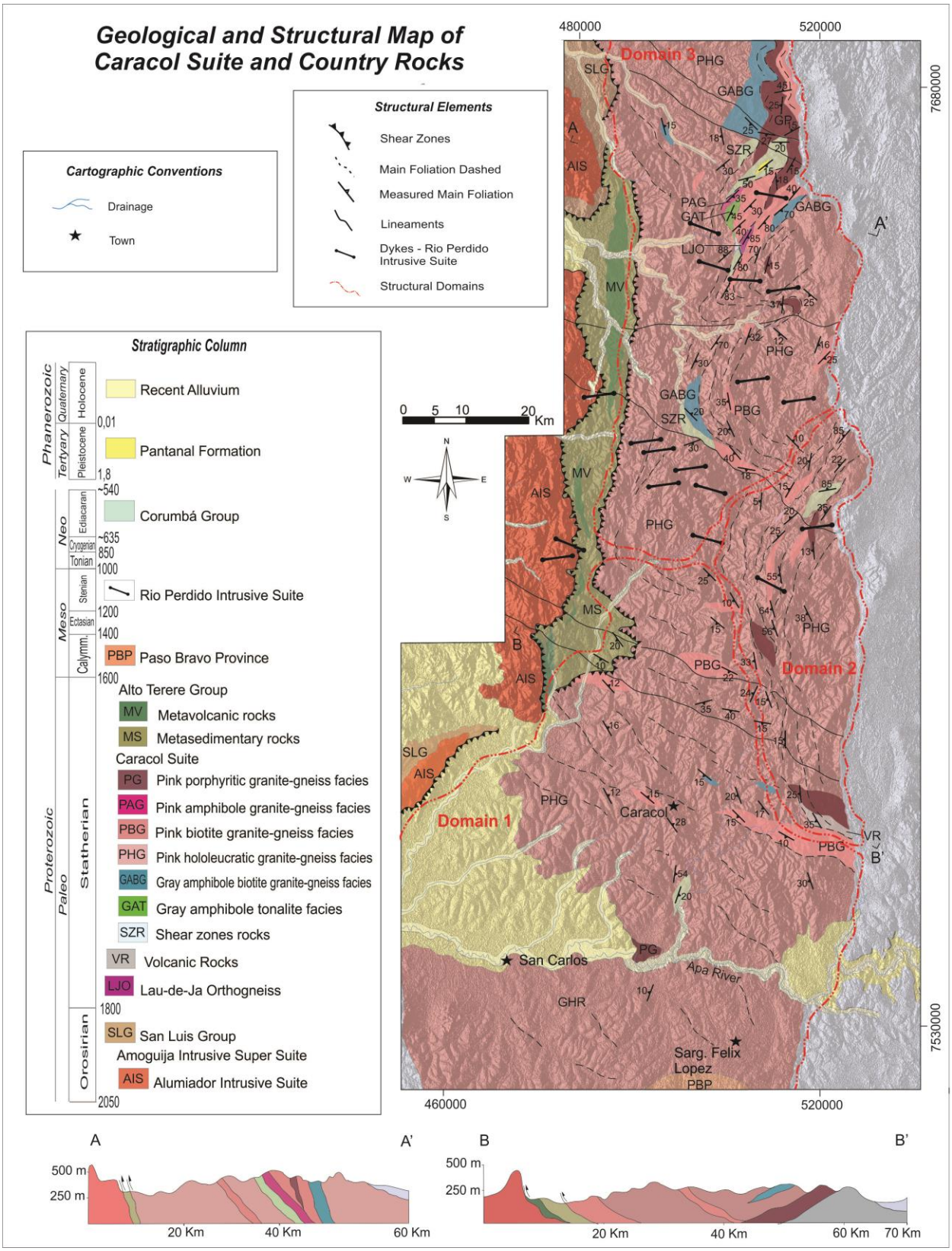

Figure 2.3. Geological and structural map of the Caracol region (MS) with emphasis on the Caracol Suite of the eastern terrane. The division into three structural areas is highlighted.

2.4.2. STRUCTURAL ANALYSIS

The structures described below were interpreted based on the processing and interpretation of the structural data collected in the field, observations of satellite images and aerogeophysical surveys (previously described), and the analysis of the microstructures in the microscopy laboratory. The observed structures included foliations, lineations, folds, and mylonitic shear zones.

The main foliation, S_2, which is interpreted as schistosity and crenulation cleavage, is present throughout the study area and dips at low angles to the NW. In the northern part of the study area, S_2 dips at higher angles with azimuths that follow the pattern of open folds that are easily observed at a regional scale. Local shear zones are observed throughout the study area but are more evident in the northern portion. Open and smooth folding is observed in the S_2 foliation where new axial planes (S_3) are developed.

Foliation S_1 is observed in the basement (Lau de Já orthogneiss) as a compositional banding foliation. As a result of the later progressive deformation, this banding was folded to form F_1 folds. In the granitic-gneiss rocks of the Caracol Suite, S_1 is interpreted as poorly preserved crenulation cleavage and schistosity as a result of the transposition by main foliation.

All of these structures, in addition to those described below, were subdivided into three groups that were attributed to three contractional deformation phases, labelled D_1, D_2 and D_3, as well as a shallow, brittle extensional deformation event that is not addressed in this study. The traditional superposition criteria of Ramsay (1967) and the progressive deformation concepts suggested by Fossen et al. (in press) were used. These authors describe the term progressive deformation as a period of continuous deformation during which composite structures may be formed, such as overlapping cleavages and refolding, typically with significant variations in style and orientation.

2.4.2.1.First Deformation Phase - D_1

The S_1 foliation was initially restricted to the northern portion of the area, where the gneissic rocks are located. It is represented by metamorphic banding defined by the compositional segregation of felsic and mafic minerals (Fig. 2.4A) in the basement rocks.

With the progression of this deformation, folding of the basement compositional banding occurred, which generated D_1 folds. The S_1 foliation has dips between 50° and 65° and an average strikes between 255° and 325°. S_1 is represented in the axial planes of folds as crenulation cleavage foliation (Fig. 2.4B, C).

The S_1 foliation in the facies of the Caracol Suite is classified as a penetrative schistosity foliation that is generally defined by the preferential orientation of mafic minerals (almost always biotite) as well as potassium feldspar, quartz, and plagioclase; however, crenulation cleavage is also present. The S_1 foliation is common in quartz-feldspar injections; however, in both the oriented minerals and the quartz-feldspar injections, it has usually been folded by the subsequent phase (Fig. 2.4B, C). A pole distribution analysis of this foliation indicates a maximum of approximately 145°/20° and a dispersion of azimuths between 120° and 160° with plunges between 5° and 30°. Another concentration of measurements includes azimuths between 240° and 265° with dip angles of 35° to 60°, and a third concentration includes azimuths between 300° and 340° and steep dips between 70° and 85° (stereogram in Fig. 2.5A).

The deformational phase (D_1) that contains these structures included an initial development period that is only observed in the basement rocks, during which the gneissic compositional banding was generated. During the subsequent progression of this deformational phase, this banding was folded to expose crenulation cleavages. The granite-gneiss were apparently affected by only the progressive deformation phase; they show penetrative schistosity and a common crenulation cleavage. Figures 2.4B, C and D show the relationship between folding and the foliation, and Figure 2.5 shows a schematic representation of the development of the structures in each deformation event in addition to stereographic projections of the structures.

2.4.2.2. Second Deformation Phase - D_2

As previously discussed, S_2 is the main foliation in the study area. In the gneissic lithotypes of the basement, S_2 is classified as a crenulation cleavage-type spaced penetrative foliation (Fig. 3.4A). In the granite-gneiss rocks of the Caracol Suite, the S_2 foliation is considered to be a crenulation cleavage (Fig. 2.4 B and C); however, it is more often a continuous schistosity, which is defined mainly by the preferential orientation of biotite and the as potassium feldspar, quartz,

and plagioclase (Fig. 2.4D). The schistosity is also observed in the metasedimentary rocks of the Alto Tererê Group.

The S_2 foliation generally has NW orientations and near horizontalized dips throughout the central-southern portion of the study area. However, in the northern portion, the measurements show distortions where the strikes are consistent with the morphology of large regional folds in the area, and the dips become steeper to nearly vertical. These changes in the S_2 foliation's orientation are also interpreted in the western portion of the area, where structures that are preferentially oriented N-S are present.

Fossen et al. (in press) suggest that the lithology and rheology played an important role during the structural evolution; in addition, high temperatures and partial melting can change the rheological properties of a region. The term deformation partitioning (Carreras et al., 2013, in Fossen et al., in press) thus defines a common result of variations in composition- and/or temperature-controlled rheology.

The observed changes in the orientation of the S_2 foliation that show (as described below) areas with greater numbers of folds in locations with greater numbers of shear zones lead us to use the term deformation partitioning of Fossen et al. (in press). For a better understanding of such changes in deformation, in the case of only one phase of deformation (D_2), we suggest the division of three structural domains in the mapped area from south to north as structural domains 1, 2 and 3.

The first structural domain is observed in the southern portion of the study area and contains crenulation cleavage and schistosity that form a NW-vergent roof thrust and near horizontalized dip angles. The field data were projected on a pole distribution diagram (Fig. 2.5B) and show two concentrations of measurements with large dispersions of values. The most significant contains azimuths between 150° and 250°, and the second contains azimuths between 20° and 70°; both have dip angles between 10° and 30°. The lineation is interpreted as slightly oblique to the S_2 foliation; it has low plunge angles between 5° and 20° and azimuths with dispersions following the S_2 measurements.

At the western end of the eastern terrane, S_2 is preferentially oriented N-S. Structural domain 2 has a distribution of poles with a concentration of azimuths between 150° and 220° and low-angle dips (Fig. 2.5B).

Domain 3 extends from the central portion of the study area to the northern end, where the satellite images (LANDSAT, Geocover, and SRTM) show that the deformation becomes more intense, which creates the morphology of meanings regional folds. The strikes of S_2 collected in the field corroborate the preliminary investigations because they follow the pattern of folds and also show dip angles that are generally higher at several locations than in the southern portion. The pole distribution analysis, which is shown in Figure 2.5B for domain 3, shows two major maximum concentrations surrounded by large dispersions of values. The first set contains azimuths between 120° and 150°, and the second set contains azimuths between 200° to 250°. The dip angles are also scattered: they are low (between 5° and 30°), but near-vertical dips between 65° and 80° are not uncommon. The azimuths of mineral lineation L_2 vary significantly in this domain, as is the case with the foliation measurements, and the plunges are between 10° and 30°.

In all rocks, S_2 is interpreted as being parallel to the axial planes of the F_2 folds. These are in turn poorly preserved with rare quartz-feldspar veins and are characterized as asymmetric, closed to isoclinal and often recumbent folds with hinge zones oriented approximately 160° and near horizontalized dips (Figure 2.4 B, C and Fig. 2.5 B).

The shear zones that formed during this deformational phase are also associated with the deformation described for each structural domain. In the northern portion of the study area, the shear zones follow the imposed deformation pattern, which clearly experienced more compression and a greater thermal energy than the rocks of domains 1 and 2, in which fewer shear zones are observed with low-angle dips. The rocks located near the shear zones are associated with the development of metamorphic reactions and are extremely deformed and sometimes schistose (Plens et al., submitted b).

The kinematic indicators in the shear zones in the three domains are S-C structures (Figure 2.4E) with stretched and rotated clasts that have asymmetric tails, both in the porphyroclasts and in the main minerals that form the different facies of the suite. Recrystallization of the minerals is often present at the edges of the crystals, forming pressure shadows. Porphyroclasts of plagioclase and oriented amygdales that are filled with quartz are observed in the effusive rocks.

The second phase of deformation was responsible for the main ductile compression observed throughout the mapped area. In the gneissic lithotypes, D_2 caused the refolding of the pre-existing folded compositional banding (S_1), which generated D_2 folds (Fig. 2.5B). Crenulation cleavage (S_2) developed on the axial surfaces of these folds. In the granite-gneiss of the Caracol Suite,

deformation phase D_2 is responsible for the folding of the previous S_1 foliation, which generated F_2 folds as well as crenulation cleavage (S_2; Fig. 2.5 B) in the axial planes of these folds. The decrease in the spacing of this foliation generated schistosity, which is the most significant characteristic of the second deformation phase (Fig. 2.4B, C, D). A schematic sketch is shown in Figure 2.5B. The intensity of the schistosity becomes more intense with proximity to the regional and local shear zones in the eastern terrane as well as throughout the Rio Apa Block.

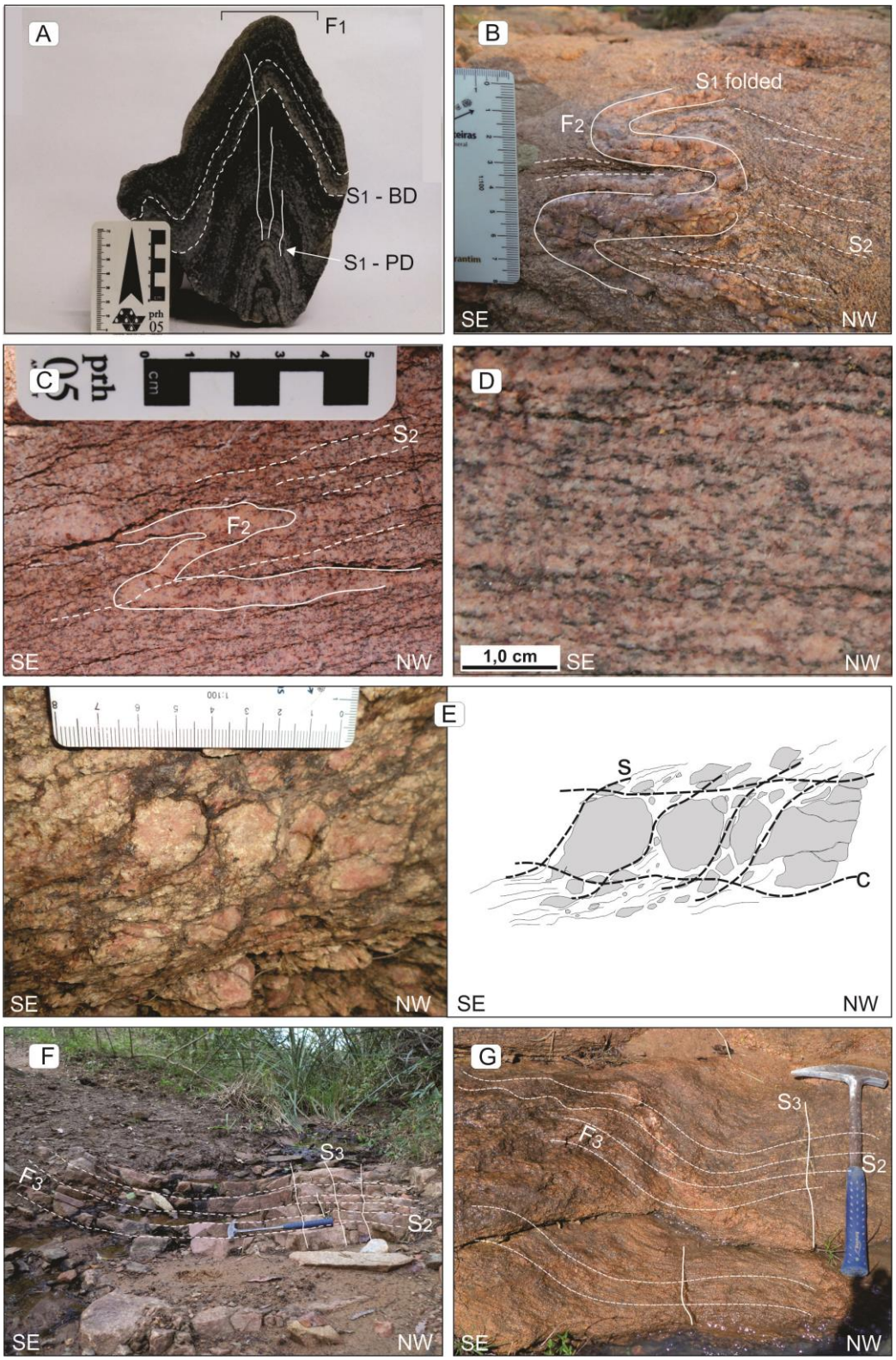

Figure 2.4. Deformation phases of the eastern terrane: (A) Lau de Já orthogneiss: compositional metamorphic banding (S_1 foliation) with subsequent folding during progressive deformation. (B) Caracol Suite, pink hololeucocratic granite-gneiss facies: penetrative S_1 foliation represented by schistosity folded during the second deformation phase D_2, which generated F_2 folds and S_2 foliation.

Cont. Figure 2.4. (C) Caracol Suite, pink hololeucocratic granite-gneiss facies: F_2 fold preserved in quartz-feldspar portions with foliation (S_2) parallel to the axial plane of the folds; (D) Caracol Suite, pink biotite granite-gneiss facies: S_2 foliation that is well-marked by the presence of mafic minerals; (E) Caracol Suite, pink porphyritic granite-gneiss facies: porphyroclasts of potassium feldspar that are rotated and oriented by the regional deformation, showing S-C structures - diagram on the right; (F and G) Caracol Suite, pink hololeucocratic granite-gneiss facies: penetrative S_2 foliation folded during the third deformational phase, which resulted in F_3 folds and crenulation cleavage foliation (S_3).

2.4.2.3.Third Deformation Phase - D_3

The S_3 foliation is present throughout the mapped extent of the eastern terrane. However, because they cover a larger area, the granite-gneiss rocks of the Caracol Suite more clearly expose these structures. The foliation is represented by crenulation cleavage (Fig. 2.4E, F, and Fig. 2.5C) with high-angle dips and NE strikes. The stereographic projection of the S_3 foliation measurements (Fig. 2.5 C) shows a maximum at 60°/60°, but the dispersion of the values also shows concentrated azimuths in the SE quadrant between 90° and 110° and between 160° and 180° as well as in the SW quadrant between 250° and 270°. The dip angles are always high (between 60° and 85°) and perpendicular to S_2.

The L_3 intersection lineation, generated by the intersection between the S_1 and S_2 foliations, was rarely observed and has azimuths between 165° and 180° with shallow plunges between 5° and 10°, as shown in the isofrequency stereogram (Fig. 2.5C).

The F_3 folds are abundant throughout the entire area, and they are smooth to open and symmetric (Fig. 2.4 F, G) to slightly asymmetric with shallow plunges at the outcrop scale. At the centimetric scale, they appear as discrete open to closed micro-wrinkles, symmetric to asymmetric and concentric, which are present in the southeastern portion of the Caracol Suite.

Deformation phase D_3 was a ductile-brittle compressive event that affected all of the rocks of the eastern terrane and the Rio Apa Block. The compression during this deformation event generated open F_3 folds at the outcrop and microscopic scales. The diagram in Figure 2.5C shows the relationships between the F_3 folds and the S_2 and S_3 foliations.

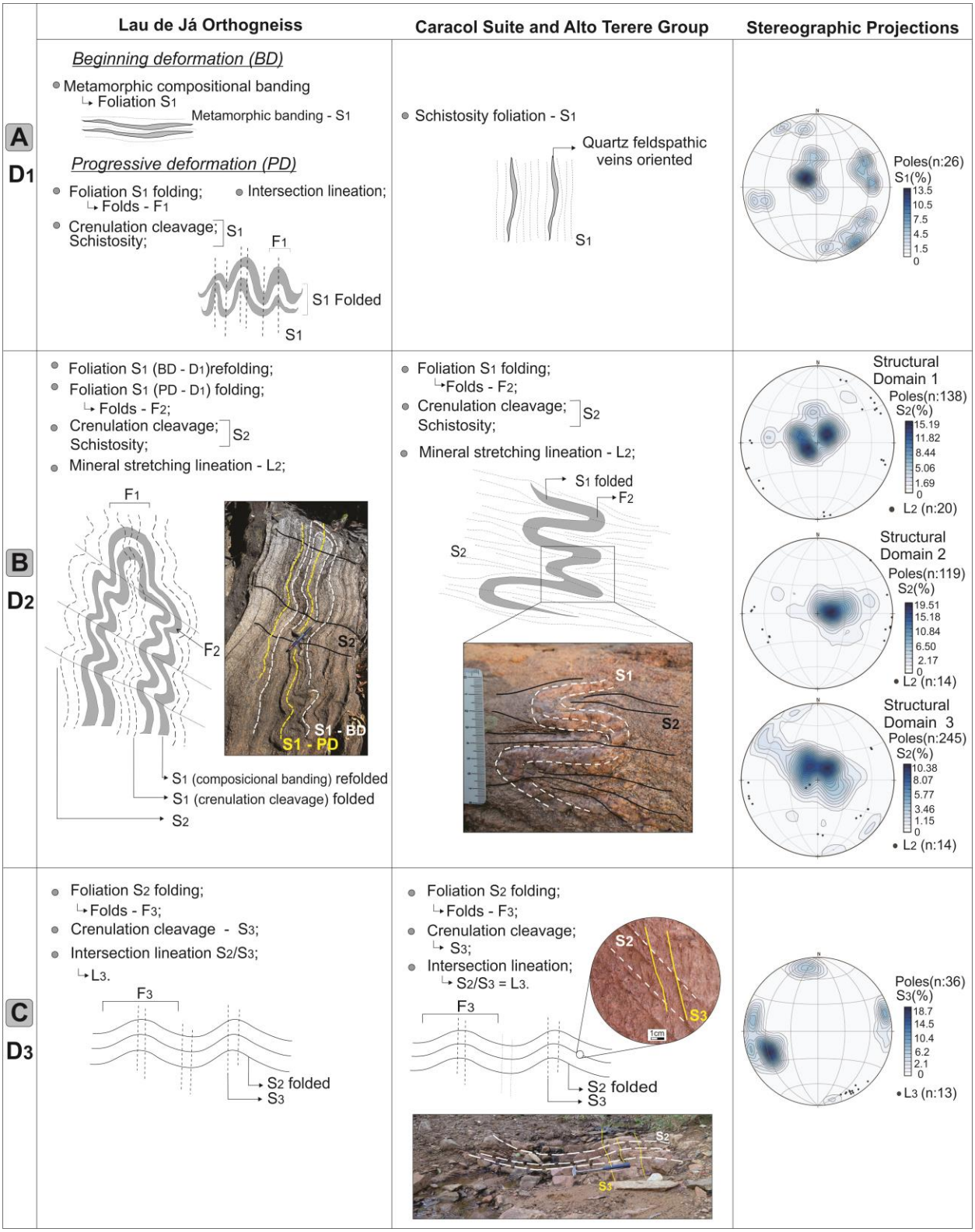

Figure 2.5. Summary of the deformation phases in the eastern terrane of the Rio Apa Block.

2.4.3. MICROTECTONICS

Kinematic structures and indicators for the first deformation phase are not observed microscopically because they were dominantly obliterated by subsequent events. The D_2 phase is recorded at a microscopic scale over the entire mapped area in gneissic, granite-gneiss and metasedimentary rocks. The deformation and metamorphism occurred gradually, and they were more intense in the vicinity of local and regional shear zones and more intense in structural domain 3.

The development mechanisms of the dominant intracrystalline deformation in the rocks of the eastern terrane are brittle to slightly plastic, low temperature, and mostly responsible for wavy extinction, twinning, and kinking as well as recrystallization by bulging. At higher temperatures, crystal-plastic deformation occurred, such as the recovery and dynamic recrystallization of quartz and feldspar crystals by subgrain rotation and boundary migration as well as the crystallization of oriented metamorphic minerals (biotite and muscovite). The terms used for the recrystallization in the text and figures (BLG: bulging; SGR: subgrain rotation; GBM: grain boundary migration) follow the descriptions of Passchier & Trouw (2005), who describe BLG as a low-temperature dynamic recrystallization mechanism with mobility at the grain boundary. A high-density grain can bulge into the boundary of a low-density grain and form new, independent small crystals. SGR is a continuous process of the former, and dislocations are continuously added to the subgrain boundaries. In this case, the angle between the crystalline lattices on both sides of the subgrain boundary increases gradually until the subgrain can no longer be classified as part of the same grain. GBM occurs at relatively high temperatures when the mobility of the grain boundaries increases to the point where the grain boundaries can sweep entire crystals while removing dislocations and possibly subgrain boundaries (Passchier & Trouw, 2005).

In the distal portions of the shear zones, the quartz crystals show wavy extinction (Figure 2.6A) and deformation lamellae in addition to BLG, in which tiny subgrains formed at the edges of older crystals (Figure 2.6B). Such intracrystalline structures are characteristic of low-grade temperatures between 300 and 400 °C (Passchier & Trouw 2005) and are abundant throughout the mapped extent of the eastern terrane, especially in the most common facies of the Caracol Suite (pink hololeucocratic granite-gneiss , pink biotite granite-gneiss , pink porphyritic granite-gneiss). At medium temperatures, between 400 and 500 ºC (Passchier & Trouw 2005), SGR also occurs

somewhat commonly and is usually associated with BLG. In this case, older crystals are flattened and stretched and are surrounded by a second generation of freshly formed crystals (subgrains rotated to become individual grains; Figure 2.6C).

Shear zones from the D_2 deformation phase are common at both regional and local outcrop scales. In areas sheared at high temperatures (between 500 and 700 °C; Passchier & Trouw 2005), GBM is observed in the quartz crystals, in which older grains are completely replaced by the recrystallized material, and is generally combined with SGR. In the Lau de Já orthogneiss rocks, GBM and SGR dominate, and the boundaries of irregular grains have lobed and ameboid shapes.

The deformation mechanisms of the feldspar and quartz crystals have a gradational behavior relative to their proximity to shear zones. Twinning in plagioclase grains as well as wavy extinction and concentric zoning in potassium feldspar characterize low to medium temperatures between 400 and 500 °C (Passchier & Trouw, 2005). At these temperatures, BLG recrystallization is also observed in potassium feldspar crystals (Fig. 2.6D) and, subordinately, plagioclase. The structures that were generated at medium temperatures, such as in the quartz crystals, are intracrystalline deformations that are more common in the rocks of the eastern terrane. At higher temperatures near 600 °C (Passchier & Trouw 2005), the SGR mechanisms occur along with BLG (Fig. 2.6 E, F). Perthitic intergrowths are observed in potassium feldspar crystals, and there are rare myrmekitic intergrowths in plagioclase crystals, especially at the boundaries with potassium feldspar crystals.

The biotite crystals appear as preferentially oriented plates between quartz grains (Figure 2.6G, H) at lower temperatures, some of which have wavy extinction. At temperatures above 250 °C (Passchier & Trouw, 2005), they begin to show plastic deformation with GBM at medium to high grade temperatures.

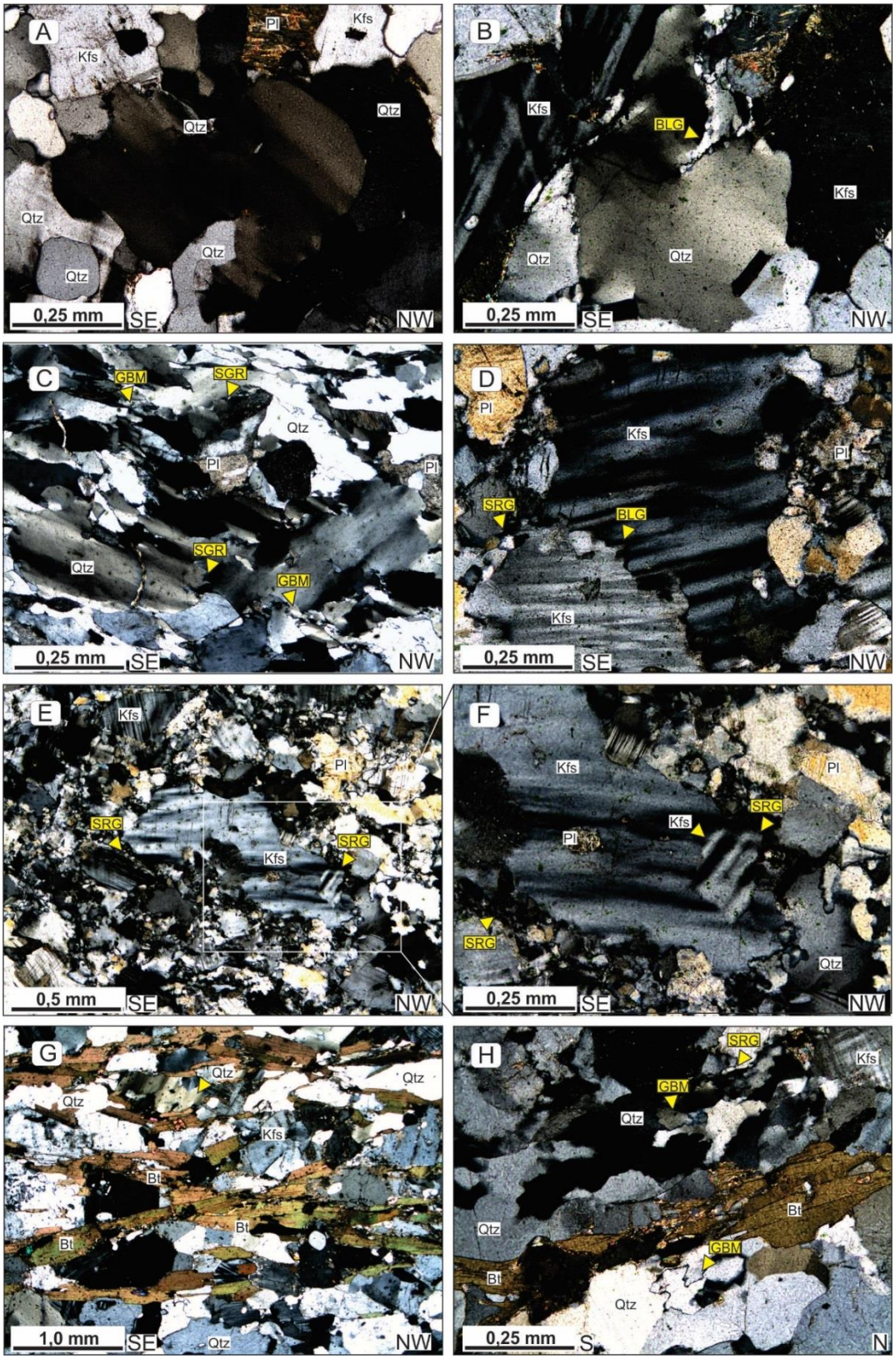

Figure 2.6. Mechanisms of intracrystalline deformation acting on the rock-forming minerals of the eastern terrane: (A) Caracol Suite, pink amphibolite granite-gneiss facies: quartz crystals with wavy extinction; (B) Caracol Suite, pink hololeucocratic granite-gneiss facies: quartz crystal with wavy extinction and BLG.

Cont. Figure 2.6. (C) Caracol Suite, pink porphyritic granite-gneiss facies: quartz crystals with wavy extinction, SGR and GBM; (D) Caracol Suite, pink hololeucocratic granite-gneiss facies: potassium feldspar crystals with concentric twinning, BLG and SGR; (E) Caracol Suite, pink hololeucocratic granite-gneiss facies: general view of potassium feldspar, quartz and plagioclase strongly recrystallized by the three mechanisms; (F) detail of the previous image with an emphasis on a potassium feldspar crystal with conical twinning and SGR throughout the edge of the older crystal; (G) Caracol Suite, pink biotite granite-gneiss facies: biotite lamellae oriented according to the preferential direction; (H) oriented biotite lamellae between SGR and GBM recrystallized quartz grains. Abbreviations: Qtz – quartz, Mc – microcline, Pl – plagioclase, Bt – biotite; BLG - bulging; SGR - subgrain rotation; GBM - grain boundary migration.

Quartz crystals, potassium feldspar and rare plagioclase occur as asymmetric kinematic indicators in S-C structures (Figure 2.7A, B) accompanied by pressure shadows (Figure 2.7C, D). These structures are mainly related to dynamic recrystallization mechanisms by means of BLG and SGR at medium to high temperatures and near shear zones. The biotite forms sigmoidal and/or folded structures in kink bands (Figure 2.7E). At high deformation rates in the mylonitic structures, muscovite forms sigmoidal kinematic indicators (Figure 2.7F). In both quartz and feldspar grains as well as in micas, the characteristic structures of the kinematic indicators follow the imposed deformation for each described domain consistent with the observations at larger scales.

The D_3 deformation phase formed a crenulation cleavage. The septa are weak and spaced with a parallel relationship and a discrete transition between the septa and microliths. The shortening of the S_3 foliation that generated the F_3 folds is microscopically highlighted by the subtly folded orientation of the biotite crystals as well as by the rupture and recrystallization of quartz and feldspar crystals, which were rotated in the form of microliths into discrete curvatures (Fig. 2.H). The crenulation cleavage appears in the hinge zones of the F_3 folds as an intercrystalline ductile-brittle mechanism.

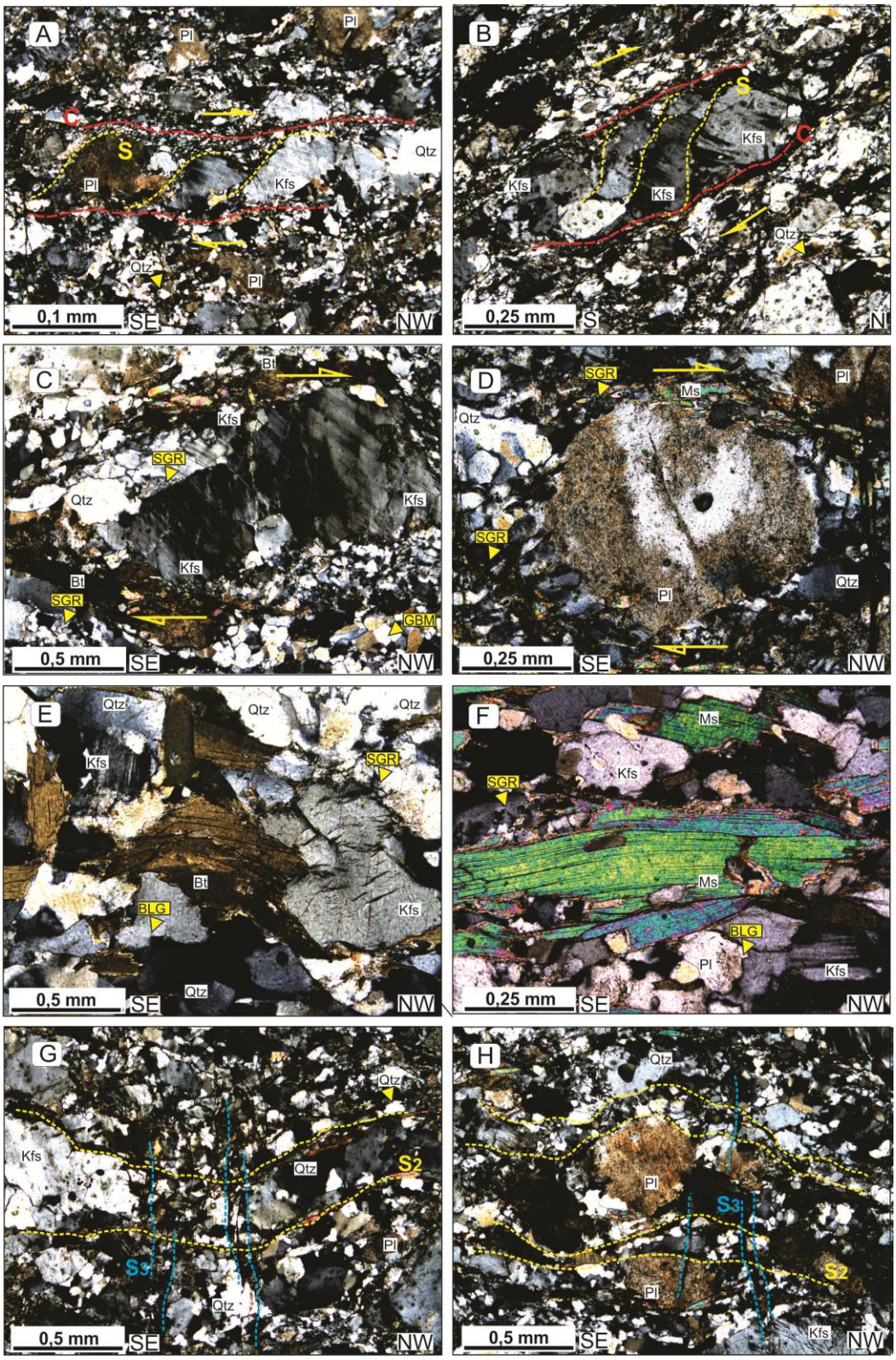

Figure 2.7. **Kinematic indicators:** (A and B) Caracol Suite, pink hololeucocratic granite-gneiss facies: potassium feldspar, plagioclase and quartz crystals forming sigmoids, S-C structures and pressure shadows in addition to recrystallization by the BLG, SGR and GBM mechanisms throughout the area shown.

Cont. Figure 2.7. (C) Caracol Suite, pink hololeucocratic granite-gneiss facies: sigmoidal potassium feldspar porphyroclast with pressure shadows generated by recrystallization; (D) rotated plagioclase grain with SGR and GBM recrystallization at the edges; (E) Caracol Suite, pink biotite granite-gneiss facies: crystals of folded biotite generating discrete kink bands between grains of potassium feldspar, quartz and subordinate plagioclase recrystallized by BLG and SGR; (F) Caracol Suite, shear zone rocks: muscovite crystals in subtle mica fish structures amid recrystallized minerals. **Microstructures representing the D_3 deformation phase:** (G and H) Caracol Suite, pink hololeucocratic granite-gneiss facies: folded S_2 foliation showing S_3 crenulation cleavage. Abbreviations: Qtz – quartz, Mc – microcline, Pl – plagioclase, Bt – biotite; BLG - bulging; SGR - subgrain rotation; GBM - grain boundary migration.

2.5. DISCUSSIONS

The mapping and structural analysis of the study area allowed the interpretation of structures such as foliations, lineations, folds, and mylonitic shear zones as well as their kinematic indicators.

The main schistosity (S_2) and subordinate crenulation cleavage is present in all of the rocks of the eastern terrane of the Rio Apa Block, and its main characteristics are NWW azimuths and low-angle dips. However, the orientation of this foliation varies, which led us to apply the concepts of progressive deformation and deformation partitioning suggested by Fossen et al. (in press). Open and smooth folding is observed in the S_2 foliation where new axial planes (S_3) are developed.

The S_1 foliation is observed in the basement (Lau de Já orthogneiss) as compositional banding and later as a result of progressive deformation in the folding of this banding, which formed F_1 folds. In the granite-gneisses of the Caracol Suite, S_1 is interpreted as crenulation cleavage and poorly preserved schistosity because of the strong transposition of the main foliation.

The correlation of the structures between the outcrops in all of the rocks is made possible by the dominance of the S_2 foliation. The subsequent foliation is also easily observed because it is the exposed crenulation cleavage on the axial surfaces of the F_3 folds, which are abundant in the area. Thus, it was possible to interpret it as well as S_2 and the lineations observed in both foliations. However, the previous foliation, S_1, which is classified as schistosity and crenulation cleavage in the orthogneisses of the basement and as schistosity in the other rocks (Caracol Suite and Alto Tererê Group), is not very evident in the outcrops in the area. In the basement rocks, this structure (S_2) is interpreted as the compositional banding and the axial plane surfaces of F_1 folds; in the granite-gneisses facies of the Caracol Suite, this is only possible when it is preserved in quartz-feldspar veins.

The traditional structural superposition criteria described by Ramsay (1967) were used to subdivide the proposed deformation phases. The structures described above were separated into three groups that were attributed to three contractional deformation phases, called D_1, D_2 and D_3, in addition to a shallow brittle extensional deformation event.

In addition to using the traditional criteria of Ramsay (1967) to identify these deformational phases, it was necessary to reassess the structural data obtained in the field and to re-examine our understanding of the deformational phases and progressive deformation topics.

Fossen et al. (in press) describe the term progressive deformation as a period of continuous deformation during which composite structures with significant variations in style and orientation may be formed. An analysis of the field data shows that the term progressive deformation is appropriate for the D_1 deformation phase. The metamorphic compositional banding identified in the basement, the Lau de Já orthogneiss, was interpreted as the initial phase of the D_1 deformation event.

Fossen et al. (in press) explain that regional deformation phases must be related to large tectonic events or at least to significant changes in tectonic conditions, such as the collision of a microcontinent or magmatic arc with a continental margin. According to the traditional method of interpreting deformation phases, the compositional banding in the basement appeared to be a single deformational phase. However, it was not possible to correlate this compositional foliation with an orogenic event that has been described in the literature. Because the Lau de Já orthogneiss is a newly described rock (Plens et al., subsmitted b) and is also limited to a small area, considering that no reliable kinematic indicators were found in these structures, we chose to interpret the compositional banding as the beginning of the deformation of the first deformational phase.

At some point after the compositional banding formed (not yet identified), progressive deformation occurred, which affected the gneissic rocks of the basement in addition to the granitic and gneisses rocks of the Caracol Suite. In the Lau de Já orthogneiss, folding of the metamorphic compositional banding generated F_1 folds and spaced crenulation cleavage (S_1) on the axial surfaces of the folds. Penetrative schistosity formed in the granite-gneiss facies of the Caracol Suite.

The subsequent deformation phase, D_2, is also broadly consistent with the term progressive deformation. Although the S_2 foliation strikes NW with near horizontal dip angles over the entire central to southern portions of the study area, this foliation has different orientations in two

locations in the eastern block. In the northern portion, the strikes measurements corroborate the morphology of large regional folds as well as steeper and vertical dip angles. These variations in the S_2 foliation orientation were also interpreted at the western end of the study area, where structures trend preferentially N-S.

Fossen et al. (in press) suggest the term deformation partitioning, and they highlight the importance of lithology and rheology during the structural evolution of a region. These authors state that the partitioning of deformation occurs as a result of geological variations controlled by the lithologic composition or thermal conditions of the region during the deformation.

We suggest that the eastern part of the Rio Apa Block is a sufficiently large area for a given deformation phase to occur with different intensities, either due to lithological compositions, the amount of thermal energy involved, or even stress heterogeneity. Therefore, we suggest that the D_2 deformational phase can be subdivided into three structural domains that are described from south to north as structural domains 1, 2 and 3.

Structural domain 1 is located in the central to southern portion of the study area and is represented by the previously reported low-angle foliation with transport to the NW (Lacerda Filho et al., 2006, 2016; Cordani et al., 2010). In this study, structural measurements with dominant SE-NW orientations and subhorizontalized dips were observed. Shear zones with low-angle dips are also observed.

Structures that are preferentially oriented N-S are interpreted in the extreme western part of the eastern terrane. In structural domain 2, the D_2 deformation phase shows a pole distribution with a concentration at approximately 150º to 220º and low-angle dips.

The third domain encompasses the northern portion of the study area, where SRTM, LANDSAT and Geocover images reveal more intense compressive deformation that is recorded in meaning regional folds. Foliations measurements collected in the field corroborate the preliminary investigations and indicate generally higher dip angles than in the southern portion of the study area. Numerous shear zones follow the pattern imposed by the deformation and expose kinematic indicators typical of high temperatures, which indicates more significant compressional deformation than in the rocks of the southern portion of the study area.

The kinematic indicators observed in all of the domains include S-C structures and stretched and rotated clasts with asymmetric tails, often with recrystallization of the minerals at

the edges of the crystals that form pressure shadows oriented according to the deformation in each structural domain.

At the eastern portion of the mapped area, where structural domain 2 is located, Faleiros et al. (2015), Remédio et al. (2015) and Lacerda Filho et al. (2016) identify a third terrane of the Rio Apa Block. Faleiros et al. (2015) call it the southeast terrane, and Lacerda Filho et al. (2016) call it the eastern terrane because they rename the eastern terrane of Cordani et al. (2010) as the central terrane (Figure 2.2). In this study, a possible local alteration in the foliation path is suggested, which shows a change in orientation from SE-NW to N-S in structural domain 2. The causes for this variation are unclear. However, although we cannot exclude the possibility of a third terrane that amalgamated with the Rio Apa Block, we chose to maintain the subdivision into two terranes.

The tectono-deformational D_2 event is possibly related to the metamorphism at approximately 1300 Ma that has been described in the literature with the methods Ar-Ar and K-Ar (Cordani et al., 2010; Ruiz et al., 2014; Faleiros et al., 2015; Lacerda Filho et al., 2016).

Faleiros et al. (2015) propose that ages between 1310 and 1270 Ma (Ar-Ar hornblende, muscovite and biotite; Cordani et al., 2010; and U–Pb, monazite, Lacerda Filho et al., 2015) are related to the collisional orogeny that joined the terranes of the Rio Apa Block. Plens et al. (submitted b), relate the average age of 1300 Ma to the juxtaposition of the eastern terrane over the western terrane by means of a NW-directed roof thrust, which caused low angle deformation to NW that is observed in all of the rocks in the Rio Apa Block, most prominently in structural domain 1 in the southern portion of the study area.

Cordani et al. (2010) also suggest that the regional heating related to the 1.3 Ga metamorphism reached temperatures between 350 and 400 °C, which are indicated by temperature blocking in the micas identified using the Ar-Ar method with crystals of hornblende, muscovite and biotite. Using temperature as an accessory deformation indicator, Faleiros et al. (2015) propose that the constituent rocks of the eastern terrane underwent a moderate temperature deformation phase (~500 °C) followed by a low temperature phase (300 - 400 °C) based on the analysis of quartz and feldspar microstructures.

The analysis of the intracrystalline structures performed in this study, which was based on observations of the main rock-forming minerals in the eastern terrane (feldspar and quartz), demonstrated that the dominant mechanisms show evidence of brittle to slightly plastic intracrystalline deformation that was generally responsible for recrystallization by bulging in

addition to wavy extinction, twinning and kinking. In quartz crystals, these structures are characteristic of low temperatures between 300 and 400 ºC, and potassium feldspar grains show intracrystalline deformations characteristic of temperatures between 400 and 500 °C (Passchier & Trouw, 2005).

However, SGR recrystallization mechanisms are not uncommon, and they are observed more often near shear zones. SGR occurs at temperatures between 400 and 500 °C in quartz crystals and at 600 °C and higher in feldspar grains. Even higher temperatures are responsible for GBM, which is common in shear zones.

The data suggest that during the D_3 deformation event, the prevailing temperature conditions were between 300 and 400 °C throughout the terrane and mainly in structural domains 1 and 2, where the deformation was less intense. In the northern part of the study area, and especially in regions of sheared rocks, which are often mylonitized and even schistose and where numerous shear zones are located, the temperatures may have been higher than 600 °C.

Fossen et al. (in press) argue that flow patterns can be complex around interconnected shear zones and areas of deformation partitioning; they further claim that high temperatures and partial melting can change the rheological properties of a region. We agree with the high temperatures indicated by the microscopic analyses because these temperatures are located in highly sheared areas.

Because the eastern and western terranes were juxtaposed during the second deformation phase, the subsequent phase, D_3, was the ductile-brittle compressional event that affected the entire Rio Apa Block. The structures interpreted at the meso- and micro-scales are F_3 folds, which resulted from shortening of the previous foliation, S_3, which is represented by crenulation cleavage associated with the folds and L_3 intersection lineations between the S_2 and S_3 foliations. The crenulation cleavage relative to this shortening has azimuths oriented to the NE with less pronounced dispersions toward the SE and SW. The dip angles are steep, in contrast to the lower S_2 dips. The mineral intersection lineation is not very apparent, and the azimuths are oriented to the SE with low dips. Figure 2.8 shows a diagram of the deformation structures that were generated and overlapped in each deformation phase as well as the affected rocks. The ductile-brittle deformational conditions indicate that the depths for the D_2 event have decreased since the subsequent deformation; consequently, the temperatures have also decreased. No ages have yet been attributed to the accompanying metamorphism of this deformation phase in the literature.

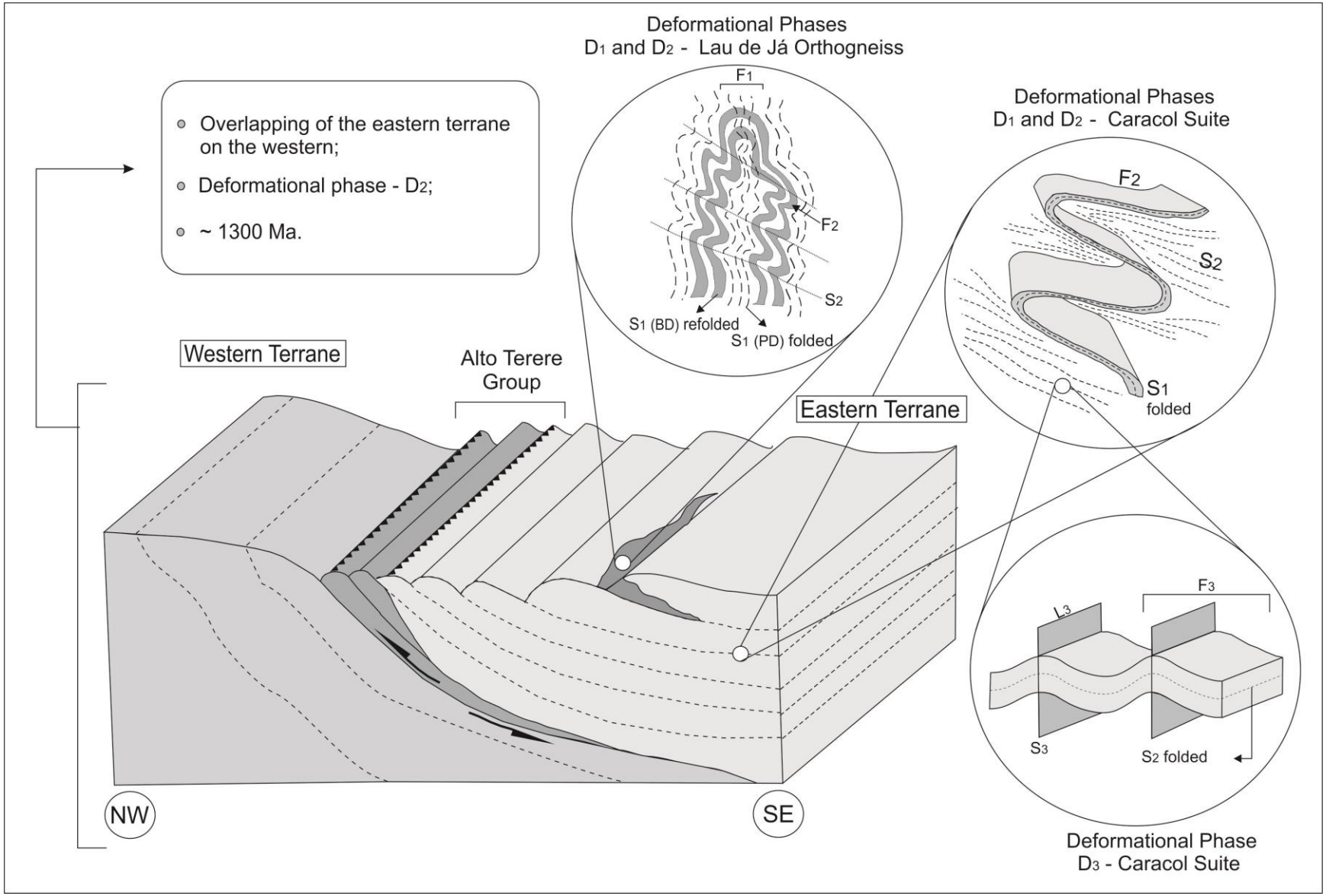

Figure 2.8. Schematic diagram illustrating the deformation structures generated by the overlapping phases of deformation in the eastern terrane.

As for the crystallization ages established for the eastern terrane present the following results which were obtained by the U-Pb zircon method (LA-ICP-MS): Lau de Já orthogneiss (1822 Ma); Caracol Suite (1783 to 1760 Ma) and Alto Tererê Group (1777 Ma; maximum sedimentation age). These data are consistent with those obtained by Cordani et al. (2010), Faleiros et al. (2015) and Lacerda Filho et al. (2016).

The rocks of the Chiquitania Complex in the Paraguá Terrane, located to the southwest of the Amazonian Craton, were dated to 1764 ± 12 Ma (U-Pb, SHRIMP, zircon; Boger et al., 2005), which may be temporally correlated with those studied herein.

Following the same conclusions, Redes et al. (2015, 2016) and Faleiros et al. (2015) correlate the rocks of the western portion of the Rio Apa Block (the Alumiador Intrusive Suite, age ~1.8 Ga, in the western terrane) with the granitic and gneissic rocks of the Correreca Granite in the region between Rincon del Tigre and Santo Corazon in eastern Bolivia. The Correreca Granite has crystallization ages of 1894 ± 13 Ma (U-Pb, SHRIMP, zircon; Vargas-Mattos, et al., 2010) and 1855 ± 5 Ma (Pb-Pb, evaporation, zircon; Redes et al., 2016).

The suggestion that the Rio Apa Block is an southern extension of the Amazonian Craton (Ruiz, 2005; Lacerda Filho et al., 2006, 2016; Cordani et al., 2010; Faleiros et al., 2015) is consistent with the division of the Amazonian Craton that was initially proposed by Almeida (1967).

Among the arguments presented by these authors, the following stand out: i) the existence of outcrops of the Alumiador Intrusive Suite throughout the western portion of the Rio Apa Block and also in the Corumbá and Santo Corazón regions of Bolivia, which demonstrates the extent of the Rio Apa Block; ii) occurrences of Proterozoic dikes and mafic sills of the Rio Perdido and Huncavaca Suites (1.1 Ga; U-Pb, SHRIMP, badeleite; Teixeira et al., 2016) are reported in eastern Bolivia, Mato Grosso and Mato Grosso do Sul; (iii) the Paraguay Belt extends from the Nova Xavantina region (Mato Grosso) to Serra do Bodoquena (Mato Grosso do Sul), where rocks from the Rio Apa block outcrop; iv) the Paraguay Fold Belt also limits the Paraguá, Jauru, and Rio Alegre terranes to the southwest of the Amazonian Craton as well as the Rio Apa Block to the south; v) the Tucavaca Aulacogen (Brasiliano) is based on the rocks of the Paraguá Terrane/Sunsás Belt and the Rio Apa Block (Corumbá and Santo Corazon); and (iv) under the interpreted conditions, the Amazonian Craton, including the southern portion of the Rio Apa Block, would

have behaved as a passive continental margin during the deposition of part of the Paraguay Fold Belt units along its length.

The Ar-Ar and K-Ar age of 1.3 Ga, which was mainly determined in micas (Cordani et al., 2010), is considered a regional cooling event that affected the entire Rio Apa Block and is temporally correlated with the San Ignácio Orogeny (Litherland et al., 1986; Bettencourt et al., 2010) in the Paraguá Terrane.

Other geotectonic correlations between the cratonic masses in South America have been proposed. Ramos & Vujovick (1993) assume that the Rio Apa Block belongs to the Rio de la Plata Craton, and Ramos et al. (2010) suggest that the Rio Apa Block is located in the Pampia Block, but these authors still refer to the Rio de la Plata Craton when they relate the Rio Apa Block to the plutonic and volcanic rocks of the Caapucú Block, southern Paraguay (Fúlfaro, 1996). Ramos et al. (2010) argue that a deep trough is located between the two blocks (Rio Apa and Caapucú) where gravimetric and magnetometric data define grabens with NNW- to NW-oriented normal faults, which as the same are those present in the Rio Apa Block.

Casquet et al. (2012) assume that an important continental mass, called the Mara Craton, was formed of the Rio Apa Block, the Maz Terrane, which is located west of the Sierras Pampeanas (Argentina), and the Arequipa Terrane (Peru), and that was attached to the Amazon Block at approximately 1.3 Ga.

Through gravity mapping, Dragone et al. (2017) suggest that the Rio Apa Block is larger than the area mapped by Cordani et al. (2010) and that it coverage part of the Pantanal basin as well as the southern boundary of the Sunsás Province (Tassinari & Macambira, 1999). Dragone et al. (2017) state that crustal growth may have occurred in two different tectonic configurations in which the Rio Apa Block had a thinner continental crust than the Amazonian Craton.

In view of the various arguments put forward, as well as the geochronological analyses obtained by the U-Pb method (LA-ICP MS on zircon) added to the isotopic data (Sm-Nd and Lu-Hf), to the petrographic analyses, presented in Plens et al. (submitted b), and also the field mapping established in the present work, leads us to conclude that the eastern terrain and, consequently, the Rio Apa Block as a whole is an extension to the south of the Amazonian Craton, as proposed by several authors in the recent literature (Ruiz, 2005; Lacerda Filho et al., 2006, 2016, Cordani et al., 2010, Faleiros et al., 2015). However, the eastern terrane of the Rio Apa Block is presented in this work as correlated with the Chiquitania Complex rocks in the Paraguá Terrane, southwest of the

Amazonian Craton, since the San Ignacio Orogeny that affected the southwestern portion of the Craton at about 1.3 Ga is also recorded as responsible of the juxtaposition of the eastern and western terranes.

2.6.CONCLUSIONS

The data collected during geological mapping, the observations from satellite images, and the macroscopic and microscopic analyses of the deformation mechanisms as well as an extensive review of the recent literature on the eastern terrane of the Rio Apa Block allow us to conclude that:

- Three main compressive deformational phases, D_1, D_2 and D_3, were identified in the study area;
- The first deformational phase included an initial period that was observed only in the basement rocks and that generated the gneissic compositional banding. Subsequently, through the progression of this deformational phase, this banding was folded, which exposed crenulation cleavages. The granite-gneisses were apparently affected by only the initial progressive deformation phase and show penetrative schistosity and crenulation cleavage;
- The subsequent phase, D_2, was more significant. In the gneissic lithotypes of the basement, S_2 is classified as a penetrative crenulation cleavage. In the granite-gneiss of the Caracol Suite, the S_2 foliation is considered to be a crenulation cleavage; however, S_2 is more often a continuous schistosity, which is evidenced mainly by the preferential orientation of the biotite crystals as well as minerals like feldspars and quartz. Schistosity is also observed in the the metasedimentary rocks of the Alto Tererê Group;
- The S_2 foliation generally has NW strikes and subhorizontal dip angles throughout the central-southern portion of the study area. However, the orientations vary in the northern and westernmost portions of the study area, which allows us to propose three structural domains that are described from south to north as structural domains 1, 2 and 3:
    - Structural domain 1: the central to southern portions of the study area with predominantly SE-NW orientations and subhorizontal dip angles;

  - Structural domain 2: the western end of the eastern terrane with structures that are preferentially oriented N-S;
  - Structural domain 3: the northern portion of the area with the most intense compressive deformation.
- The D_3 deformational event appears to have been ductile-brittle throughout the Rio Apa Block; the structures observed at meso- and microscales include the F_3 folds, S_3 crenulation cleavage and L_3 intersection lineation between the S_1 and S_2 foliations;
- The eastern terrane of the Rio Apa Block is presented in this work as correlated with the Chiquitania Complex in the Paraguá Terrane, southwest of the Amazonian Craton. The 1.3 Ga age taken as marking the justapoxition of the eastern terrain over the weastern terrain can be associated with the San Ignacio Orogeny which took place in the southwestern portion of the Amazonian Craton.

ACKNOWLEDGEMENTS

The authors acknowledge the Laboratory of Geochronology of the University of Brasilia, the Postgraduate Program in Geology of the University of Brasilia, the Grupo de Pesquisa em Evolução Crustal e Tectônica (Guaporé), the Comissão de Aperfeiçoamento de Pessoal do Nível Superior (Capes), the Fundação de Amparo à Pesquisa do Estado de Mato Grosso (FAPEMAT), and the Instituto Nacional de Ciências e Tecnologia de Geociências da Amazônia (GEOCIAM) for the support during the development of this research.

REFERENCES

Almeida, F.F.M., 1965. Geologia da Serra da Bodoquena (Mato Grosso), Brasil. Boletim de Geologia e Mineralogia, Departamento Nacional de Produção Mineral-DNPM, Rio de Janeiro. 219, 1-96.

Almeida, F. F. M., 1967. Origem e evolução da plataforma brasileira Rio de Janeiro, Boletim da Divisão de Geologia e Mineralogia. Boletim 241, 01-36.

Araújo, H.J.T., Montalvão, P.E.N., 1980. Geologia da Folha SF.21 e parte das Folhas SF.21-V-D e SF.21-X-C, sudoeste do Estado de Mato Grosso do Sul: operação 578/80 - DIGEO. Projeto Radam Brasil, Relatório Interno, Goiânia, 15 p.

Bettencourt, J. S., Leite Jr., W. B., Ruiz, A. S., Matos, R., Payolla, B. L., Tosdal, R. M., 2010. The Rondonian-San Ignacio Province in the SW Amazonian Craton: An Overview. Jounal of South American Earth Sciences, 29: 28-46.

Boger S.D., Raetz M., Giles D., Etchart E., Fanning C.M. 2005. U-Pb Age data from the Sunsas Region of eastern Bolivia, evidence for the allochthonous origin of the Paragua Block. *Precambrian Research*, **139**:121-146.

Brittes, A.F.N., Sousa M.Z.A., Ruiz A.S., Batata E.F., Lafon J.M., Plens D.P., 2013. Geology, petrology and geochronology (Pb-Pb) of the Serra da Bocaina Formation: evidence of an Orosirian Amoguijá Magmatic Arc in the Rio Apa Terrane, south of the Amazonian Craton. Brazilian Journal of Geology, 43(1): 48-69.

Brittes, A.F.N., Sousa M.Z.A., Ruiz A.S., Batata E.F., Lafon J.M., (em prep..). Petrologia e Geocronologia (U-Pb/SHRIMP e Sm-Nd) Da Formação Serra Da Bocaina: Implicações Sobre A Evolução Do Arco Magmático Amoguijá No Bloco Rio Apa – Sul Do Craton Amazônico

Casquet, C., Rapela, C.W., Pankhurst, R.J., Baldo, E.G, Galindo C., Fanning C.M., Dahlquist, J.A. Saavedra, J. 2012. A history of Proterozoic terranes in southern South America: From Rodinia to Gondwana. Geoscience Frontiers, 3(2):137- 145 p.

Cordani, U, G., Teixeira, W., Tassinari, C. C. G., Ruiz, A. S., 2010. The Rio Apa Craton in Mato Grosso do Sul (Brazil) and Northern Paraguay: geochronological evolution, correlations and tectonic implications for Rodinia and Gondwana. American Journal of Science, 310, 1-43.

Corrêa, J.A., Corrêa Filho, F.C.L., Scislewski, G., Cavallon, L.A., Cerqueira, N.L.S., Nogueira, V.L., 1976. Projeto Bodoquena - Relatório Final, MME/DNPM, Convênio DNPM/CPRM, Superintendência Regional de Goiânia.

Faleiros, F. M., Pavan, M., Remédio, M., Rodrigues, J.B., Almeida, V.V., Caltabeloti,V.V., Caltabeloti, F.P., Pinto, L., Oliveira, A. A., Pinto de Azevedo, E. J., Costa,V.S., 2015. Zircon U-Pb ages of rocks from the Rio Apa Crátonic Terrene (Mato Grosso do Sul, Brazil): New insights for its connection with the Amazonian Craton in pre-Gondwana times. Gondwana Research, 34: 187 – 204.

Fossen H. 2012. *Geologia Estrutural*. Trad. de Fabio R.D. de Andrade. São Paulo: Oficina de Texto, 584 p.

Fossen, H., Cavalcante, G. C. G., Pinheiro, R. V. L., Archanjo, C. J.,. Deformation Progressive or multiphase? - Journal of Structural Geology.

Fúlfaro, V.J., 1996. Geology of Eastern Paraguay. In: Comin-Chiaramonti, P., Gómes C.B., (Eds.) Alkaline Magmatism in Central and Eastern Paraguay: Relationship with Coeval Magmatism in Brazil. Fapesp, 17–29, Sao Paulo.

Godoi, H.O., Martins, E.G., Mello, C.R., Scislewski, G., 1999. Geologia MME/SG. Projeto Radam Brasil. Programa Levantamentos Geológicos Básicos do Brasil. Folhas Corumbá (SE. 21-Y-D), Aldeia Tomázia, (SF. 21-V-B) e Porto Murtinho (SF. 21-V-D), Mato Grosso do Sul, escala 1: 250.000.

Lacerda Filho, J.V., Brito, R.S.C., Silva, M.G., Oliveira, C.C. De., Moreton, L.C., Martins, E.G., Lopes, R.C., Lima, T.M., Larizzatti, J.H., Valente, C.R., 2006. Geologia e Recursos Minerais do Estado de Mato Grosso do Sul. Programa integração, atualização e difusão de dados de geologia do Brasil. Convênio CPRM/SICME - MS, MME. 10 - 28.

Lacerda Filho, J. V. 2015. Bloco Rio Apa: Origem e evolução tectônica. Tese de Doutorado, Instituto de Geologia. Universidade de Brasília, 181 p.

Lacerda Filho, J.V., Fuck, R. A., Ruiz, A. S., Dantas, E. L., Scandolara, J. E., Rodrigues, J. B., Nascimento, N. D. C., 2016. Palaeoproterozoic tectonic evolution of the Alto Tererê Group, southernmost Amazonian Craton, based on field mapping, zircon dating and rock geochemistry. Journal of South American Earth Science. 65, 122 – 141.

Lima, G. A., Macambira, M. J. B., Sousa, M. Z. A., Ruiz, A. S., submetido. Suíte Intrusiva Rio Perdido: magmatismo intraplaca no sul do Cráton Amazônico – Terreno Rio Apa. Revista de Geologia da USP – Série Científica.

Litherland, M., Annells, R.N., Appleton, J.D., Berrangé, J.P., Bloomfield, K., Burton, C.C.J., Darbyshire, D.P.F., Fletcher, C.J.N., Hawkins, M.P., Klinck, B.A., Lanos, A., Mithcell, W.I., O Connor, E.A., Pitfield, P.E.J., Power, G. E Webb, B.C. 1986. The Geology and Mineral Resources of the Bolivian Precambrian Shield. British Geological Survey. Overseas Memoir 9. London, Her Majesty's Stationery Office. 140 p.

Paschier C.W., Trouw R.A.J. 2005. *Microtectonics*. (2 Ed). Berlin: Springer, 353 p.

Pavan, M., Faleiros, F.M., 2014. Geologia da borda W do Terreno Rio Apa, SE do Craton Amazônico, SW do Mato Grosso do Sul. In: Anais do 47° Congresso Brasileiro de Geologia, Salvador, p. 1668.

Plens, D.P., Ruiz, A.S., Sousa, M.Z.A., Batata, E.F., Lafon, J.M., Brittes, A.F.N., 2013. Cerro Porã Batholith: post-orogenic A-type granite from the Amoguijá Magmatic Arc – Rio Apa Terrane – South of the Amazonian Craton. Brazilian Journal of Geology, 43 (3): 515-534.

Plens, D.P., Pimentel, M. M., Ruiz, A.S., Fuck, R. A., Sousa, M. Z. A., Nascimento, N. D. C. Geology and geochronology (U-Pb, Sm-Nd And Lu-Hf) of the Caracol Suite and country rocks: implications to evolution magmatic and tectonics of Rio Apa Block - south of Amazonian Craton. Journal of South American Earth Science – Submitted b.

Ramos, V. A; Vujovick, G I. 1993. Alternativas de la evolución del borde occidental de America del Sur durante el Proterozoico. Revista Brasileira de Geociências, 23(3): 94-200.

Ramos, V.A., Vujovich, G., Martino, R., Otamendi, J. 2010. Pampia: a large Cratonic block missing in the Rodinia supercontinent. Journal of Geodynamics, 50, 243-255.

Ramsay J.G. 1967. Folding and Fracturing of Rocks. New York, McGrawHill.

Redes, L. A., Sousa, M. Z. A., Ruiz, A. S., Lafon, J. M., 2015. Petrogeneses and U-Pb and Sm-Nd geochronology of the Taquaral granite: record of an Orosirian continental magmatic arc in the region of Corumbá – MS. Brazilian Journal of Geology. 45(3), 431 – 451.

Redes, L. A., Pimentel, M. M., Ruiz, A. S., Matos, G. R. S., 2016. Granito Correreca - um registro magmático orosiriano no oriente boliviano: implicações tectônicas e estratigráficas. In: Anais do 48 Congresso Brasileiro de Geologia – Porto Alegre – Brazil.

Remédio, M.J., Costa, V.S., Almeida, V.V., Pinto-Azevedo, E.J.H.C.B., Ferrari, V.C., Brumatti, M., Pinto, L.G.R., Caltabeloti, F.P., Faleiros, F.M., 2013. Programa Geologia do Brasil –

PGB. Fazenda Margarida. Folha SF.21-X-C-IV. Estado de Mato Grosso do Sul. Carta Geológica. São Paulo: CPRM, 2013, 1 mapa colorido, 95 x 70 cm. Escala 1:100.000.

Ruiz, A. S., 2005. Evolução geológica do sudoeste do Cráton Amazônico região limítrofe Brasil-Bolívia – Mato Grosso. Tese de Doutorado, Instituto de Geociências e Ciências Exatas, Universidade Estadual Paulista, 14-245p.

Ruiz, A. S., Sousa, M. Z. A., Lima, G. A., D'agrella Filho, M. S. (2014). Ar-Ar step heating ages for milonitic low angle shear zones rocks in the Rio Apa Terrane, South of the Amazonian Craton. *9th South American Symposium on Isotope Geology*. São Paulo: CPGEO.

Santos, J. O. S., Hartmann, L. A., Gaudette, H. E., Groves, D. I., Mcnaughton, N. J., Fletcher, I. R., 2000. A new understanding of the Amazon Craton Provinces based on integration of field mapping and U-Pb and Sm-Nd Geochronology Gondwana Research, 3, 453-488.

Santos, J.O.S., Rizzotto, G.J., Potter, P.E., Mcnaughton, N.J., Matos, R.S., Hartmann, L.A., Chemale Jr, F. & Quadros, M.E.S., 2008. Age and Autochthonous Evolution of The Sunsás Orogen in the West Amazon Craton based on mapping and U-Pb Greochronology. Precambrian Research, 165, 120-152.

Schobbenhaus, C. & Neves B. B. B., 2003. A Geologia do Brasil no Contexto da Plataforma Sul-Americana. In: Brasil L. A. Bizzi, C. Schobbenhaus, R. M. Vidotti e J. H. Gonçalves (eds.) Geologia, Tectônica e Recursos Minerais do CPRM, Brasília, 2003. 64 p.

Tassinari, C.C.G., & Macambira, M.J.B., 1999. Geochronological provinces of the Amazonian Craton. Episodes. 38, 174-182.

Tassinari, C.C.G., Bettencourt, J.S., Geraldes, M.C., Macambira, M.J.B. & Lafon, J.M., 2000. The Amazonian Craton. In: Cordani, U.G., Milani, E.J., Thomaz-Filho, A. & Campos, D.A. (eds.). Tectonic Evolution Of South America, Rio de Janeiro. p. 41- 95.

Tassinari, C.G.C., Macambira, M.J.B., 2004. A Evolução Tectônica do Cráton Amazônico. In: Neto-Mantesso, V., Bartorelli, A, Carneiro, C. D. R., Brito-Neves, B.B. (eds). Geologia do Continente Sul-Americano: Evolução da Obra de Fernando Flávio Marques de Almeida. p. 471-486.

Teixeira, W., Hamilton, M. A., Girardi, V. A. V., Faleiros, F. M., 2016. Key dolerite dyke swarms of Amazonia: U-Pb constraints on supercontinent cycles and geodynamic connections with global LIP events through time. *Acta Geologica Sinica (English Edition)*, 90 (supp. 1), 84-85, DOI: 10.1111/1755-6724.12902.

Vargas-Mattos G.L. 2010. Caracterização geocronológica e geoquímica dos granitos proterozoicos: implicação para a evolução crustal da borda SW do Cráton Amazônico na Bolívia. Faculdade de Geologia, Universidade do Estado do Rio de Janeiro, Tese de Doutoramento, 164 p

Wiens, F.M.S. 1986. Zur lithostratigraphischen, petrographischen und strukturellen Entwicklung des Rio-Apa Hochlandes, Nordost Paraguay: Clausthal, Geologisches Institut der Technischen Universitat Clausthal, Clausthaler Geowissenschaftliche, Ph. D. dissertation, 19, 280 p.

Capítulo 3

GEOLOGY AND GEOCHRONOLOGY (U-Pb, Sm-Nd and Lu-Hf) OF THE CARACOL SUITE AND COUNTRY ROCKS: IMPLICATIONS OF MAGMATIC EVOLUTION AND TECTONICS IN THE RIO APA BLOCK - SOUTH AMAZONIAN CRATON

Dalila Pexe Plens
Márcio Martins Pimentel
Amarildo Salina Ruiz
Reinhardt A. Fuck
Maria Zélia Aguiar de Sousa
Newton Diego Couto do Nascimento

Submetido: *Journal of South American Earth Sciences*
21-Jun-2018

Dear Mrs. Plens,

Thank you for submitting your manuscript for consideration for publication in Journal of South American Earth Sciences. Your submission was received in good order.

To track the status of your manuscript, please log into EVISE® at: http://www.evise.com/evise/faces/pages/navigation/NavController.jspx?JRNL_ACR=SAMES and locate your submission under the header 'My Submissions with Journal' on your 'My Author Tasks' view.

Thank you for submitting your work to this journal.

Kind regards,

Journal of South American Earth Sciences

3. GEOLOGY AND GEOCHRONOLOGY (U-Pb, Sm-Nd and Lu-Hf) OF THE CARACOL SUITE AND COUNTRY ROCKS: IMPLICATIONS OF MAGMATIC EVOLUTION AND TECTONICS IN THE RIO APA BLOCK - SOUTH AMAZONIAN CRATON

Dalila Pexe Plens[1,4,5*], Márcio Martins Pimentel[1,2], Amarildo Salina Ruiz[3,5], Reinhadt A. Fuck[1, 2], Maria Zélia Aguiar de Sousa[3,5], Newton Diego Couto do Nascimento[4,5].

[1]Postgraduate Program in Geology/UNB; [2]Geochronology Laboratory/UNB; [3]Faculty of Geology/UFMT; [4]Engineering Institute/Mining Engineering Course; [5]Research Group on Crustal and Tectonic Evolution; *Corresponding author: dalilaplens@ufmt.br

ABSTRACT

The Rio Apa Block, exposed in southwest Mato Grosso do Sul (it is locatedin the south of the central-west region of Brazil) and in north of Paraguay, is divided into two tectonic terranes with different characteristics: western and eastern. New field, petrographic, gechronologic and isotopic data for rocks of the eastern portion of the Rio Apa Block are discussed in the present work. The studied area covers almost all of the eastern terrane and is represented by the Lau de Já orthogneiss, as well as by granite-gneisses rocks of the Caracol Suite, and by volcano-sedimentary rocks of the Alto Tererê Group. The basement presents the oldest age in the area (1822±6 Ma, LA-ICPMS U-Pb age) and a positive ε_{Nd} value of 0.69, suggesting some old crust participation in its generation, with model age Sm-Nd T_{DM} of 2.03 Ga. The Caracol Suite includes high-K calc-alkaline plutonic rocks represented by the following facies: (i) pink hololeucocratic granite-gneiss, (ii) pink biotite granite-gneiss, (iii) pink porphyritic granite-gneiss, (iv) pink amphibole granite-gneiss, (v) gray amphibole biotite granite-gneiss, (vi) gray amphibole tonalite. The suite presents crystallization ages between 1776±13 and 1748±19 Ma (LA-ICPMS U-Pb data). The ε_{Nd} values are positive to slightly negative, varying from 3.25 to -1.75 while ε_{Hf} values are negative to positive ranging from -4.64 to 5.32, which reflect assimilation of older crust by the parental magma. The model ages T_{DM} Lu-Hf is between 1.92 and 2.30 Ga, and Sm-Nd is 1.82 to 2.25 Ga. The Alto Tererê Group, exposed in the studied area, is represented by silimanite-quartz schist, with maximum sedimentation age of ca. 1777 Ma. Positive ε_{Nd} values of 1.03 and 2.00 are presented for these metasedimentary rocks,

which suggests no participation of older crust by the parental mantle magma. It shows model ages T_{DM} Sm-Nd of 1.90 to 2.01 Ga, consistent with the eastern terrane rocks. Tentatively, it is suggested that the rocks investigated here may be correlated with the granites and gneisses of the Chiquitania Complex, in the southwestern Amazonian Craton.

Keywords: Rio Apa Block, eastern terrane, Caracol Suite, geochronology.

3.1. INTRODUCTION

The Rio Apa Block is located in southwestern Mato Grosso do Sul, and extends towards Paraguay. It comprises a set of lithostratigraphic units that include infra- and supracustral segments. Their tectonic evolution took place largely during the Orosirian and Statherian, and is therefore an important part of the accretion of the Rodinia Supercontinent.

The model proposed by Almeida (1965), Ruiz (2005) and Cordani et al. (2010), based on geological/geochronological data, considers the Rio Apa Block as an integral part of the Amazonian Craton. Cordani et al. (2010) divided the Rio Apa Block into two different tectonic terranes: the western and eastern, a model which has been debated in the Brazilian scientific community.

The rock units investigated here are located in the eastern portion of the Rio Apa Block, represented by the Lau de Já orthogneiss, the Caracol Suite, that is composed of granite-gneisses and the metavolcanic-sedimentary sequence of the Alto Tererê Group. A small volume of volcanic rocks of dacitic composition was described in the eastern portion of the area.

The basement rocks were recognized for the first time in this work, as well as the volcanic previous cited. This suite, named by Cordani et al. (2010) as the Caracol Gneiss, is composed of orthogneisses, slightly to moderately foliated, gray to pink, medium- to coarse-grained, granoblastic, with crystallization ages of 1721±25 Ma (U-Pb, SHRIMP, zircon; Cordani et al., 2010). The Alto Tererê Group is represented by a Paleoproterozoic metavolcanic-sedimentary sequence, folded and metamorphosed under amphibolite facies conditions (Godoi et al., 1999; Lacerda Filho et al., 2006, 2016; Godoy et al., 2009).

Although recent petrogenetic and geochronological studies provided new information about the crustal evolution of the Rio Apa Block (Cordani et al., 2010; Brittes et al., 2013; Plens et al., 2013; Redes et al., 2015; Faleiros et al., 2015; Lacerda Filho et al., 2016), there are still

important issues related to the chronology of magmatic events in the eastern part of the Rio Apa Block. The main objective of this work is to describe the petrographic features of the Caracol Suite, and to attempt to understand the chronology of the magmatic events that generated the suite and its country rocks on the basis of zircon U-Pb dating. Investigation of crustal accretion episodes and crustal reworking processes using Lu-Hf isotopic methods in zircon and whole-rock Sm-Nd method is also presented.

3.2. METHODS

3.2.1. GEOLOGICAL MAPPING

The geological mapping was preceded by interpretation of remote sensor images LANDSAT and Geocover, SRTM images (Shuttle Radar Topography Mission), besides aerogeophysical sensor images (Ternary images and Analytic Signal 3D), as well as integration of geological data previously obtained (Lacerda Filho et al., 2006, 2016; Cordani et al., 2010; Brittes et al., 2013; Plens et al., 2013; Ruiz et al., 2014; Redes et al., 2015; Faleiros et al., 2015; Lacerda Filho, 2015). Field survey was carried out in several stages. The first stage was performed in the recognition scale of 1:250.000 for sampling, structural data collection, and identification of the main lithological units. Key areas were then selected from regional field survey for a detailed scale study (1:10.000) whose aim was to clarify geological relationships, and to establish the chronology and tectonic significance of structures.

Samples were selected for petrographic studies carried out in the labs of the University of Brasilia and Federal University of Mato Grosso. The definition of different types of ficies in the granite-gneissic rocks of the Caracol Suite was determined based on the essential geological mapping that, besides being the key to the possible delimitation of the outlying lithologies, characterizes them with the structural behavior. From microscopic analyzes specific structural, structural and mineralogical characteristics were identified, together with the quantification of minerals by visual estimation. The description and interpretation of the facies, as well as, the classification and denomination of then were based on Ulbrich et al. (2001).

Considering the most representative samples, their distribution in the study area, textural and mineralogical diversity, selected samples were forwarded to isotopic and geochronological

analyses by zircon U-Pb and Lu-Hf methods using LA-ICP-MS as well as whole-rock Sm-Nd analyses.

3.2.2. GEOCHRONOLOGY AND ISOTOPE GEOLOGY

Zircon crystals were used for U-Pb and Lu-Hf analyses by LA-ICPMS, in agreement with the systematics of Bühn et al. (2009) and Matteini et al. (2010), respectively. Sample preparation was carried out according to the conventional procedure with gravimetric and magnetic techniques in the Geochronology Laboratory of the University of Brasília. After separation, the zircon crystals were selected, cast in epoxy resin, and polished. This was followed by cleaning with dilute HNO_3 (2%). To investigate the internal structure of crystals and obtain the best location for the spot, backscattered electron images were recorded.

The LA-ICPMS analyses were performed at the Geochronology Laboratory of the University of Brasilia using a Neptune coupled to a Nd-YAG (λ = 213nm) Laser Ablation System. A mixture of helium and argon was used to carry the ablated material into the equipment. Two international standards were used (GJ-1 and 91500). The GJ-1 standard (Jackson et al., 2004) was used as a correction factor every seven analyses, including one laboratory blank and one standard. The 91500 standard (Wiedenbeck et al., 1995) is analysed at the beginning and at the end of each sequence, as well as every two cycles of the previous pattern.

For the isotopic analyses of Hf, zircon crystals previously analysed by the U-Pb method were used, and grains which usually showed ± 5% concordance were selected. Spots for Hf analysis were located next to that of U-Pb analysis. Before initiating laser ablation analyses, the spectrometer was calibrated with standard solution JMC 475 (Yb/Hf=0.02 and Lu/Hf=0.02) at the beginning of each analytical session. During the analyses, GJ-1 standard was also applied to monitor the values of $^{176}Hf/^{177}Hf$. The T_{DM} values were calculated using the continental crust comparison, according to Bouvier et al. (2008).

The raw data of U-Pb and Hf were worked out and reduced in the ISOPLOT version 3.0 program (Ludwig, 2003) and the presented errors are of 1σ for the systemmatic analyses and of 2σ for the isotopic analyses, both represented in percentage.

Sm-Nd isotopic analyses were also performed at the Geochronology Laboratory of the University of Brasilia according to the method described by Gioia and Pimentel (2000).

Approximately 50 mg of powdered sample was mixed with ^{149}Sm-^{150}Nd spike and dissolved in Savillex® capsules in HF, HNO3 and HCl. The contents of Sm and Nd are extracted into cation exchange columns, made in Teflon and deposited on double rhenium filaments. Nd and Sm analyses were carried out on a multi-collector Finnigan MAT 262 mass spectrometer in static mode. The uncertainties for the Sm/Nd and $^{143}Nd/^{144}Nd$ ratios are usually less than ± 0.5% (2σ) and ± 0.005% (2σ), respectively, based on repeated analyses of the international BHVO-1 and BCR-1 standards. $^{143}Nd/^{144}Nd$ ratios were normalized using the $^{146}Nd/^{144}Nd$ ratio of 0.7219. T_{DM} values were calculated using the model of De Paolo (1981).

3.3. REGIONAL GEOLOGY

The Amazonian Craton consists of several Archean and Proterozoic geochronological provinces which are progressively younger from east to west (Tassinari & Macambira, 1999, 2004; Tassinari et al., 2000): Maroni-Itacaíunas, Ventuari-Tapajós, Rio Negro- Juruena, Rondoniana-San Ignacio and Sunsás, located around an Archean nucleus, the Central Amazonian Province.

In recent models (Ruiz, 2005; Lacerda Filho et al., 2006, 2016; Cordani et al., 2010), the Rio Apa Block is considered the southern most extension of the Amazonian Craton (Fig. 3.1). One of the evidences that these authors use to suggest this hypothesis is that both the Cuiabá Group and the other units of the Paraguay Belt extend bordering the eastern region of Mato Grosso and southern portions of Mato Grosso do Sul, in the region of Serra do Bodoquena, and in northern Paraguay. An extensive carbonate sequence covers the southwestern part of the Amazonian Craton, the Tucavaca rift, and the Rio Apa Block. This suggests that the Amazonian Craton, including the Rio Apa Block, behaved as a passive continental margin during the deposition of part of the Paraguay Belt. In the figure 3.1, the Rio Apa Block is represented with the color of San Ignacio Province, since the last orogeny (San Ignácio Orogeny) of the province is proposed as correlated to the deformation of the same age in the Rio Apa Block.

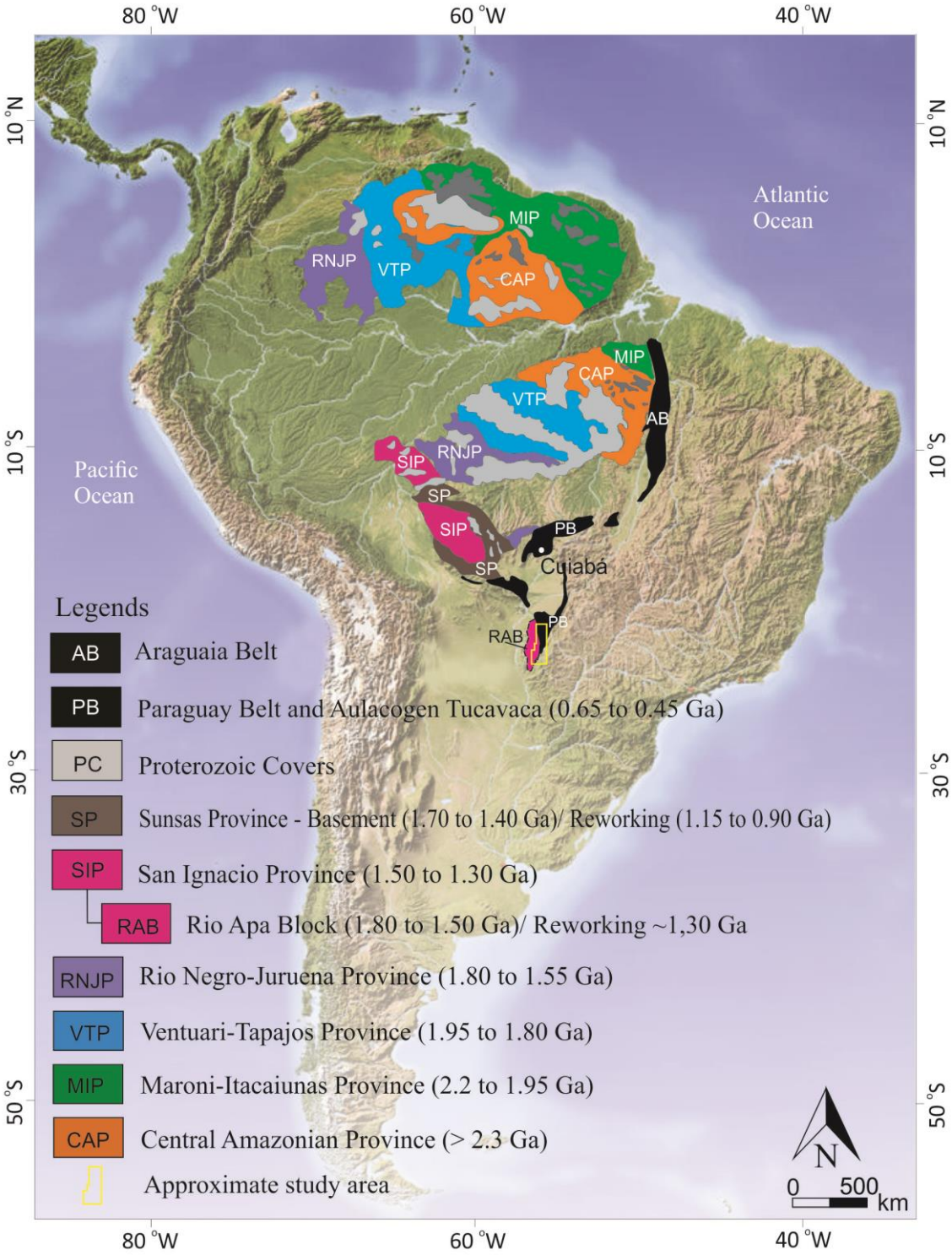

Figure 3.1. Geochronological and tectonic compartmentalization of the Amazonian Craton, considering the Rio Apa Block as an integral part in sthe south. Extracted and modified from Tassinari & Macambira (1999) and Ruiz (2005).

Other ideas are put forward in this regard: Ramos & Vujovick (1993) admit that the Rio Apa Block represents the northwestern portion of the Rio de la Plata Craton; Ramos et al. (2010)

suggest that the Rio Apa Block is located in the eastern portion of the Pampia Craton bordering the northwest of the Paranapanema Block; Casquet et al. (2012) advocate that the Rio Apa Block should constitute the eastern portion of the Mara Craton; based on gravity maps, Dragone et al. (2017) suggest that the Rio Apa Block can cover a wider region than that mapped by Cordani et al. (2010), separate of Amazonian Craton.

Regard of geotectonic subdivision of the Rio Apa Block, four main models are proposed (Lacerda Filho et al., 2006; Cordani et al., 2010; Faleiros et al., 2015; Lacerda Filho; 2015).

Lacerda Filho et al. (2006) subdivided the Rio Apa Block into three distinct geotectonic compartments: i) Remnants of Oceanic Crust, of Rhyacian age, represented by the Alto Tererê Metamorphic Complex; ii) Rio Apa Magmatic Arc, of Orosirian age, equivalent to the gneisses of the Rio Apa Complex; and iii) the Amoguijá Magmatic Arc, including mafic intrusions and dikes of Statherian or Tonian age. The area investigated in the present study is located within the Rio Apa Magmatic Arc.

Considering the distribution of Sm-Nd model ages, Cordani et al. (2010) proposed the existence of two different tectonic terranes in the Rio Apa Block (western and eastern), with distinct evolutionary histories, limited by a N-S suture zone (Fig. 3.2). Describing the eastern terrane, these authors abandon the term Rio Apa Complex and point out to the presence of the Caracol Gneiss and Morraria Complex, as well as of metasedimentary rocks of the Alto Tererê Group and of granites and gneisses of the Paso Bravo Province in Paraguay (Wiens , 1986). The geochronological data provided by zircon U-Pb dating (SHRIMP) indicate an age of 1721 ± 25 Ma, which is interpreted as crystallization of the Caracol Gneiss (Cordani et al., 2010).

In addition to the western and eastern terranes proposed by Cordani et al. (2010), Faleiros et al. (2015) individualized a third terrane in the southeast (Fig. 3.2). According to the authors, the terrane is limited by shear zones and its magmatic evolution took place through successive accretion events, which reflect are extremely mobile tectonic regime. In this model, the studied area is located in the eastern and southeastern terranes of the Rio Apa Block. The eastern terrane consists of the Morraria and Caracol gneisses and the Baía das Garças Suite, formed ofby the Sanga Bonita Granite (1721 ± 25 Ma; U-Pb, SHRIMP, zircon; Remédio et al., 2013), Santa Clarinha and Espinilho orthognaisses (Remédio *et al.*, 2013; 1716 ± 11Ma and 1735 ± 12 Ma, U-Pb, SHRIMP, zircon; respectively), as well as of the Cerro Porã Granite (1749 ± 45 Ma, U-Pb, SHRIMP, zircon; Plens et al., 2013). In the Southeastern terrane, the João Candido Gneiss,

Scardine Granite (1791 ± 19 Ma, U-Pb, LA-ICP MS, zircon; Faleiros et al., 2015) and the Rio Areia Gneiss (1809 ± Ma, U-Pb, LA-ICP MS, zircon; Faleiros et al., 2015) are recognized.

Lacerda Filho et al. (2016) divided the Rio Apa Block in three segments (western, central and eastern), with their own characteristics, all marked by a succession of magmatic events (between ca. 1.87 and 1.71 Ga). The authors suggest five main magmatic events between 2.07 and 1.71 Ga, that constitute a progressive evolution and represent the several stages of assembly of the Amoguijá Magmatic Arc. The rocks studied would be in the final stages of this magmatic arc, between 1760 and 1750 Ma, interpreted as late-orogenic A type granites. The area of the present work covers the central (Rio Apa Complex and Alto Tererê Group) and the eastern terranes (Paraíso Complex).

The central terrane is composed of the Rio Apa Complex and the Alto Tererê as described by Cordani et al. (2010) and Faleiros et al. (2015), together with unpublished terminologies such as Tamanduá Granite (1736±19 Ma, U-Pb, LA-ICP MS, zircon; Lacerda Filho et al., 2016) and Santo Antônio Granite (1794± 14 Ma, U-Pb, LA-ICP MS, zircon; Lacerda Filho et al., 2016); as well as the Paso Bravo Province (1559±55 Ma; U-Pb, SHRIMP, zircon; Cordani et al., 2010) exposed in Paraguayan territory. The Paraíso Complex consists of gneisses and granites described as part of the southeastern terrane (Faleiros et al., 2015). The subdivisions and nomenclatures cited are shown in table 3.1 along with the initial names used by previous authors (e.g. Almeida, 1965).

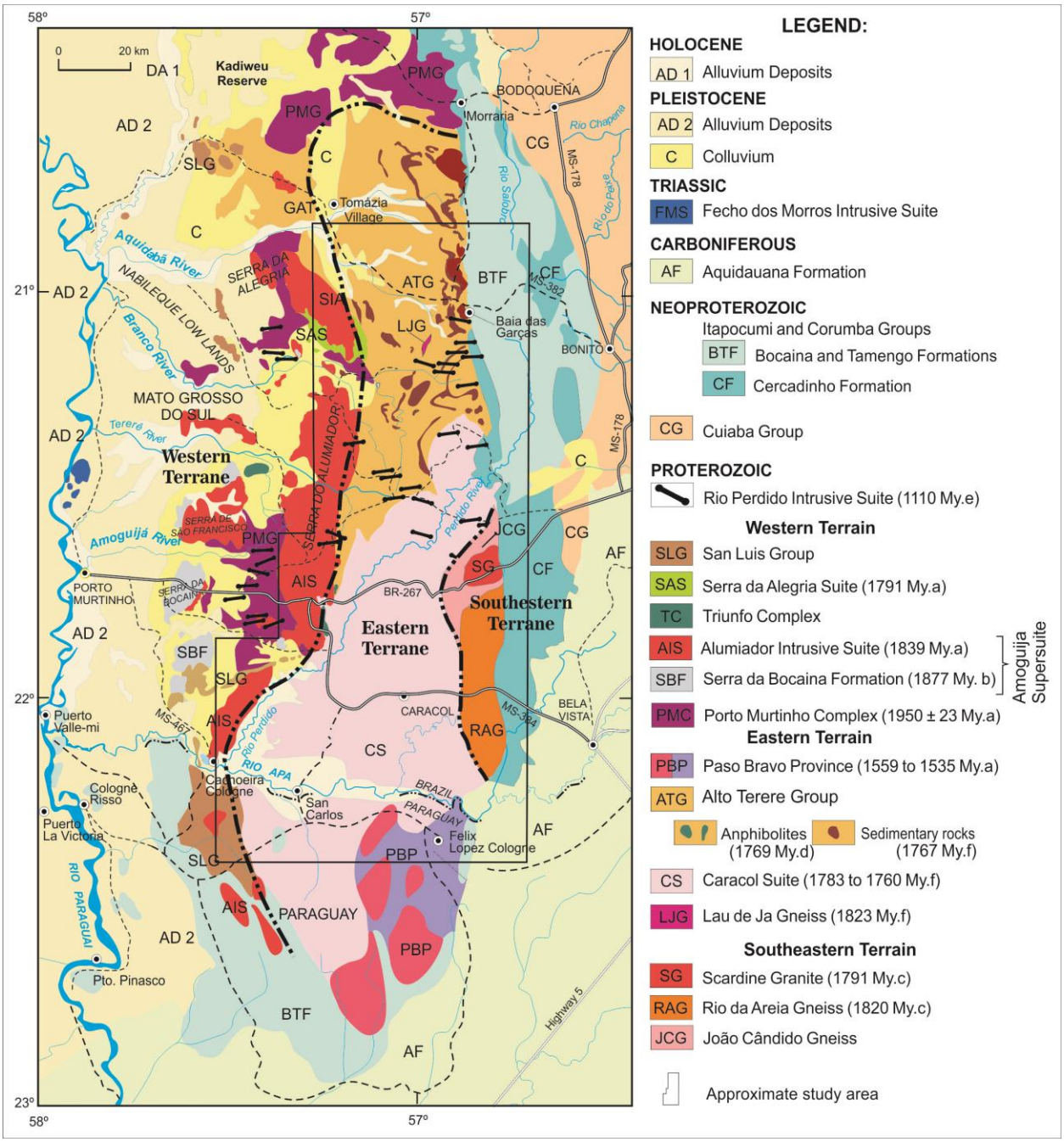

Figure 3.2. Geological outline of the Rio Apa Block in southwestern Mato Grosso do Sul (Brazil) and northwestern Paraguay (extracted and modified from Cordani et al., 2010 and Lima et al., Subm). The geochronological data were obtained by the following authors: a (Cordani et al., 2010); b (Brittes et al., 2013); c (Faleiros et al., 2015); d (Lacerda Filho et al., 2016); e, (Teixeira et al., 2016); f, this work.

Table 3.1. Granites and gneisses of the eastern and southeastern terranes; U-Pb ages are from a Wiens (1986), b Cordani et al. (2010), c Plens et al. (2013), d Remédio et al. (2013), e Pavan et al., (2014), f Faleiros et al. (2015); g Lacerda Filho (2015). Zircon SHRIMP ages*, Zircon U-Pb U-Pb LA-ICP-MS ages**, U-Pb Zircon Detrital***.

Authors	Lithostratigraphic Units	Subdivisions	U-Pb Ages
Almeida (1965)	Brazilian Crystalline Complex		
Correa et al. (1976)	Base Complex		
	Alto Tererê		
Araújo & Montalvão (1980)	Rio Apa Complex		
Godoi et al. (1999)	Rio Apa Complex		
	Alto Tererê Group		
Lacerda Filho et al. (2006)	Rio Apa Complex	Porto Murtinho Gneiss	
		Morraria Gneiss	
		Caracol Gneiss	
	Alto Tererê Group		
Cordani et al. (2010)	Caracol Gneiss		1774 ± 26 Ma (b)*
	Morraria Gneiss		1721 ± 25 Ma (b)*
	Alto Tererê Group (Metavolcanic and metasedimentary)		
Faleiros et al. (2015)	Caracol Gneiss		
	Santa Clarinha Orthogneiss		1750 ± 9 Ma (f)**
	Espinílho Orthogneiss		1719 ± 11 Ma (f)**
	Rio de Areia Gneiss		
	Scardine Gneiss		
	Alto Tererê Group		
Lacerda Filho (2015)	Rio Apa Complex	Espinilho Gneiss (d)	1719 ± 11 Ma (f)**
		Sanga Bonita Granite (e)	1721± 26 Ma (b)*
		Baía das Garças Granite (b)	1727±29 Ma (b)*
		Santa Clarinha Gneiss (d)	1750±9 Ma (f)**
		Tamanduá Granite (g)	1736± 19 Ma (g)**
		Cerro Pora Granite (c.)	1749± 45 Ma (c.)*
		Caracol Gneiss (b)	1768± 27 Ma (b)*
		Santo Antônio Granite (g)	1794± 14 Ma (g)**
		Córrego Cervo Granite (f)	1841± 7,5 Ma (f)*
		Paso Bravo Province (a)	1839± 33 Ma (b)*
	Alto Tererê Group	Metavolcanic Rocks	1769±9 Ma (g)**
		Metasedimentary Rocks	1727 Ma (g)***

Lacerda Filho et al. (2016) also presents a lot of datas about the Alto Tererê Group and describes it as represented by a metavolcan-sedimentary sequence. The basic metavolcanic unit as consisting of three lithofacies: (i) fine-grained banded amphibolite (metabasalt); (ii) medium-grained amphibolite with relic subophitic texture (metagabbro) and; (iii) amphibolite with relic cumulate texture (metapyroxenite); and had crystallization ages of 1769 ± 36 Ma (U-Pb in zircon; LA-ICP-MS). The metasedimentary rocks are composed of garnet-kyanite-muscovite schist, muscovite-quartz schist, garnet-muscovite schist, biotite-quartz schist, chlorite-muscovite-quartz schist, epidote-chlorite-quartz schist and muscovite quartzite metamorphosed to medium amphibolites facies, with retrometamorphism to greenschist facies. The isotopic data for these rocks showed ages obtained by the U-Pb method in zircon (LA-ICP-MS) with last sedimentation peak in 1728 and 1700 Ma for two samples of garnet-kyanite-muscovite schist.

Cordani et al. (2010) report a T_{DM} model age of 2.23 Ga as well as a slightly negative ε_{Nd} (t) value, -1.94 Ga for the Caracol Gneiss. Lacerda Filho et al. (2016) indicate values of T_{DM} model ages ~2,09 Ga for rocks of the Rio Apa Complex, and negative values of ε_{Nd} (t) between -1.1 and -4.75, which are indicative of crustal contamination of parental magmas.

Cordani et al. (2010) presented cooling and metamorphic ages of approximately 1300 Ma obtained by K-Ar and Ar-Ar methods in micas crystals to the Rio Apa Block.

3.4. RESULTS

3.4.1. FIELD AND PETROGRAPHIC ASPECTS

3.4.1.1.Lau de Já orthogneiss

The Lau de Já orthogneiss, identified for the first time in this work, occurs in the NE portion of the area as a narrow xenolith within the pink hololeucratic granite-gneiss facies of the Caracol Suite, constituting a strip of discontinuous outcrops (Fig. 3.3). It presents gray color, medium to fine granulation and well developed gneissic banding. Under the microscope, it is characterized by felsic bands of quartz, plagioclase and microcline alternating with mafic bands of biotite, muscovite, epidote and opaque minerals (Fig. 3.4). The accessory minerals are titanite, apatite,

monazite, zircon and opaque minerals; epidote, chlorite, white mica and opaque minerals constitute the paragenesis of alteration.

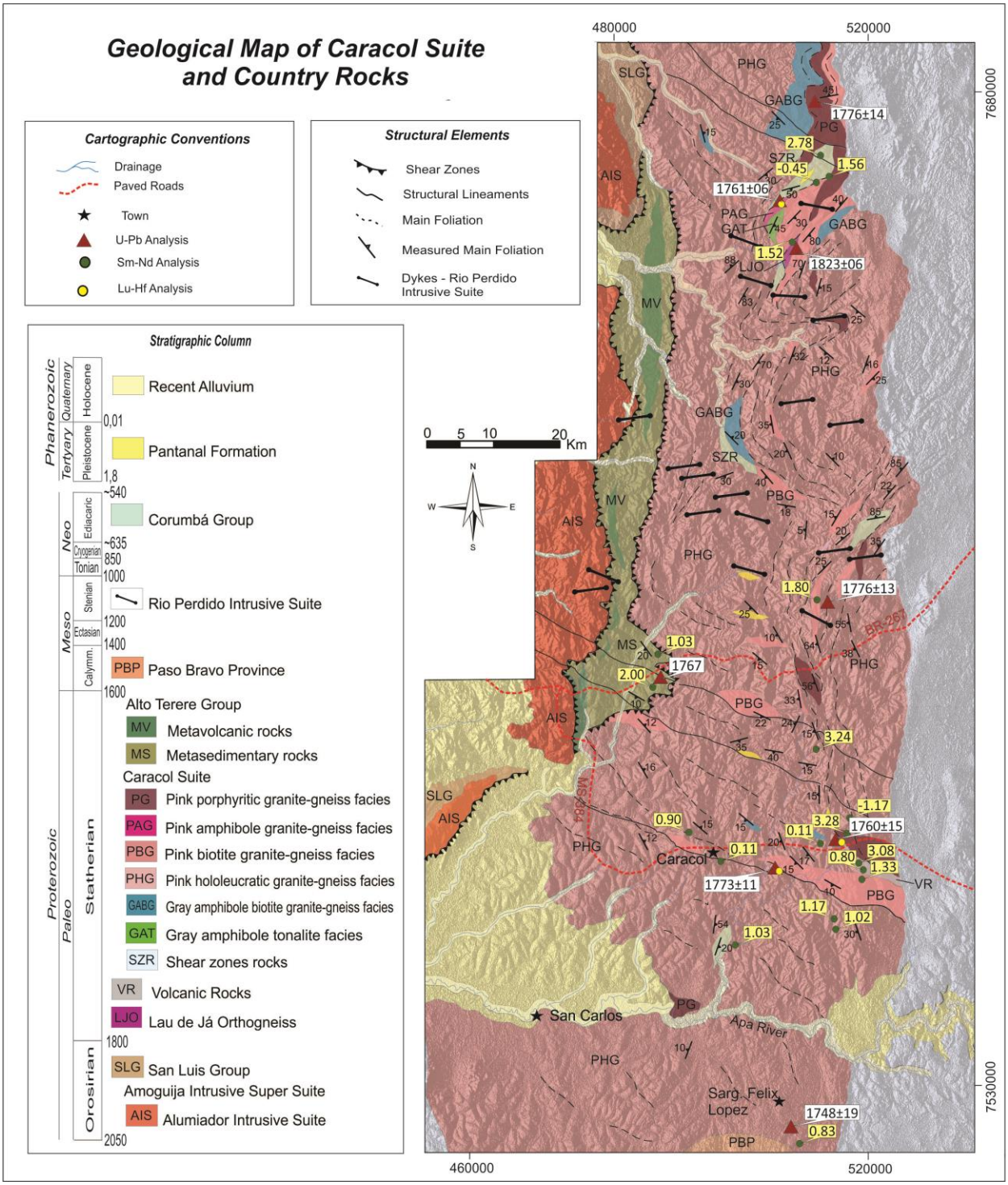

Figure 3.3. Geological map of the Caracol region (MS), showing location of analyzed samples.

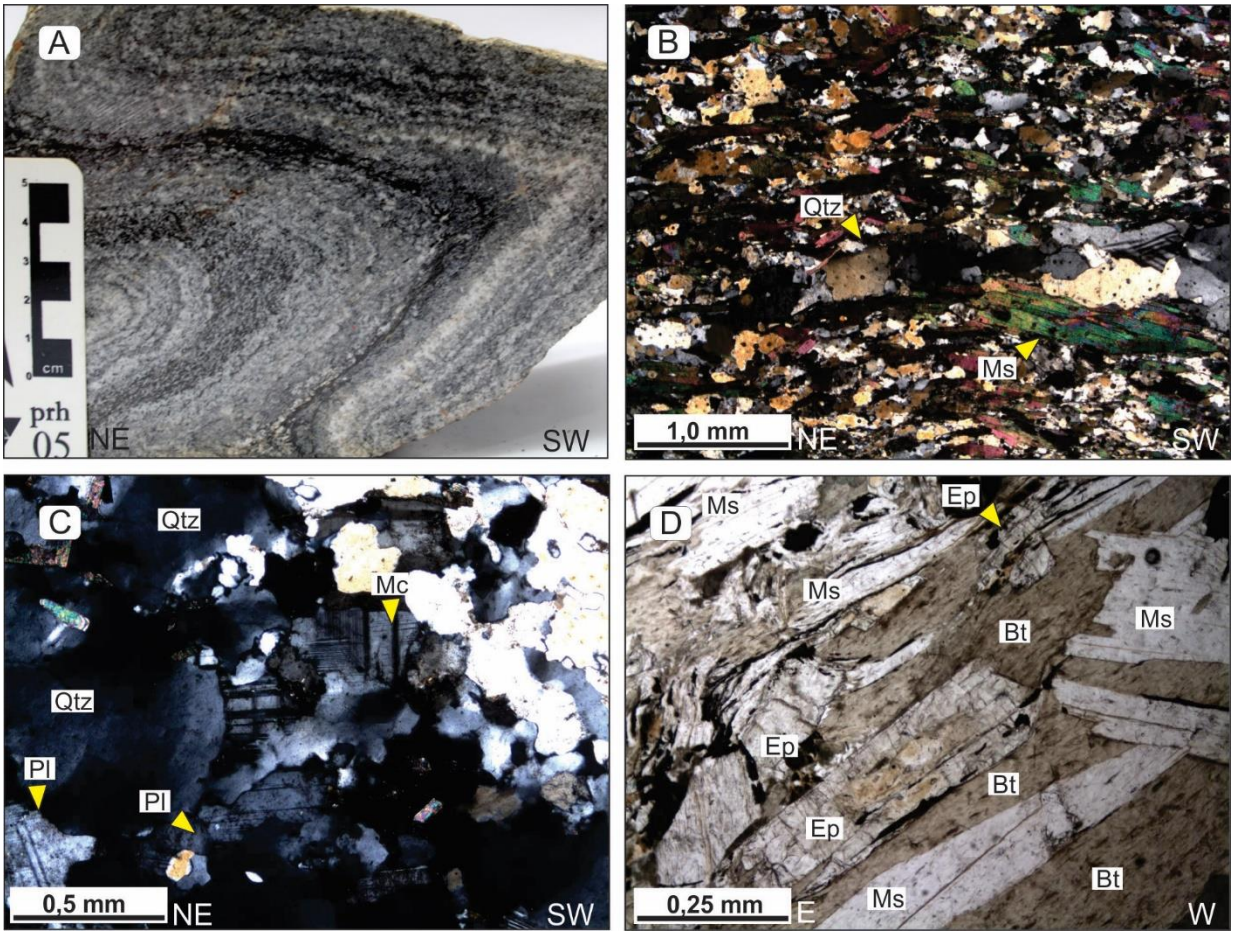

Figure 3.4. Lau de Já orthogneiss: **(A)** folded gneiss banding; **(B)** granolepidoblastic texture and gneiss banding; **(C)** detail of felsic band; **(D)** detail of mafic band formed of biotite and epidote. Parallel polarizers in D and crossed polarizers in B and C. Abbreviations: Qtz – quartz, Mc – microcline, Pl – plagioclase, Bt – biotite, Ep – epidote, Ms – muscovite.

3.4.1.2.Caracol Suite

The Caracol Suite consists of voluminous granitic-gneissic magmatism occupying most of the eastern terrane. It is exposed along the N-S direction for approximately 190 km, and extending for about 65 km to Paraguay, with width between 80 and 30 km. It is in contact to the west with the rocks of the Alto Tererê Group and to the east with rocks of the Corumbá Group; in the southwestern portion, it is partially covered by sediments of the Pantanal Formation.

The rocks are foliated and, when affected by local or regional shear zones, form mylonites and schists. Evidence of hydrothermal processes causing the formation of chlorite and muscovite may be related to metamorphic events under greenschist facies conditions.

Based on field and petrographic characteristics, six petrographic facies were identified: (i) pink hololeucratic granite-gneiss facies; (ii) pink biotite granite-gneiss facies; (iii) pink porphyritic

granite-gneiss facies; (iv) pink amphibole granite-gneiss facies; (v) gray amphibole biotite granite-gneiss facies; (vi) gray amphibole tonalite facies.

The pink hololeucocratic granite-gneiss facies is the dominant facies, comprising approximately 80% of the Caracol Suite. It is essentially composed of granite-gnaisses (Fig. 3.5A). These rocks are foliated, whose intensity of deformation increses nearlocal or regional shear zones. They present less than 5% of mafic minerals, xenomorphic to hipidiomorphic texture, medium granulation, and are made of microcline, quartz, and plagioclase (Fig. 3.5B). The mafic minerals are biotite, amphibole, opaque minerals and rare garnet. The accessory minerals are represented by epidote, amphibole, garnet, and opaque minerals.

The pink biotite granite-gneiss facies, characterized by the occurrence of biotite as the primary mafic phase (Fig. 3.5C), is exposed as kilometer-long lenses throughout the Caracol Suite, oriented in the northwest direction. Under the microscope, the rocks of this facies show medium- to fine-grained texture, xenomorphic to hipidiomorphic texture, consisting of quartz, microcline, plagioclase and biotite in proportions that classify them as syenogranites and, subordinately, monzogranites. When foliated, they exhibit granolepidoblastic texture, mainly due to the alignment of biotite crystals (Fig. 3.5D). Epidote, titanite and opaque minerals are the most common accessories, however hornblende may also occur.

The pink porphyritic granite-gneiss facies also occurs as lenses in the principal facies, generally oriented along the main deformational fabric and it is composed of pink to light gray syenogranite. It is distinguished from the pink hololeucocratic granite-gneiss facies due to the presence of anhedral to subhedral alkaline feldspar phenocrysts with dimensions up to 3 cm immersed in a fine matrix. When affected by shear zones, it displays a protomylonitic to mylonitic foliation showing stretched and rotated feldspar porphyroclasts generating sigmoids (Fig. 3.5E). Under the microscope they present alkaline feldspar phenocrysts in a fine matrix, composed of quartz, plagioclase and microcline. Plagioclase is subhedral with a cloudy appearance due to alteration. Intergrowth with quartz in droplets and films is frequent, characterizing the mirmechitic texture. Microcline is anhedral to subhedral and occurs as deformed phenocrysts that constitute a porphyroblastic texture. It is also found as smaller grains in the matrix (Fig. 3.5F). Biotite is the dominant mafic phase, and is partially altered to chlorite. Titanite and apatite often occur associated with lamellar aggregates of biotite. The accessory paragenesis is represented by titanite, apatite, epidote, and opaque minerals.

The pink amphibole granite-gneiss facies is only observed in the northern portion of the area as a small syenogranite lens. Prominent penetrative foliation is marked by the orientation of mafic minerals (Fig. 3.5G). Under the microscope, it consists of 10% hornblende in a matrix with quartz and alkali feldspar as the dominant phases. The texture is medium- to fine-grained, xenomorphic and, in places, granoblastic, with a composition of microcline, plagioclase, quartz and hornblende (Fig. 3.5H). Accessory minerals generally occur in association with hornblende aggregates and are represented by titanite, opaque minerals, apatite and zircon; epidote, biotite and opaque minerals are alteration products.

The gray anphibole tonalite facies is the least evolved portion of the suite; it occurs as a lens with up to 20% hornblende, and a high amount of plagioclase and seldom microcline restricted to the northern region of the area. It shows intense deformation like the pink amphibole granite-gneiss facies, previously mentioned (Fig. 3.6A). Under the microscope, the tonalite exhibits medium- to fine-grained hypidiomorphic inequigranular texture composed of quartz, plagioclase, and hornblende (Fig. 3.6B). Zircon occurs in tiny disseminated bipyramidal prisms, while titanite aggregates border the hornblende; both make up the accessory minerals. Epidote, white mica, opaque and clay minerals represent alteration paragenesis.

The gray amphibole biotite granite-gneiss facies occurs in the eastern portion of the area and is formed of monzo- to subordinate syenogranites with around 10% of biotite. Under the microscope, they exhibit fine-grained and equi- and inequigranular xenomorphic texture composed of quartz, microcline, plagioclase and biotite. Biotite is the main accessory phase, hornblende, titanite and zircon also occur. Epidote, calcite, muscovite and white mica are alteration products; opaque minerals are rare. Small intrusions of the pink amphibole granite-gneiss facies are observed.

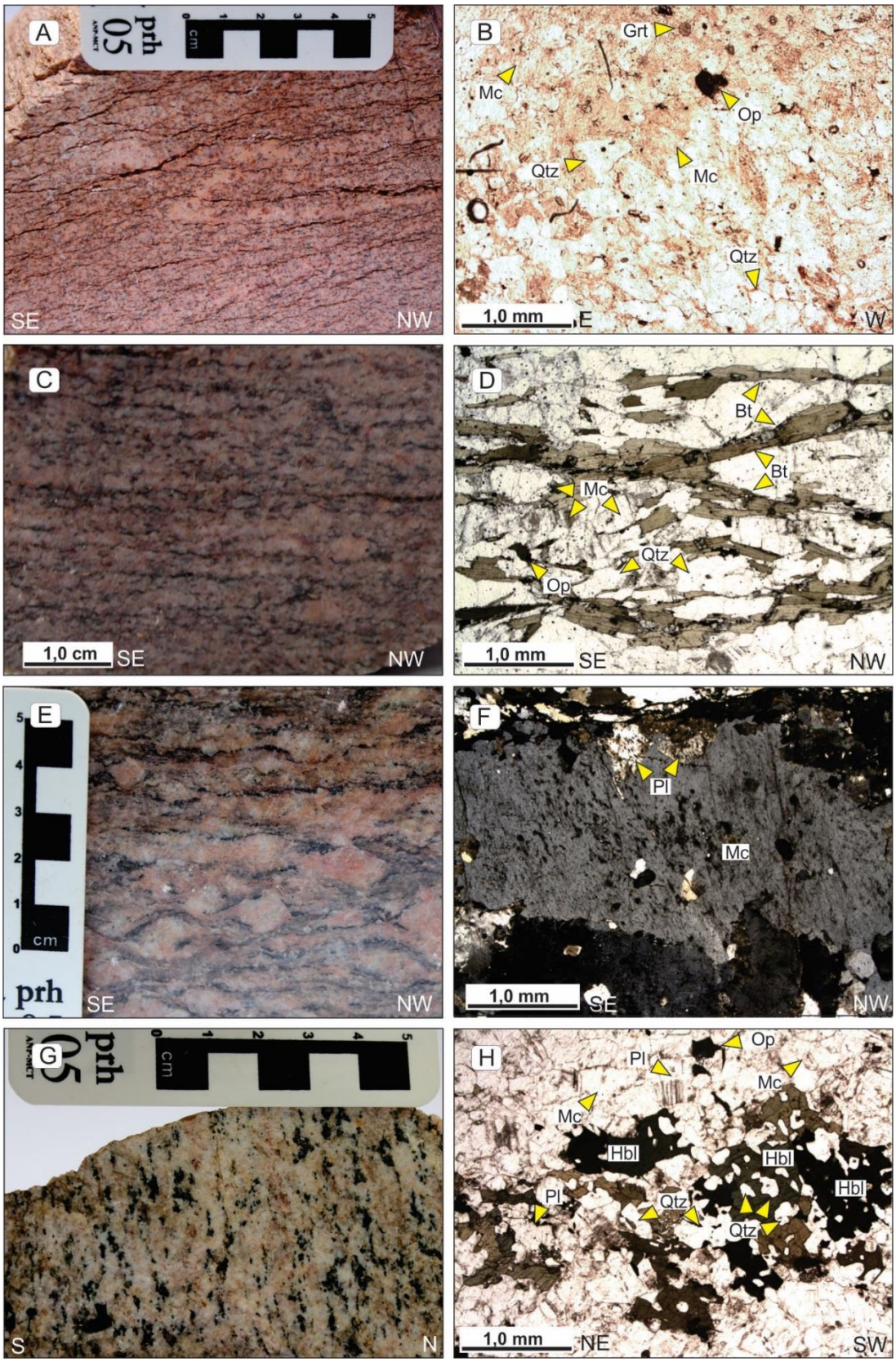

Figure 3.5**.** Pink hololeucocratic granite-gneiss facies: (A) granitic texture and foliation commonly marked by mafic minerals; (B) xenomorphic texture in alkali-feldspar granite.

Continuation Figure 3.5. Pink biotite granite-gneiss facies: (C) oriented biotite crystals; (D) granolepidoblastic texture showing alignment of biotite crystals; Pink porphyritic granite-gneiss facies: (E) alkali-feldspar sigmoidal porphyroclasts; (F) microcline phenocrystal in a recrystallized quartz-feldspathic matrix; Pink amphibole granite-gneiss facies: (G) foliation marked by the orientation of mafic minerals; (H) xenomorphic granonematoblastic texture, formed of microcline, plagioclase, quartz and hornblende. Hand-sample photographs on the left; and microphotographs on the right. Parallel polarizers in B, D and H and crossed polarizers in F. Abbreviations: Qtz – quartz, Mc – microcline, Pl – plagioclase, Bt – biotite, Ep – epidote, Hbl – hornblende, Ms – muscovite, Grt – garnet, Op – opaque minerals.

3.4.1.2.1. **Shear zone rocks**

Shear zones are present throughout the whole Caracol Suite, with greater frequency and intensity in the the northern portion of the area. The sheared rocks have a porphyroclastic texture and granolepidoblastic matrix characterized by garnet blasts in a fine-grained matrix of quartz, muscovite and microcline (Fig. 3.6F). The orientation of these minerals defines a schistosity. In addition, abrupt textural variation is observed, giving rise to medium-grained granolepidoblastic layers.

3.4.1.2.2. Volcanic rocks

Extrusive rocks were also recognized and they occur in the southeastern area as hills, blocks and low-lying outcrops. Despite the high degree of alteration, very fine-grained amygdaloidal dacitic flows are observed, which are red to dark-gray in color, with pseudomorphic phenocrystals of plagioclase and mafic minerals, as well as amygdals filled by quartz and calcite (Fig. 3.6C). Under the microscope, trachyitic to intergranular texture is observed consisting of euhedral and subhedral tabular crystals of plagioclase with apatite, opaque and zircon as the accessory phases; white mica, clay minerals, epidote, and opaque minerals are the alteration phases. The amygdules are filled by quartz and calcite (Fig. 3.6D), and exhibit common fibrorradiated pattern. They also have zoned plagioclase phenocrystals in which calcium-rich cores are revealed by the greater degree of alteration.

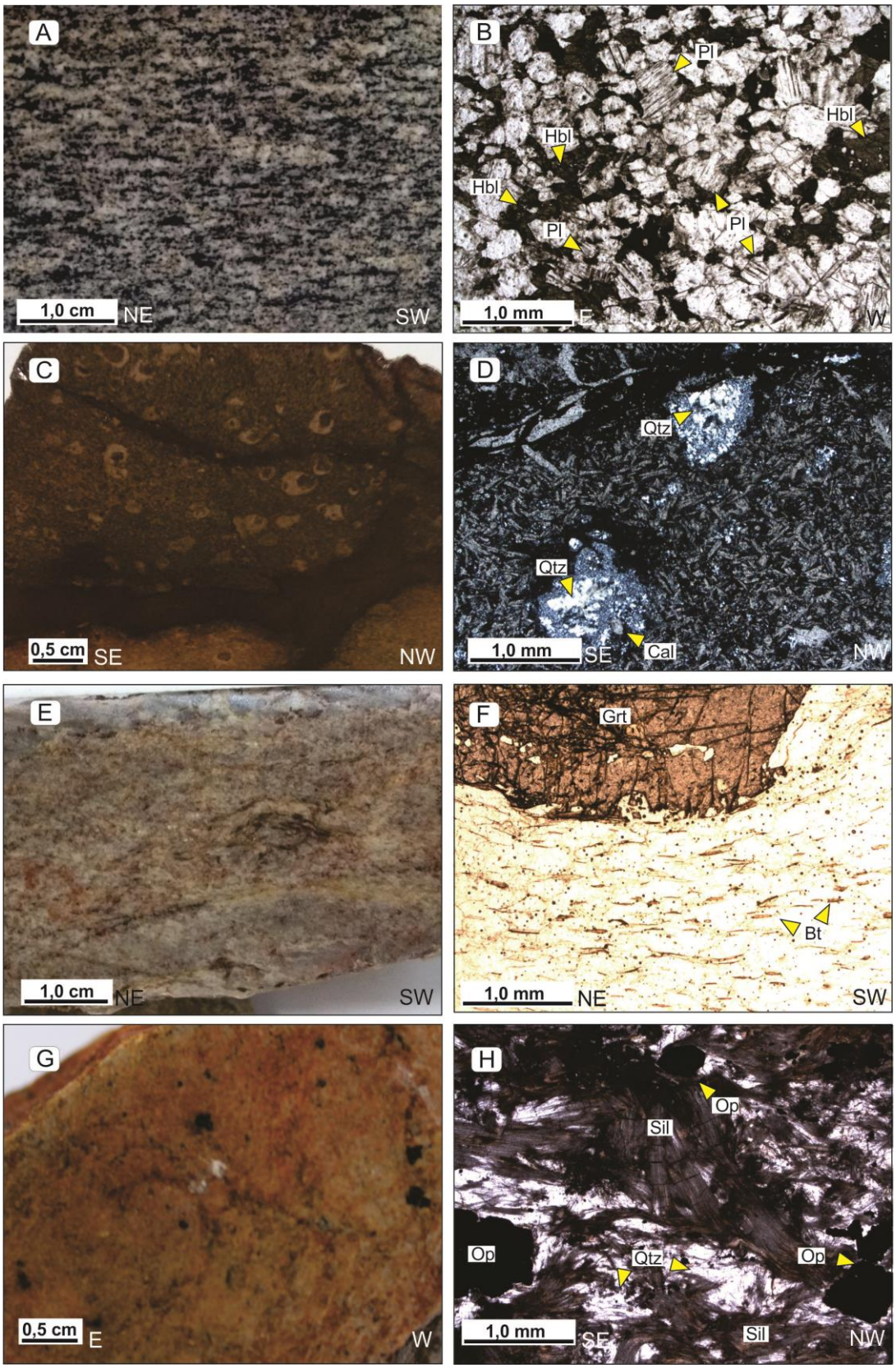

Figure 3.6**. Gray amphibole tonalite facies:** (A) oriented mafic minerals; (B) fine-grained hypidiomorphic equigranular texture consisting of quartz, plagioclase and hornblende.

Continuation Figure 2.6. **Volcanic rocks:** (C) amygdules filled by quartz; (D) trachytic to intergranular texture with amygdales filled by feldspar, quartz and calcite. **Shear zone rocks**: (E) garnet porphyroblasts in a fine-grained matrix ; (F) part of garnet porphyroblasts immersed in a granolepidoblastic matrix. **Sillimanite-quartz schist (Alto Tererê Group):** (G) porphyroblastic texture with opaque mineral phenocrystals; (H) close-view of porphyroblast of opaque minerals, interstitial quartz and fibrous sillimanite. Hand-sample photographs on the left; and microphotographs on the right. Parallel polarizers in B, F; and crossed polarizers in D, H. Abbreviations: Qtz – quartz, Mc – microcline, Pl – plagioclase, Bt – biotite, Ep – epidote, Hbl – hornblende, Grt – garnet, Cal – calcite, Sil – sillimanite, Op – opaque minerals.

3.4.1.3.Alto Tererê Group

The sedimentary rocks of the Alto Tererê Group are represented mainly by sillimanite-quartz schists and occur in the eastern portion of the area. To the west, it is in contact with rocks of the Alumiador Intrusive Suite in the western Rio Apa Block, and to the east, it is in contact with the Caracol Suite. These rocks exibit orange to beige colors while their alteration results in the formation of rounded fragments that are stretched preferably in the east-west direction (Fig. 3.6G).

The sillimanite-quartz schists, metamorphosed under amphibolite facies conditions (sillimanite zone), have porphyroblastic texture marked by porphyroblasts of opaque minerals in a fine-grained matrix of quartz, fibrous sillimanite and opaque minerals (Fig. 3.6H).

3.4.2. GEOCHRONOLOGICAL AND ISOTOPIC RESULTS

3.4.2.1.U-Pb in Zircon

3.4.2.1.1. Lau de Já orthogneiss

The sample FS-98, UTM coordinates 506357/7655590 (Fig. 3.3), is a phaneritic rock, of fine- to medium-grained inequigranular texture and characteristic gneissic banding. The zircon crystals are dark yellow, smoky, and rarely colorless, mostly prismatic, euhedral, 150 to 250 μm in length, with ratios of 2/1 and rarely 2/2. Backscattered images (Fig. 3.7A to C) show oscillatory zoning.

In the concordia diagram, this sample (Fig. 3.8A) presented an alignment of 14 zircon crystals, (Table 3.2) indicating an upper intercept age of 1822±6 with MSWD of 2.80.

3.4.2.1.2. Caracol Suite

From the six facies identified on the basis of petrography, we selected two samples of the pink hololeucratic granite-gneiss facies (DP-12 and SQ-29), one of the pink biotite granite-gneiss facies (DP-09), two sample of the pink porphyritic granite-gneiss facies (DP- 27), and one of the pink amphibole granite-gneiss facies (FS-63).

Sample DP-12 of the pink hololeucratic granite-gneiss facies was collected near the town of Sargento José Felix Lopes in Paraguay (UTM coordinates 506816/7523971). The rock is light-pink, syenogranitic in composition, foliated, with inequigranular to, essentially, equigranular texture. Biotite is considered to be a primary mafic mineral and accounts for less than 5% of the modal composition. The sample SQ-29, located in the mid-eastern portion of the Caracol Suite (UTM coordinates 510732/7604507), is light-pink to gray in color, fine-grained, equigranular, with small amounts of mafic minerals.

The zircon crystals from the pink hololeucocratic granite-gneiss facies are dark yellow and smoky, rarely colorless, and range from 50 to 400 μm in length. Crystals with size from 150 to 300 μm are more common and show prismatic and euheral habits, with well-developed pyramids; such crystals have a length-to-width ratio of 2/1. In backscattered images (Fig. 3.7D to H), they generally exhibit relatively regular bright and dark oscillatory zoning bands. DP-12 sample shows a Discordia diagram formed of 6 analytical points, several of which are concordant to sub-concordant, producing an upper intercept age of 1748±19 Ma, with MSWD of 0.80 (Fig. 3.8B). The calculated age of the SQ-29 sample is of 1776±13 Ma (MSWD = 1.9; Fig. 3.8C).

Sample DP-09 was collected from the southwest portion of the area (505720/7563229; Fig. 3.3), and is characterized by a pink to reddish-pink, fine-grained, equigranular rock; biotite along with opaque aggregates define a penetrative foliation. Zircon crystals are smoky, yellow and also colorless, mostly ranging in size from 150 to 200 μm. Subordinate smaller grains of approximately 50 μm, and larger, with sizes up to 400 μm long are also observed. The most abundant crystals exhibit prismatic and euhedral habits, as commonly observed in grains of most magmatic rocks (Vavra et al., 1996); the length-to-width ratio is 2/1. Backscattered images (Fig. 3.7I to K) show zircons crystals with relative regular dark-bright zoning bands (different levels of U). Twelve spot analyses indicate an upper intercept age of 1773±11 Ma (MSWD=2.1; Fig. 3.8D).

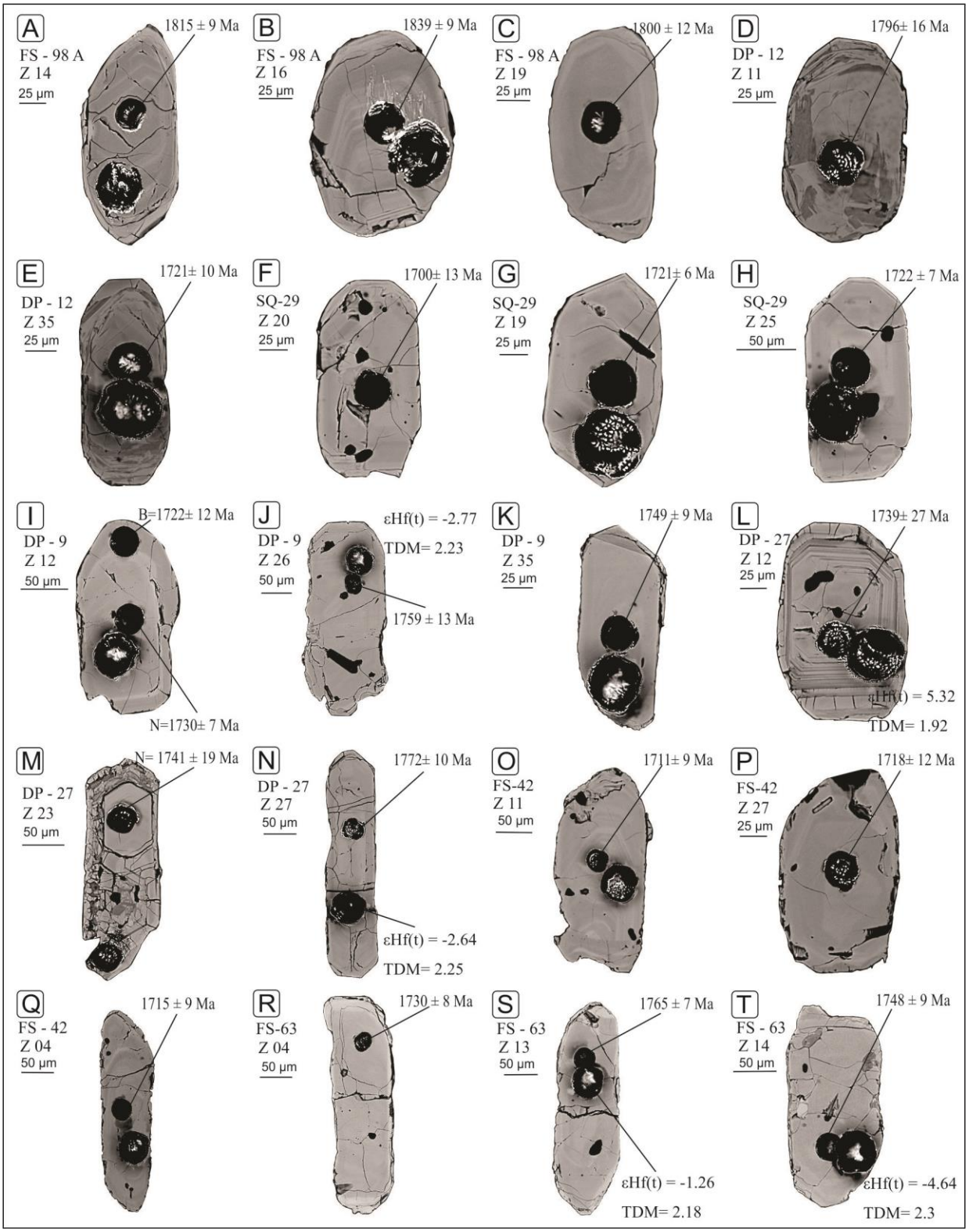

Figure 3.7. Backscattered images of the crystals of the Lau de Já orthogneiss and of the Caracol Suite. A, B and C: Lau de Já orthogneisses; D to H: pink hololeucratic granite-gneiss facies; I to K: pink biotite granite-gneiss facies; L to Q: pink porphyritic granite-gneiss facies; R to T : pink amphibole granite-gneiss facies.

Sample DP-27 of pink porphyritic granite-gneiss facies, located at UTM coordinates 515264/7566546, eastern portion of the eastern terrane, is light pink, sienogranitic in composition, and shows phenocrystals of potassium feldspar in a fine-grained matrix. Deformation in this facies is characterized by penetrative foliation with stretched, sigmoidal and rotated porphyroclasts. The sample FS-42, located in the north portion of the area (coordinates 512808/7671960) is light gray, with a fine-grained quartz-feldspathic matrix and porphyroclasts of potassium feldspar.

The zircon crystals to this facies are larger than the crystals of the previous facies. They range between 150 and 400 μm, however most crystals belong to the size fractions between 200 and 250 μm. They are often dark and light yellow, show oscillatory zoning, and are prismatic, euhedral, with well-developed bipyramidal shapes. The length-to-width-ratio is 2/1 and more often 3/1 (Fig. 3.7L to Q). In this facies, overgrowths are more frequent. For the diagram in Figure 3.8E, a total of 15 crystals have yielded a discordia indicating the upper intercept age of 1760±15 Ma (MSWD=4.8). However, this sample presents crystals with high values of 204 Pb, which makes its results uncertain. For the FS-42 sample was noted an upper intercept of 1748±19 Ma with MSWD of 1.3 (Figure 3.8F).

Located at the north end of the area (UTM coordinates 504423/7662118), the sample FS-63 represents the pink amphibole granite-gneiss facies and is characterized as fine- to medium-grained, equi- to inequigranular, with hornblende, mafic aggregates and opaque minerals defining the rock foliation. The zircon grains range between 50 and 400 μm, more frequently from 100 to 200 μm. They are displayed in dark yellow to light colors and colorless, and are prismatic. The length-to-width- ratio is 2/1 to 3/1. Observed in backscattered images (Fig. 3.7R to T), they show, as in previous cases, oscillatory zoning. In the diagram of figure 3.8G, 10 analysed grains show a Discordia with alignment upper intercept of 1761.3±6.6 Ma (MSWD of 1.8).

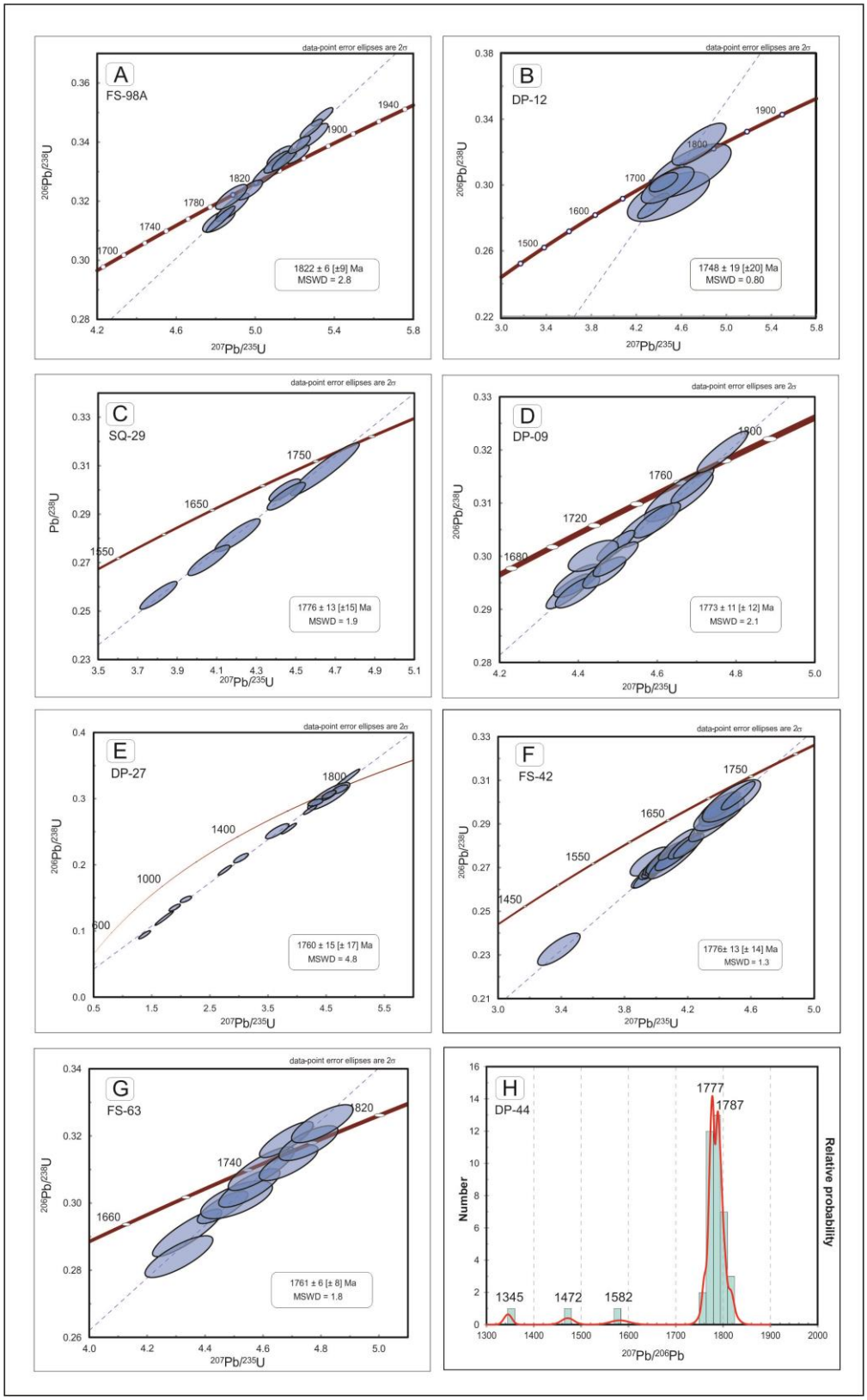

Figure 3.8. Representation of U-Pb data for rocks and backscattered images of zircon crystals of the Lau de Já orthogneiss, Caracol Suite and Alto Tererê Group. (A) FS 98A: Lau de Já orthogneiss; (B and C); (D) DP-9: Pink biotite granite-gneiss facies - Caracol Suite; DP-12 and SQ-29: Pink hololeucocratic granite facies - Caracol Suite.

Continuation Figure 3.8. (E) DP-27: Pink porphyritic granite-gneiss facies - Caracol Suite; (F) FS-42: Pink porphyritic granite-gneiss facies - Caracol Suite; (G) FS-63: Pink amphibole granite-gneiss facies - Caracol Suite; (H) DP-44: Sillimanite-quartz schist – Alto Tererê Group.

3.4.2.1.3. Alto Tererê Group

Located in the central-western portion of the area, UTM coordinates 487027/7591458, the sample DP-44 is a sillimanite-quartz schist. Zircon crystals have different shades of yellow, but is also smoky and rarely colorless; they are 250 to 50 μm in length and present high degree of roundness. In the backscattered images, the predominant internal structure is oscillatory zoning and some grains show some thin overgrowths. The probability frequency diagram (Figure 3.8H) shows results of 40 zircon grains analysed that present two mains peakes: 1787 and 1777 Ma, this last, considered as the maximum age of sedimentation. However, three younger crystals were dated to the following ages: 1582, 1472, and 1345 Ma. Because they are few grains (only one for each age), it shows the need for this sample to be complemented with more crystals to be analyzed for better understanding respect to the younger ages related to these three crystals.

B Table 3.2. U-Pb LA-ICPMS data from sample FS 98 A – Lau de Já orthogneiss.

Sample	^{204} Pb	∫ 206%	Th/U	^{206}Pb / ^{204}Pb	^{207}Pb / ^{206}Pb	Err (%) 1 sigma	^{207}Pb / ^{235}U	Err (%) 1 sigma	^{206}Pb / ^{238}U	Err (%) 1 sigma	Apparent ages (Ma) ^{207}Pb / ^{206}Pb	Err (%) 1 sigma	^{207}Pb / ^{235}U	Err (%) 1 sigma	^{206}Pb / ^{238}U	Err (%) 1 sigma	Rho	Conc (%)
004-Z01	10.678	0.025	0.344	62158.500	0.111	0.945	4.818	1.394	0.313	1.025	1772	18	1788	12	1758	16	0.72	98
013-Z06B	31.621	0.030	0.599	51178.995	0.110	0.810	4.881	1.344	0.321	1.073	1749	15	1799	11	1797	17	0.79	100
014-Z07	16.263	0.035	0.388	44475.031	0.111	0.654	5.069	1.354	0.330	1.186	1771	12	1831	11	1838	19	0.87	100
018-Z11	15.898	0.006	0.512	240990.432	0.111	0.407	5.341	0.834	0.349	0.728	1766	8	1875	7	1928	12	0.85	103
019-Z12N	28.294	0.038	0.295	40470.627	0.112	0.476	5.149	0.992	0.334	0.870	1777	9	1844	8	1858	14	0.86	101
024-Z13	24.052	0.025	0.252	61985.056	0.113	0.545	5.217	0.927	0.336	0.750	1791	10	1855	8	1867	12	0.78	101
025-Z14	18.444	0.035	0.347	44705.900	0.111	0.683	4.973	1.088	0.324	0.847	1770	13	1815	9	1808	13	0.76	100
027-Z16	16.368	0.027	0.533	56822.964	0.111	0.628	5.116	1.117	0.333	0.924	1769	12	1839	9	1855	15	0.81	101
029-Z30B	36.395	0.009	0.375	176847.287	0.111	0.446	5.286	0.876	0.345	0.755	1768	8	1867	7	1909	12	0.84	102
033-Z31	43.202	0.007	0.532	213849.591	0.112	0.501	5.225	0.868	0.339	0.709	1776	9	1857	7	1883	12	0.79	101
038-Z35	103.419	0.163	0.448	9572.376	0.111	0.425	4.826	1.230	0.314	1.155	1772	8	1790	10	1760	18	0.93	98
046-Z39	13.180	0.007	0.745	209246.469	0.111	0.617	5.126	1.018	0.335	0.810	1761	12	1840	9	1864	13	0.77	101
057-Z27B	16.478	0.010	0.398	158580.642	0.112	0.648	5.291	1.232	0.342	1.048	1783	12	1867	11	1896	17	0.84	102
059-Z29	13.458	0.013	0.502	118334.501	0.111	0.711	4.886	1.414	0.318	1.222	1771	13	1800	12	1780	19	0.86	99

Table 3.3. U-Pb LA-ICPMS data from sample DP 12 – pink hololeucocratic granite-gneiss facies – Caracol Suite.

Sample	^{204} Pb	∫ 206%	Th/U	^{206}Pb / ^{204}Pb	^{207}Pb / ^{206}Pb	Err (%) 1 sigma	^{207}Pb / ^{235}U	Err (%) 1 sigma	^{206}Pb / ^{238}U	Err (%) 1 sigma	Apparent ages (Ma) ^{207}Pb / ^{206}Pb	Err (%) 1 sigma	^{207}Pb / ^{235}U	Err (%) 1 sigma	^{206}Pb / ^{238}U	Err (%) 1 sigma	Rho	Conc (%)
005-Z02	28.816	0.306	0.699	5183.998	0.111	2.573	4.489	3.320	0.293	2.098	1766	48	1729	28	1657	31	0.63	96
007-Z04	16.783	0.062	0.526	25648.590	0.108	1.517	4.481	2.141	0.300	1.511	1719	29	1728	18	1691	22	0.70	98
010-Z07	9.242	0.072	0.392	21663.766	0.110	2.353	4.679	3.201	0.309	2.171	1746	44	1764	27	1735	33	0.67	98
017-Z13	11.685	0.037	0.431	42538.571	0.106	1.295	4.761	2.064	0.325	1.607	1684	25	1778	17	1813	25	0.77	102
024-Z19	35.883	0.016	0.356	96447.602	0.110	0.724	4.354	1.312	0.287	1.094	1745	14	1704	11	1629	16	0.82	96
045-Z35	11.172	0.017	0.618	90748.617	0.107	0.855	4.446	1.168	0.302	0.795	1693	16	1721	10	1700	12	0.65	99

Table 3.4. U-Pb LA-ICPMS data from sample SQ-29 pink hololeucocratic granite-gneiss facies – Caracol Suite.

Sample	^{204} Pb	∫ 206%	Th/U	^{206}Pb ^{204}Pb	^{207}Pb ^{206}Pb	Err (%) 1 sigma	^{207}Pb ^{235}U	Err (%) 1 sigma	^{206}Pb ^{238}U	Err (%) 1 sigma	Apparent ages (Ma) ^{207}Pb ^{206}Pb	Err (%) 1 sigma	^{207}Pb ^{235}U	Err (%) 1 sigma	^{206}Pb ^{238}U	Err (%) 1 sigma	Rho	Conc (%)
004-Z01	38.970	0.022	0.745	72912.647	0.108	0.431	3.807	1.010	0.257	0.914	1707	8	1594	8	1472	12	0.89	92
009-Z05B	10.636	0.013	0.438	121746.513	0.108	0.510	4.207	1.112	0.281	0.988	1721	10	1675	9	1598	14	0.88	95
023-Z17	29.441	0.007	0.514	219172.464	0.109	0.511	4.650	1.528	0.309	1.440	1735	10	1758	13	1734	22	0.94	99
025-Z19	30.182	0.012	0.497	127484.945	0.107	0.388	4.446	0.731	0.300	0.620	1705	7	1721	6	1691	9	0.81	98
034-Z24B	34.823	0.011	0.338	142651.267	0.109	0.484	4.062	1.063	0.271	0.947	1725	9	1647	9	1546	13	0.88	94
035-Z25	36.259	0.012	0.540	132197.643	0.109	0.420	4.454	0.888	0.297	0.783	1724	8	1722	7	1679	12	0.86	97

Table 3.5. U-Pb LA-ICPMS data from sample DP 09 – pink biotite granite-gneiss facies – Caracol Suite.

Sample	^{204} Pb	∫ 206%	Th/U	^{206}Pb ^{204}Pb	^{207}Pb ^{206}Pb	Err (%) 1 sigma	^{207}Pb ^{235}U	Err (%) 1 sigma	^{206}Pb ^{238}U	Err (%) 1 sigma	Apparent ages (Ma) ^{207}Pb ^{206}Pb	Err (%) 1 sigma	^{207}Pb ^{235}U	Err (%) 1 sigma	^{206}Pb ^{238}U	Err (%) 1 sigma	Rho	Conc (%)
015-Z09	19.148	0.011	0.500	146373.543	0.108	0.479	4.767	1.104	0.320	0.994	1716	9	1779	9	1788	16	0.89	101
018-Z12N	21.730	0.029	0.659	53534.747	0.108	0.415	4.496	0.877	0.302	0.772	1713	8	1730	7	1701	12	0.86	98
021-Z14	13.233	0.016	0.475	99217.334	0.108	0.713	4.570	1.301	0.306	1.088	1721	13	1744	11	1719	16	0.83	99
030-Z20	18.391	0.007	0.714	214875.851	0.109	0.392	4.690	0.948	0.313	0.863	1723	7	1766	8	1757	13	0.90	100
031-Z21	23.788	0.030	0.549	52991.105	0.107	0.860	4.438	1.172	0.300	0.796	1701	16	1720	10	1692	12	0.65	98
032-Z22	16.487	0.017	0.577	95215.475	0.109	0.593	4.466	1.008	0.297	0.815	1732	11	1725	8	1676	12	0.79	97
035-Z23	40.593	0.042	0.628	37795.927	0.109	0.535	4.495	1.039	0.299	0.890	1728	10	1730	9	1689	13	0.84	98
036-Z24	16.418	0.022	0.529	70519.304	0.109	0.627	4.398	1.049	0.293	0.841	1726	12	1712	9	1658	12	0.78	97
037-Z25	11.733	0.018	0.579	89500.462	0.108	0.548	4.376	1.062	0.293	0.910	1716	10	1708	9	1659	13	0.84	97
038-Z26	12.718	0.037	0.480	42083.115	0.108	0.891	4.656	1.527	0.311	1.239	1722	17	1759	13	1747	19	0.80	99
039-Z27	14.231	0.021	0.369	74376.641	0.108	0.698	4.397	1.105	0.295	0.857	1713	13	1712	9	1668	13	0.75	97
051-Z35	15.572	0.021	0.803	75503.273	0.109	0.592	4.600	1.063	0.307	0.884	1726	11	1749	9	1725	13	0.81	99

Table 3.6. U-Pb LA-ICPMS data from sample DP-27 - pink porphyritic granite-gneiss facies - Caracol Suite.

Sample	^{204} Pb	∫ 206%	Th/U	^{206}Pb / ^{204}Pb	^{207}Pb / ^{206}Pb	Err (%) 1 sigma	^{207}Pb / ^{235}U	Err (%) 1 sigma	^{206}Pb / ^{238}U	Err (%) 1 sigma	Apparent ages (Ma) ^{207}Pb / ^{206}Pb	Err (%) 1 sigma	^{207}Pb / ^{235}U	Err (%) 1 sigma	^{206}Pb / ^{238}U	Err (%) 1 sigma	Rho	Conc (%)
004-Z01	63.061	0.094	0.523	17170.624	0.110	0.473	3.855	1.378	0.255	1.294	1741	9	1604	11	1465	17	0.94	91
007-Z04	308.510	0.892	0.325	1819.447	0.106	1.292	3.654	2.245	0.251	1.836	1671	24	1561	18	1444	24	0.83	93
008-Z05	366.326	0.151	0.285	10270.841	0.107	0.441	4.862	1.787	0.331	1.731	1689	8	1796	15	1843	28	0.97	103
010-Z07	29.824	0.014	0.372	116617.640	0.107	0.543	4.365	1.268	0.296	1.146	1698	10	1706	10	1670	17	0.90	98
023-Z13	263.163	1.220	0.436	1456.292	0.105	1.487	1.372	3.051	0.095	2.664	1667	27	877	18	582	15	0.89	66
024-Z14	575.397	0.792	0.841	2212.144	0.104	0.935	1.709	3.783	0.119	3.665	1639	17	1012	24	728	25	0.97	72
025-Z15	354.635	0.785	0.413	2119.685	0.104	1.024	3.031	1.711	0.210	1.371	1652	19	1415	13	1231	15	0.81	87
027-Z34	415.819	0.647	0.400	2599.617	0.104	0.656	2.752	1.723	0.192	1.594	1643	12	1343	13	1132	17	0.93	84
028-Z16	249.264	0.306	0.561	5201.534	0.108	0.464	4.219	1.109	0.284	1.007	1713	9	1678	9	1609	14	0.90	96
030-Z18	441.877	1.992	0.350	864.892	0.102	1.402	2.083	1.914	0.148	1.303	1608	26	1143	13	890	11	0.72	78
036-Z22	218.995	0.916	0.465	1726.630	0.106	1.003	4.312	1.239	0.294	0.727	1683	18	1696	10	1664	11	0.57	98
037-Z23N	14.334	0.006	0.464	255938.449	0.108	0.537	4.552	1.103	0.305	0.964	1719	10	1741	9	1715	15	0.86	99
044-Z26	366.484	2.158	0.402	804.044	0.101	1.360	1.890	2.094	0.136	1.592	1592	25	1078	14	819	12	0.80	76
045-Z27	36.771	0.058	0.527	27151.143	0.109	0.835	4.727	1.219	0.314	0.888	1731	16	1772	10	1762	14	0.71	99
046-Z28	52.101	0.006	0.533	250405.845	0.108	0.689	4.545	1.086	0.307	0.839	1706	13	1739	9	1724	13	0.75	99

Table 3.7. U-Pb LA-ICPMS data from sample FS-63 - pink amphibole granite-gneiss facies – Caracol Suite.

Sample	^{204} Pb	∫ 206%	Th/U	^{206}Pb/^{204}Pb	^{207}Pb/^{206}Pb	Err (%) 1 sigma	^{207}Pb/^{235}U	Err (%) 1 sigma	^{206}Pb/^{238}U	Err (%) 1 sigma	Apparent ages (Ma) ^{207}Pb/^{206}Pb	Err (%) 1 sigma	^{207}Pb/^{235}U	Err (%) 1 sigma	^{206}Pb/^{238}U	Err (%) 1 sigma	Rho	Conc (%)
006-Z03	133.104	0.510	0.574	3122.458	0.110	0.659	4.311	1.111	0.284	0.894	1748	12	1695	9	1612	13	0.80	95
009-Z06N	11.095	0.012	0.498	131739.293	0.108	0.556	4.554	0.950	0.305	0.770	1721	11	1741	8	1714	12	0.79	98
014-Z07B	22.500	0.025	0.400	63226.809	0.108	0.456	4.462	0.802	0.299	0.660	1719	9	1724	7	1685	10	0.79	98
018-Z10	60.996	0.014	0.470	108821.834	0.106	0.427	4.682	0.810	0.319	0.688	1687	8	1764	7	1785	11	0.82	101
023-Z13	9.753	0.007	0.424	216884.414	0.109	0.550	4.690	0.885	0.312	0.693	1731	10	1765	7	1751	11	0.75	99
024-Z14	11.900	0.027	0.396	59171.106	0.107	0.552	4.596	1.019	0.310	0.857	1704	10	1748	9	1742	13	0.82	100
035-Z23	16.969	0.016	0.564	98077.959	0.109	0.566	4.758	0.876	0.318	0.668	1723	11	1778	7	1779	10	0.72	100
036-Z36	35.241	0.029	0.350	53507.325	0.108	0.557	4.806	0.907	0.324	0.715	1708	11	1786	8	1808	11	0.76	101
038-Z38	39.469	0.058	0.880	27431.027	0.108	0.532	4.339	1.126	0.291	0.992	1715	10	1701	9	1647	14	0.87	97
043-Z27	13.774	0.023	0.283	69857.872	0.109	0.819	4.510	1.123	0.301	0.768	1725	15	1733	9	1696	11	0.65	98

Table 3.8. U-Pb LA-ICPMS data from sample DP-44 - sillimanite-quartz schist, metasedimentary portion of the Alto Tererê Group.

Sample	^{204} Pb	∫ 206%	Th/U	^{206}Pb/^{204}Pb	^{207}Pb/^{206}Pb	Err (%) 1 sigma	^{207}Pb/^{235}U	Err (%) 1 sigma	^{206}Pb/^{238}U	Err (%) 1 sigma	Apparent ages (Ma) ^{207}Pb/^{206}Pb	Err (%) 2 abs	^{207}Pb/^{235}U	Err (%) 2 abs	^{206}Pb/^{238}U	Err (%) 2 abs	Rho	Conc (%)
004-Z03	16.713	0.005	0.383	343092.714	0.109	0.331	4.544	0.698	0.303	0.615	1777	12	1739	12	1708	18	0.85	98
004-ZR47	27.328	0.007	1.660	111605.214	0.108	0.447	4.806	1.288	0.322	1.150	1773	16	1797	36	1786	22	0.89	99
005-Z05	14.939	0.005	0.463	328038.107	0.109	0.371	4.492	0.729	0.298	0.627	1787	7	1730	6	1683	9	0.83	97
005-ZR48	23.100	0.006	0.486	194845.956	0.109	0.433	4.706	1.017	0.313	0.842	1781	16	1757	26	1768	17	0.83	101
006-Z04	31.865	0.010	0.356	160190.077	0.109	0.465	4.409	0.755	0.292	0.595	1790	16	1714	12	1653	18	0.74	96
006-ZR49	28.184	0.011	0.737	174221.441	0.110	0.449	4.975	1.057	0.329	0.883	1795	16	1832	28	1815	18	0.83	99
007-Z06	7.014	0.005	0.442	345297.306	0.109	0.348	4.434	0.762	0.296	0.677	1775	12	1719	12	1673	20	0.87	97
007-ZR50	9.582	0.009	0.997	371058.956	0.109	0.447	4.897	1.004	0.326	0.820	1779	16	1821	26	1802	17	0.82	99
008-Z07	27.792	0.008	0.440	191485.055	0.110	0.420	4.478	0.926	0.296	0.825	1795	16	1727	16	1671	24	0.88	97
009-Z08	66.425	0.017	0.377	94055.515	0.110	0.428	4.513	0.768	0.298	0.638	1797	16	1733	12	1681	18	0.79	97

Continuation table 3.8.

Sample	^{204} Pb	∫ 206%	Th/U	^{206}Pb/^{204}Pb	^{207}Pb/^{206}Pb	Err (%) 1 sigma	^{207}Pb/^{235}U	Err (%) 1 sigma	^{206}Pb/^{238}U	Err (%) 1 sigma	Apparent ages (Ma) ^{207}Pb/^{206}Pb	Err (%) 2 abs	^{207}Pb/^{235}U	Err (%) 2 abs	^{206}Pb/^{238}U	Err (%) 2 abs	Rho	Conc (%)
009-ZR52	17.584	0.009	0.709	302836.702	0.110	0.625	4.864	1.128	0.322	0.863	1793	23	1799	27	1796	19	0.77	100
010-ZR53	27.063	0.005	0.680	86387.441	0.108	0.722	4.506	1.246	0.303	0.946	1763	26	1707	28	1732	21	0.76	101
013-ZR54N	31.712	0.005	0.761	127011.438	0.108	0.716	4.662	1.710	0.313	1.508	1766	26	1756	46	1760	28	0.88	100
016-Z13	29.945	0.007	0.325	222276.681	0.110	0.392	4.676	0.872	0.309	0.780	1796	14	1763	14	1735	24	0.88	98
017-Z14	35.789	0.017	0.333	90820.112	0.109	0.375	4.553	0.667	0.302	0.552	1790	14	1741	12	1700	16	0.77	98
017-ZR57	40.270	0.006	0.764	110315.979	0.109	0.596	4.940	1.245	0.329	1.028	1781	22	1833	33	1809	21	0.83	99
018-ZR58	10.567	0.006	0.614	251564.164	0.109	0.609	5.005	1.223	0.332	0.994	1788	22	1849	32	1820	21	0.81	98
019-ZR59	53.519	0.009	0.490	33698.622	0.110	0.556	5.158	1.156	0.340	0.943	1801	20	1886	31	1846	20	0.82	98
020-ZR60	24.116	0.006	0.717	127856.886	0.111	0.739	5.232	1.167	0.341	0.823	1818	27	1893	27	1858	20	0.71	98
023-Z18	25.482	0.006	0.582	282476.208	0.109	0.305	4.510	0.780	0.301	0.718	1779	12	1733	12	1695	22	0.91	98
024-Z39	31.502	0.008	0.446	201047.997	0.111	0.607	4.659	1.003	0.304	0.798	1817	22	1760	16	1712	24	0.77	97
026-Z20	54.198	0.017	0.424	90345.582	0.109	0.463	4.507	0.825	0.300	0.682	1784	16	1732	14	1690	20	0.80	98
026-ZR63	29.418	0.008	0.028	109448.618	0.086	0.435	2.798	0.892	0.235	0.685	1345	17	1361	17	1355	13	0.77	100
027-ZR64	23.595	0.007	0.340	136202.685	0.098	1.088	3.779	1.733	0.280	1.297	1582	40	1593	37	1588	28	0.75	100
028-Z22	34.348	0.047	0.334	33639.653	0.108	0.329	4.459	0.987	0.299	0.930	1770	12	1723	16	1685	28	0.94	98
028-ZR65	14.089	0.004	0.505	159527.510	0.109	0.623	4.890	1.104	0.325	0.833	1783	23	1816	26	1801	19	0.75	99
029-Z23	14.032	0.005	0.445	301148.525	0.109	0.300	4.501	0.612	0.300	0.534	1779	10	1731	10	1692	16	0.82	98
029-ZR66	15.423	0.003	0.661	80001.521	0.111	0.719	4.715	1.186	0.309	0.868	1812	26	1735	26	1770	20	0.73	102
033-ZR68	29.064	0.007	0.809	109812.382	0.110	0.697	4.888	1.114	0.323	0.787	1795	25	1804	25	1800	19	0.71	100
034-Z26	77.697	0.011	1.179	139603.254	0.110	0.391	4.836	0.949	0.318	0.865	1804	14	1791	16	1780	26	0.90	99
035-ZR70	54.489	0.006	0.740	27356.797	0.109	0.560	4.828	1.081	0.321	0.847	1782	20	1796	27	1790	18	0.78	100
037-ZR72	37.304	0.005	0.149	70168.542	0.092	0.706	3.221	1.217	0.253	0.920	1472	27	1456	24	1462	19	0.76	100
038-ZR73	14.383	0.006	0.769	203229.762	0.109	0.554	4.831	0.987	0.323	0.728	1775	20	1804	23	1790	17	0.74	99
039-ZR74	43.887	0.007	0.441	67275.880	0.109	0.799	4.656	1.112	0.310	0.678	1784	29	1739	21	1759	18	0.61	101
040-Z32	47.266	0.029	0.442	53255.808	0.108	0.404	4.944	0.927	0.331	0.834	1773	14	1810	16	1842	26	0.89	102
040-ZR75	15.473	0.003	0.416	75356.606	0.109	0.712	4.928	1.223	0.329	0.924	1778	26	1833	29	1807	21	0.75	99
043-Z33	28.142	0.010	0.464	155448.664	0.108	0.451	4.771	0.806	0.321	0.668	1760	16	1780	14	1797	20	0.80	101
044-Z37	66.528	0.006	0.438	274517.075	0.109	0.441	4.769	0.907	0.317	0.792	1787	16	1779	16	1773	24	0.86	100
048-Z42	36.839	0.010	0.589	154740.915	0.109	0.335	4.538	0.728	0.303	0.646	1775	12	1738	12	1708	20	0.86	98
049-Z43	22.009	0.005	0.450	297101.679	0.109	0.366	4.640	0.750	0.307	0.654	1790	14	1756	12	1728	20	0.84	98

3.4.2.2.Lu-Hf in Zircon

3.4.2.2.1. Caracol Suite

The Lu-Hf method was use analyzed in three of the four facies dated of the Caracol Suite. The touchstone that determined the choice of the three facies was the concordance of the U-Pb ages. Samples of the pink biotite granite-gneiss facies, pink porphyritic granite-gneiss facies and pink amphibole granite-gneiss facies were analysed (fig. 3.9). The results showed $^{176}Hf/^{177}Hf(t)$ ratios between 0.281568 and 0.281839, negative to positive $\varepsilon_{Hf}(t)$ values ranging from -4.64 to 5.32, with a slight dominance of negative values, and T_{DM} model ages between 1.92 and 2.30 Ga (table 3.9).

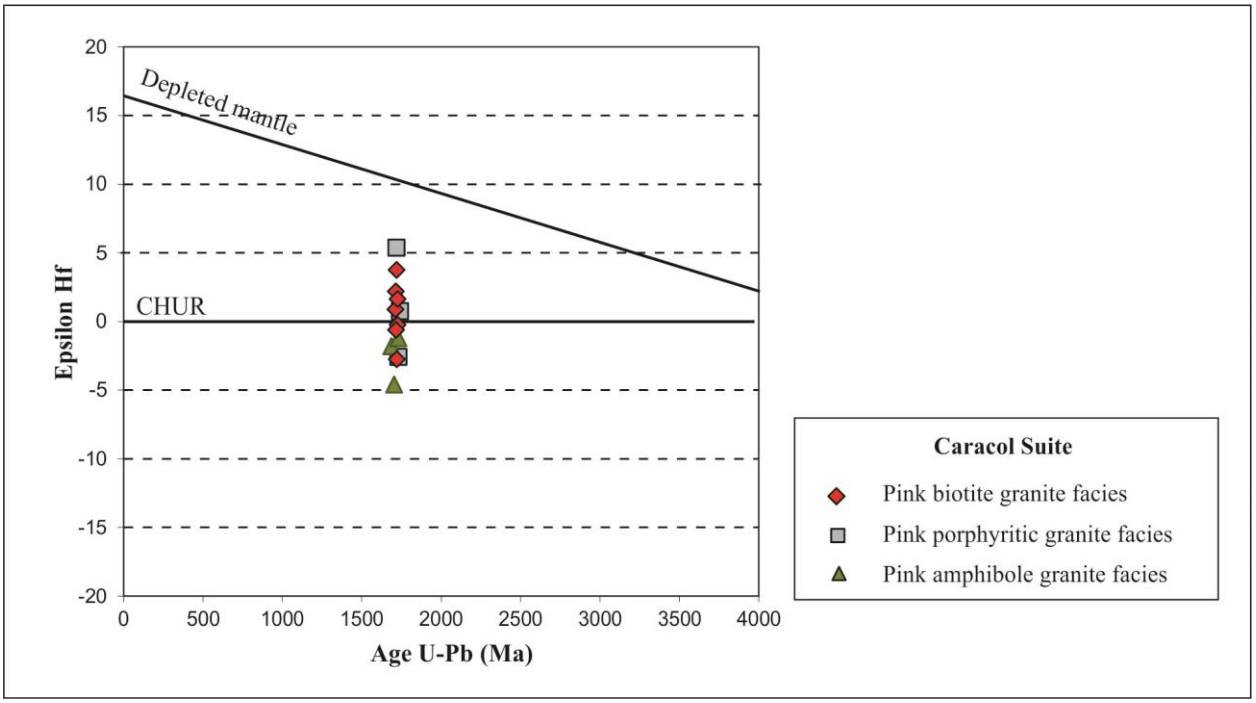

Figure 3.9. Lu-Hf analytical data for samples the -Caracol Suite.

Table 3.9. Summary of results of the Lu-Hf analyses for intrusive rocks of the Caracol Suite.

Sample	$^{176}Lu/^{177}Hf$	±2σE	$^{176}Hf/^{177}Hf$	±2σE	Age U-Pb (Ma)	$(^{176}Hf/^{177}Hf)_t$	eHf(t)	±2σE	T(DM) Ga
Caracol Suite									
Pink biotite granite-gneiss facies									
DP - 09									
003-Z9	0.001051	0.00001	0.281786	0.0002	1716	0.281752	2.17	0	2.04
004-Z14	0.001197	0.00001	0.281832	0.0001	1721	0.281793	3.73	0.1	1.98
006-Z35	0.001008	0.00001	0.28171	0.0001	1726	0.281677	-0.26	0	2.14
007-Z27	0.000975	0.00001	0.281749	0.0001	1713	0.281717	0.86	0	2.08
008-Z26	0.000845	0.00001	0.281637	0.0001	1722	0.281609	-2.77	0.1	2.23
009-Z25	0.001197	0.00001	0.281712	0.0001	1716	0.281673	-0.64	0	2.15
010-Z24	0.000785	0.00001	0.281756	0.0001	1726	0.28173	1.62	0	2.07
Pink amphibole granite-gneiss facies									
FS - 63									
005-Z4	0.000994	0.00001	0.281691	0.0001	1686	0.281659	-1.84	0	2.16
008-Z13	0.001098	0.00002	0.281682	0.0000	1731	0.281646	-1.26	0	2.18
009-Z14	0.001672	0.00010	0.281622	0.0001	1704	0.281568	-4.64	0.3	2.3
Pink porphyritic granite-gneiss facies									
DP - 27									
003-Z1	0.001048	0.000002	0.281729	0.0000	1741	0.281694	0.69	0	2.12
006-Z12	0.001178	0.00004	0.281877	0.0001	1719	0.281839	5.32	0.4	1.92
007-Z27	0.002122	0.00009	0.281677	0.0001	1731	0.281607	-2.64	0.2	2.25

3.4.2.3.Whole-rock Sm-Nd results

Sm-Nd data are presented in table 3.10 and figure 3.10. The ca. 1.82 Ga old Lau de Já orthogneiss showed ε_{Nd} (t) of 0.70, with T_{DM} model age of 2.03 Ga, which attest to the juvenile nature of the protolith.

The volcanic rocks show positive ε_{Nd} (t), between 0.12 and 3.29, and T_{DM} model ages between 1.82 and 2.16 Ga.

Granite-gneiss samples of the Caracol Suite generally exhibits positive to slightly negative ε_{Nd} values ranging from 3.25 to -1.75 with T_{DM} values of 1.82 to 2.25 Ga. Seven samples of the pink hololeucratic granite-gneiss facies show slightly negative to positive ε_{Nd}(t) values between -1.18 and 3.25 and T_{DM} model ages between 1.81 and 2.25 Ga. Three analysed samples of the pink

biotite granite-gneiss facies, present positive $\varepsilon_{Nd}(t)$ between 1.33 and 1.87 and T_{DM} values of 1.92 and 1.99 Ga.

For the Alto Tererê Group, two samples of sillimanite-quartz schist were analysed, yielding positive ε_{Nd} values between 1.03 and 2.01 and T_{DM} between 1.90 and 2.01 Ma. These data suggest that the original sediments of the Alto Tererê Group represent erosion of the nearby Caracol Suite as well as of Lau de Já orthogneiss.

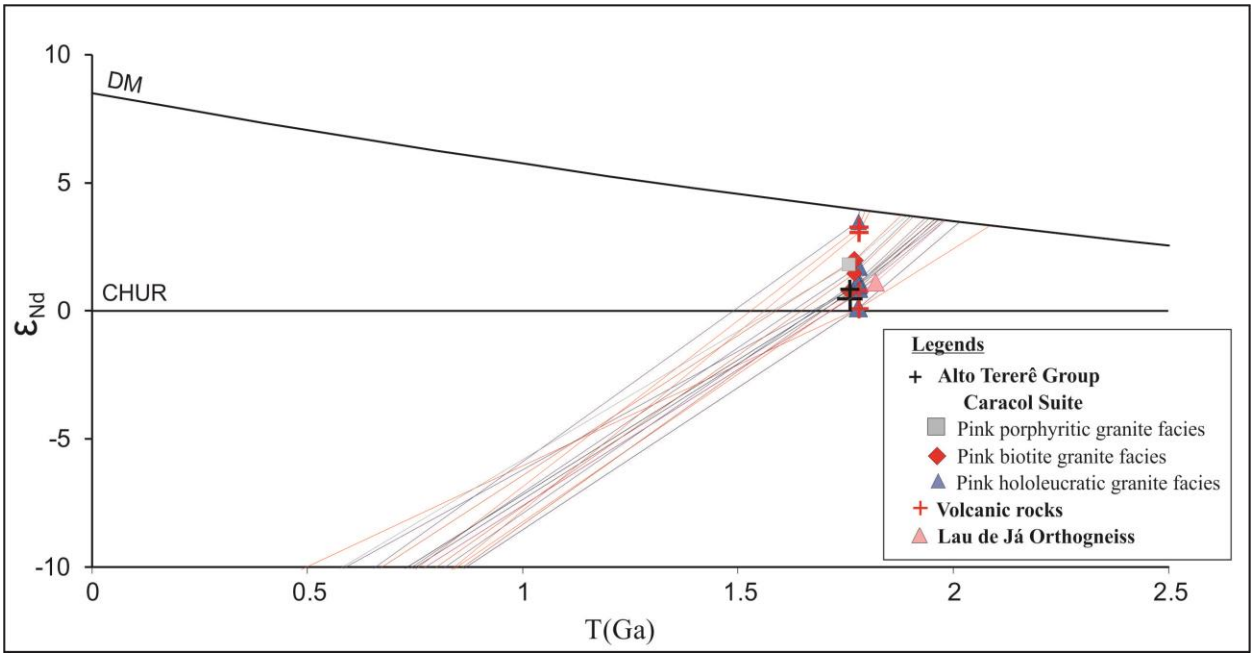

Figure 3.10. Sm-Nd for the rocks of the Lau de Já orthogneiss and Caracol Suite. Noticeable are the positive ε_{Nd} (t) values for most rock units investigated.

Table 3.10. Summary of Sm-Nd results for the studied rocks.

Sample	Sm(ppm)	Nd(ppm)	$^{147}Sm/^{144}Nd$	$^{143}Nd/^{144}Nd$ ± 2SE	$\varepsilon_{Nd\,(t)}$	T_{CHUR}	T_{DM} (Ga)	T - U-Pb (Ga)
Alto Tererê Group								
DP44	10.39	51.77	0.12	0.511819+/-1	1.03	1.65	2.01	1.76
DP68	21.67	124.65	0.11	0.511680+/-1	2.01	1.59	1.9	1.76
Caracol Suite								
Pink hololeucocratic granite-gneiss facies								
DP12	5.63	29.68	0.11	0.511730+/-5	0.83	1.68	2.01	1.78
DP16	13.62	79.93	0.10	0.511719+/-3	3.25	1.49	1.81	1.78
DP25	2.52	11.56	0.13	0.511829+/-8	-1.18	1.90	2.25	1.78
DP51	7.58	36.8	0.12	0.511846+/-4	1.02	1.67	2.03	1.78
DP52	7.23	41.3	0.11	0.511635+/-5	1.18	1.68	1.98	1.78
DP55	6.98	38.27	0.11	0.511631+/-4	0.11	1.77	2.07	1.78
DP60	9.67	51.22	0.11	0.511717+/-4	0.90	1.70	2.01	1.78
SQ29	10.49	53.46	0.12	0.511826+/-6	1.81	1.58	1.93	1.76
Pink biotite granite-gneiss facies								
DP23	10.28	55.69	0.11	0.511748+/-2	1.87	1.59	1.92	1.77
DP47	9.44	54.52	0.10	0.511641+/-5	1.33	1.65	1.95	1.77
DP57	5.4	30.02	0.11	0.511694+/-4	1.51	1.63	1.94	1.77
Pink porphyritic granite-gneiss facies								
DP27	5.	29.24	0.10	0.511596+/-4	0.75	1.70	1.99	1.76
Volcanic Rocks								
DP28B	3.1	13.8	0.14	0.511925+/-10	0.12	1.77	2.16	1.78
DP28C	15.24	96.34	0.10	0.511622+/-2	3.29	1.53	1.82	1.78
DP31	4.4	30.1	0.09	0.511526+/-3	3.08	1.56	1.83	1.78
DP33C	11.17	63.32	0.11	0.511625+/-3	0.80	1.71	2.01	1.78
Lau de Já Orthogneisses								
FS98A	4.76	25.3	0.11	0.511704+/-5	0.70	1.72	2.03	1.82

3.5. DISCUSSION

Magmatic arcs record the complex history of magma generation, segregation and transport, as subduction-related magma interacts with the preexisting crust (Matzel et al., 2006).

Schaltegger et al. (2009) reveal that the placement of magmatic liquids in the intermediate and upper crust took place at varying time intervals: the batholiths can grow during more than 100 million years (e.g. Matzel et al., 2006) due to individual magmatic pulses during a much shorter

time horizon, that is, in the range of several tens to one hundred thousand years (e.g. Michel et al., 2008).

Glazner et al. (2004) present field and geochronological evidence indicating that at least some large, superficially homogeneous plutonic bodies were formed by amalgamation of numerous repeated and discrete injections of magmatic pulses, and that field or petrological records of its composite origins may be subtle.

The arguments mentioned above allow to present the Caracol Suite here as a large NS-trending plutonic body, approximately 200 km long and 50 km wide. It comprisses relatively homogeneous rocks that are here individualized into petrographic facies, and present crystallization age between 1776±13 and 1748±19 Ma (U-Pb, LA-ICP MS, zircon). The assembly is thoroughly deformed by low-angle structures with vergence towards the west, and shows deformation increasing towards the northern portion of the area.

Taking into account the different contributions proposed for the compartmentation of the Rio Apa Block discussed above, here we corroborate the existence of the two terranes (western and eastern) previously proposed by Cordani et al. (2010), on the basis of the distribution of Sm-Nd model ages. According to the authors, the western terrane is older, with T_{DM} ages between 2.5 and 2.6 Ga, and the eastern terrane shows model ages between 2.2 and 2.3 Ga.

Geophysical images (Ternary images and Analytic Signal 3D) of aerial survey available for the study area were previously extensively explored (Faleiros et al., 2015; Lacerda Filho et al., 2016). Such images were a complement to the field work in this paper, and modifications were suggested to the various granitic-gneissic bodies with local terminologies recently presented for the eastern terrane (Remédio et al., 2014; Faleiros et al., 2015; Lacerda Filho et al., 2016).

The geochronological and isotopic data along with petrographic analyses and field mapping data have contributed to the lithological and geochronological understanding of the eastern terrane. All laboratory and field data presented so far (Araújo et al., 1980; Lacerda Filho et al., 2006, 2016; Lacerda Filho, 2015; Cordani et al., 2010; Pavan et al., 2014; Remédio et al., 2015; Faleiros et al., 2015) were considered in order to better understand the Rio Apa Block.

The lithological and geochronological framework of the eastern terrane is represented by the Lau de Já orthogneiss, intrusive and effusive rocks of the Caracol Suite, the metavolcanic-sedimentary rocks of the Alto Tererê Group, the Paso Bravo Province, which outcrops in Paraguay, and the final magmatism, represented by the Rio Perdido Suite.

The Lau de Já orthogneiss, with a Sm-Nd T_{DM} age of 2.03 Ga and crystallization age of ca. 1822 ± 6 Ma (U-Pb, LA-ICP MS, zircon), might have been formed in magmatic arc setting, likely in an intra-oceanic island arc (Fig. 3.11A). The positive ε_{Nd} value of 0.48 suggests limited contamination with older crust.

Subsequently, in a magmatic arc environment, plutons of the Caracol Suite were emplaced (Fig. 3.10B). The granite-gneisses show crystallization ages ranging from 1776±13 to 1748±19 Ma (U-Pb, LA-ICP MS, zircon), Sm-Nd T_{DM} ages from 2.25 to 1.81, and Lu-Hf model ages between 2.30 and 1.92 Ga. Values of ε_{Nd} (t) exhibit positive to slightly negative values (3.25 to -1.75). ε_{Hf} (t) range from 5.32 to -4.64, suggesting some degree of older crust assimilation in the parental mantle magma.

This work clarifies that the southern portion of the Rio Apa Block previously mapped as the Paso Bravo Province, near Sargento Luis Felix Lopes, Paraguay, is an extension of the Caracol Suite. Sample DP-12, collected from this locality, yields a crystallization age of 1748±19 Ma (U-Pb, LA-ICP MS, zircon; Fig. 3.8C) as well as share the main characteristics of the predominant facies, pink hololeucocratic granite-gneiss. Therefore, the Paso Bravo Province is presented in the geological outline of this work.

Volcanic rocks present Sm-Nd T_{DM} model ages, between 2.16 and 1.82 Ga and positive ε_{Nd} (t) values, between 0.11 and 3.29, which indicates that their parental mantle magma has not undergone significant contamination of older continental crust. These volcanic rocks are presented in this work with preliminary results. It would be very interesting to deepen in field mapping, petrographic, geochronological and isotopic analyzes for a better understanding this effusive rocks and to correlate it (or not) with the rocks already described in the eastern part of the Rio Apa Block.

Two hypotheses are raised for the Alto Tererê Group. The first one was proposed by Lacerda Filho et al. (2016) and suggests that this segment is a back-arc basin, filled with material derived from erosion of the western and eastern terranes. The second hypothesis, accepted in the present work, proposes that the original sedimentary rocks of the Alto Tererê Group are derived from erosion of rocks of the Caracol Suite and the Lau de Já Orthogneiss, in the eastern terrane, before amalgamation of the two terranes (Fig. 3.11B and C) in view of the argument that the rocks of the Alto Tererê Group are restricted to the eastern part of the Rio Apa Block.

The results of U-Pb analyses shows three mains peakes: 1817, 1787 and 1777 Ma, this last, considered as the maximum age of sedimentation. It is noteworthy that the first peak is more

discrete. However, three younger crystals were dated to the following ages: 1582, 1472, and 1345 Ma. Because they are few grains (only one for each age), it shows the need for this sample to be complemented with more crystals to be analyzed for better understanding respect to the younger ages related to these three crystals.

Nevertheless, if we still consider the largest amount of crystals and the possible final sedimentation in 1777 Ma, these ages are consistent with the arguments that the Alto Tererê Group comes from the sedimentation of the eastern terrane, since the basement rocks (Lau de Já orthogneisses) and the Caracol Suite granite-gneisses that date from 1822 to 1748 Ma. We understand that this is a daring proposal when we use as an argument only the U-Pb analysis, since they are preliminary data and need to be complemented.

However, it is indispensable to observe the Sm-Nd model ages for the Alto Tererê Group that shows provided values from 1.90 to 2.01 Ga which are also consistent with the model ages of the Caracol Suite, and Lau de Já Orthogneiss, in the eastern terrane. This comparison is made taking into account the Sm-Nd model ages as one of the criteria touchstone to distinguish the eastern and western terranes by Cordani et al. (2010).

Finally, the rocks of the Alto Tererê Group outcrops only in the eastern terrane, and are not observed in the western part of the Rio Apa Block, reinforcing the suggestion that the two terranes were not united during the sedimentation of the Alto Tererê Group.

Younger rocks are also exposed in the southern portion of the eastern terrane, such as the intrusions of the Paso Bravo Province, with age of 1559±55 Ma (U-Pb, SHRIMP, zircon; Cordani et al., 2010), which is restricted to Paraguay.

Based on Ar-Ar results and on the compilation of existing K-Ar and Ar-Ar data presented by Cordani et al. (2010), a metamorphic event likely took place at ca. 1.3 Ga throughout the whole Rio Apa Block. The accretion of the terrane may have occurred during this episode resulting in low-angle deformation with vergence towards the west, observed in all the rocks of the Rio Apa Block (Figure 3.11C).

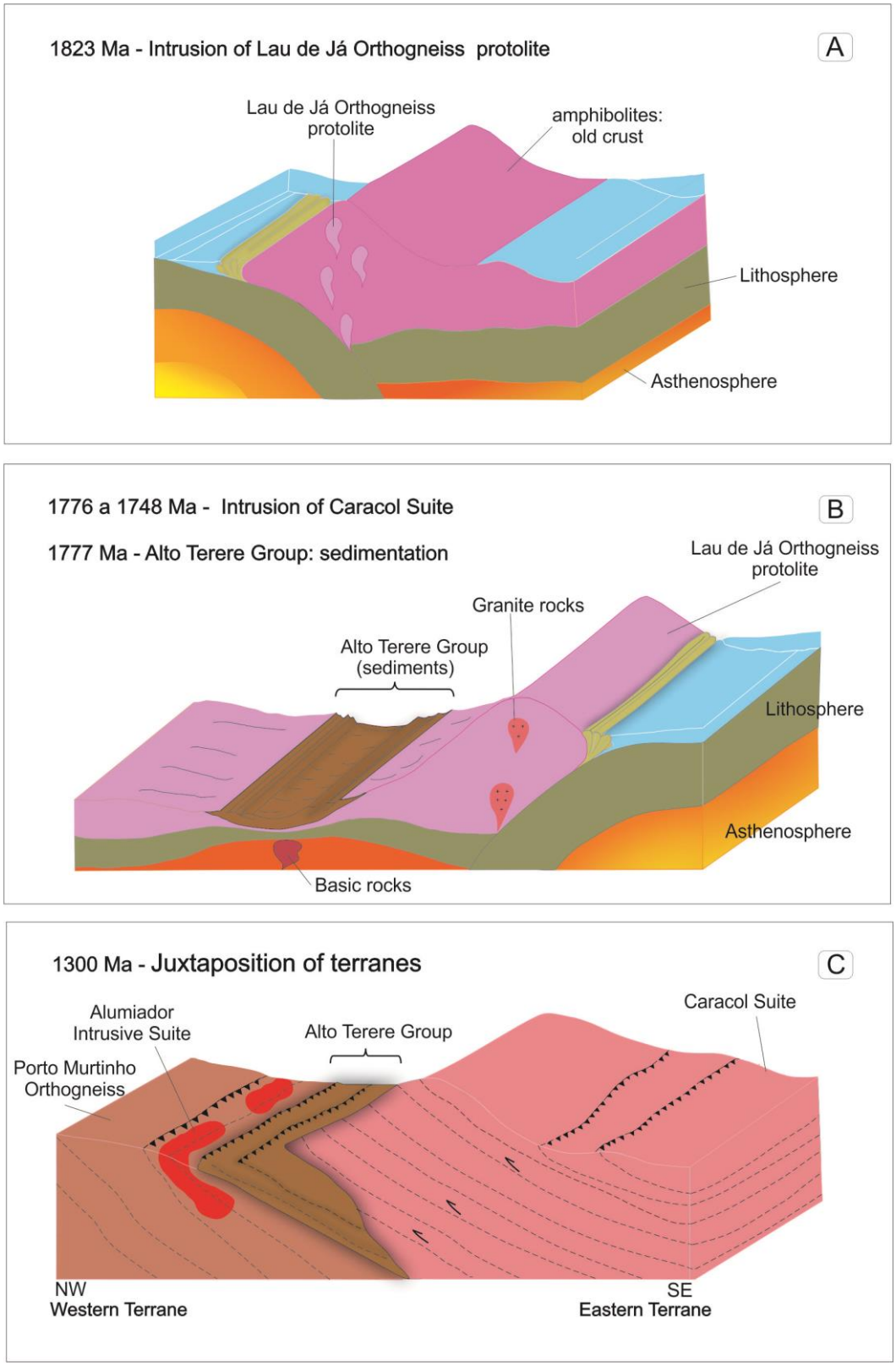

Figure 3.11. Schematic diagram for the tectonic evolution of the eastern terrane of the Rio Apa Block, including the Caracol Suite and country rocks. (A) In an older crust marked by amphibolite xenoliths, there is the intrusion (1822 Ma) of the Lau de Já orthogneiss protolith.

Continuation Figure 3.11. (B) From 1776 to 1748 Ma, the intrusion of the Caracol Suite took place. The country rock is the Lau de Já orthogneiss. The sedimentation in the back arc basin of the Alto Tererê Group may have been roughly coeval with the emplacement of the Caracol Suite; (C) Juxtaposition of both terranes through thrusting of the eastern terrane over the western terrane towards NW. Observe that the Amoguijá Intrusive Supersuite in the western terrane, here represented by the Alumiador Intrusive Suite, has already intruded into the basement, Orthogneiss Porto Murtinho.

The dike swarms of the Rio Perdido Intrusive Suite, observed in both terranes, are considered the last magmatic event in the Rio Apa Block, and represent basic magmatism in extensional settings, with baddeleyite U-Pb age of 1110 Ma (U-Pb, SHRIMP, badeleite; Teixeira et al., 2016).

Plens et al. (submitted a) sugest that all of the eastern terrane was deformed in three dephormacional phases, where the second one is more pronounced. This most prominent deformational phase had its main foliation (schistosity, normally observed with values from SE to NW) shows some changes in its characteristic trajectory. These changes are interpreted as coming from progressive deformation and deformational partitioning. Fossen et al (in press) suggest the term deformation partitioning, and they highlight the importance of lithology and rheology during the structural evolution of a region. The authors state that the partitioning of deformation occurs as a result of geological variations controlled by the lithologic composition or thermal conditions of the region during the deformation.

At the eastern portion of the mapped area, where structural domain 2 is located, Faleiros et al. (2015), Remédio et al. (2015) and Lacerda Filho et al. (2016) identify a third terrane of the Rio Apa Block. Faleiros et al. (2015) call it the southeast terrane, and Lacerda Filho et al. (2016) call it the eastern terrane because they rename the eastern terrane of Cordani et al. (2010) as the central terrane. Plens et al. (submitted a), suggest that a possible local alteration in the foliation path, which shows a change in orientation from SE-NW to N-S. These changes can be observed in the geological map of figure 3.3 where the main foliation of the deformational phase D_2 is modificated to N-S. This occurs located along the limit where the mentioned authors locate the contact between the terranes; thus, we do not rule out the possibility of a third segment for the Rio Apa Block, however, studies and complementary data are necessary to support this.

Regarding the geotectonic model, based on the geological history supported by the geochronological and isotopic results, the rocks of the Caracol Suite may be correlated with granitic and gneiss rocks of the Chiquitania Complex in the southwestern Amazonian Craton.

Borger et al. (2005) report ages of 1764±12 Ma and 1333±6 Ma (U-Pb, SHRIMP, zircon) for these rocks, the younger being interpreted as a metamorphic event.

Following the same concept, authors such as Redes et al. (2015, 2016) and Faleiros et al. (2015) correlate the Correreca Granite in the region between Rincon del Tigre and Santo Corazon, in eastern Bolivia with the plutonic rocks of the Alumiador Intrusive Supersuite, whose approximate age is 1.8 Ga in the western terrane of the Rio Apa Block. Vargas-Mattos et al. (2010) report crystallization age of 1894±13 (Pb-Pb, evaporation, zircon) for the Correreca Granite and Redes et al. (2016) the age of 1855±5 (U-Pb, SHRIMP, zircon) which may be correlated with rocks of the granitic western terrane.

The proposal of the Rio Apa Block as a crustal segment of the southwestern portion of the Amazonian Craton (Ruiz, 2005; Lacerda Filho et al.,2006, 2016; Cordani et al.,2010; Faleiros et al., 2015) corroborates the initial compartmentation of the Amazonion Craton proposed by Almeida (1967). Among the supporting arguments, the following ones are the most significant: i) the carbonate layer (Paraguay Belt) covers from the southwestern portion of the craton in the region of Nova Xavantina in Mato Grosso to Serra do Bodoquena in Mato Grosso do Sul, where rocks of Rio Apa Block crop out; ii) the extension of the Alumiador Suite/Rio Apa Block, to Corumbá and Santo Corazon in Bolivia; iii) the Rio Perdido-Huanchaca LIP (1.1 Ga; Teixeira et al., 2016) coverege from the Paraguay/ Brazil border to the Bolivia/ Brazil border; iv) the Paraguay Belt borders physically and tectonically the Rio Apa Block as well as the Paraguá, Jauru and Rio Alegre Terranes in the southwest of the Amazonian Craton; v) the Tucavaca Aulacogen (Brasiliano) overlies rocks of the Paraguá/Sunsás Belt and the Rio Apa Block (Corumbá and Santo Corazon). These statements allow to assume that the Amazonian Craton, including its southern portion, the Rio Apa Block, would have behaved as a passive continental margin during the deposition of part of the Paraguay Belt units throughout its extension.

Based on geological, geochronological and isotopic data, Faleiros et al. (2015) propose that between 1950 and 1720 Ma, the Rio Apa Block could have been part of the southwestern Amazonian Craton (Ventuari-Tapajós Province), and later fragmented and dispersed as a microcontinent.

Ruiz (2005) and Cordani et al. (2010) also propose that ages around 1300 Ma (Ar-Ar hornblende, muscovite and biotite) obtained throughout the Rio Apa Block reflectiv metamorphic heating coeval with the San Ignácio Orogeny (Litherland et al., 1986; Bettencourt et al., 2010) in

the Paraguá Terrane. Faleiros et al. (2015) also state that in the period between 1310 and 1270 Ma, the proto-craton Rio Apa changed from an accretionary orogen to a collisional orogen, and was consolidated as a cratonic mass in approximately 1270 Ma, before the formation of Rodinia.

Other geotectonic correlations were raised during the reconstruction of models involving the South American cratonic components of Rodinia. Ramos & Vujovick (1993) placed the Rio Apa Block as part of the northwestern portion of the Rio de la Plata Craton; Ramos *et al.* (2010) suggest that the Rio Apa Block is located in the eastern portion of a pre-Grenvillian continental mass called Pampia; however, these authors still make reference to the Rio de la Plata Craton when they relate the Rio Apa Block with plutonic and volcanic rocks of the Caapucú Block (Fúlfaro, 1996; northern Paraguay). Ramos *et al.* (2010) argue that there is a channel more than 5000 m deep between the two blocks (Rio Apa and Caapucú) where gravimetric and magnetometric data show grabens with NNW-to-NW normal faults, the same that truncate the Rio Apa Block.

An alternative proposal (Casquet *et al.*, 2012) suggest that the Rio Apa Block, along with the Maz Terrane (west of the Pampean Sierras, Argentina; magmatic arcs and metasedimentary rocks), and the Arequipa Terrane (southern Peru; orthogneisses and metasedimentary rocks) are part of an important continental mass, the Mara Craton, which was amalgamated with the Amazonian Block at approximately 1.3 Ga.

Dragone *et al.* (2017) used gravity maps to suggest that the Rio Apa Block may cover a wider region than the one mapped by Cordani *et al.* (2010). This region includes the substrate of the Pantanal Basin, and extends over the southern limit of the Sunsas Province (Tassinari & Macambira, 1999). Dragone *et al.* (2017) report that studies carried out with gravity maps show that the Rio Apa Block has a positive gravimetric anomaly and thin continental crust (about 35 km), while the Amazonian Craton has negative gravimetric anomalies and thicker continental crust.

Therefore, the field mapping, the petrographic discussions, the geochronological analyzes obtained by the U-Pb method (LA-ICP MS in zircon), the isotopic data (Sm-Nd and Lu-Hf), together with the discussions about the structural and metamorphic geology presented in Plens et al (submitted a), leads us to agree with the proposal that the eastern land and, consequently, the Rio Apa Block as a whole be an extension to the south of the Amazonian Craton, as also proposed a number of authors in the recent literature (Ruiz, 2005; Lacerda Filho et al., 2006, 2016; Cordani et al., 2010; Faleiros et al., 2015). The studied rocks are presented in this work then, as correlated

with the rocks of the Chiquitania Complex in the Paraguá Terrane, southwest of the Amazonian Craton. Having the San Ignacio Orogeny of approximately 1.3 Ga affected the southwest and south of the Amazon Craton.

3.6. CONCLUSIONS

Field data, petrographic, geochronological and isotopic analyses of rocks from the mapped area, including the Lau de Já orthogneiss, Caracol Suite and the Alto Tererê Group allow to conclude that:

- The Lau de Já orthogneiss has singular characteristics in comparison to the rest of the rocks observed in the area, and shows partial assimilation by rocks of the Caracol Suite. The U-Pb zircon results revealed the oldest age of the eastern terrane (1822±6 Ma), with a ε_{Nd} positive value of 0.69 indicating little crustal contamination.
- The Caracol Suite constitutes a large plutonic body, with low-angle structures that verge towards the west, and progressive increase in the intensity of deformation towards the northern portion;
- The Caracol granitic-gneissic rocks were divided into six petrographic facies (pink hololeucratic granite-gneiss facies, pink biotite granite-gneiss facies, pink porphyritic granite-gneiss facies, pink amphibole granite-gneiss facies, gray amphibole biotite granite-gneiss facies, gray amphibole tonalite facies); the U-Pb geochronological data show crystallization ages between 1776±13 and 1748±19 Ma for the plutonic rocks; values of ε_{Nd} (3.25 to -1.75) and ε_{Hf} (5.32 to -4.64) are positive and negative, suggesting some degree of older crust assimilation by the parental magma.
- The Alto Tererê Group has its sedimentary portion represented by sillimanite-quartz schist, with U-Pb data showing four mains peaks of proveniances sources (1817, 1787 and 1777 Ma) indicating provenance mainly from rocks of the eastern terrane (Lau de Já orthogneiss and Caracol Suite);
- The studied rocks are presented in this work as correlated with the rocks of the Chiquitania Complex in the Paraguá Terrane, southwest of the Amazonian Craton, having the San Ignacio Orogeny of approximately 1.3 Ga affected the southwest and south of the craton area.

ACKNOWLEDGMENTS

The authors acknowledge the Laboratory of Geochronology of the University of Brasilia, the Postgraduate Program in Geology of the University of Brasilia, the Grupo de Pesquisa em Evolução Crustal e Tectônica (Guaporé), the Comissão de Aperfeiçoamento de Pessoal do Nível Superior (Capes), the Fundação de Amparo à Pesquisa do Estado de Mato Grosso (FAPEMAT), and the Instituto Nacional de Ciências e Tecnologia de Geociências da Amazônia (GEOCIAM) for the support during the development of this research.

BIBLIOGRAPHIC REFERENCES

Almeida, F.F.M., 1965. Geologia da Serra da Bodoquena (Mato Grosso), Brasil. Boletim de Geologia e Mineralogia, Departamento Nacional de Produção Mineral-DNPM, Rio de Janeiro. 219, 1-96.

Almeida, F. F. M., 1967. Origem e evolução da plataforma brasileira Rio de Janeiro, Boletim da Divisão de Geologia e Mineralogia. Boletim 241, 01-36.

Alvarenga, C.J.S., & Saes, G. S., 1992. Estratigrafia e sedimentologia do Proterozóico Médio e Superior da região sudeste do Cráton Amazônico. Revista Brasileira de Geologia, 22: 493-499.

Araújo, H.J.T., Montalvão, P.E.N., 1980. Geologia da Folha SF.21 e parte das Folhas SF.21-V-D e SF.21-X-C, sudoeste do Estado de Mato Grosso do Sul: operação 578/80 - DIGEO. Projeto Radam Brasil, Relatório Interno, Goiânia, 15 p.

Barros, A. M., Silva, R. H. da., Cardoso, O.R.F.A., Freire, F.A., Souza Jr., J.J., Rivetti, M., Luz, D.S., Palmeira, R.C., Tassinari, C.C.G., 1982. Geologia. In: Ministério das Minas e Energia. Projecto RADAMBRASIL, Folha SD. 21, Cuiabá. Rio de Janeiro: RadamBrasil, p. 25-192. (Levantamentos de Recursos Naturais, 26).

Bettencourt, J. S., Leite Jr., W. B., Ruiz, A. S., Matos, R., Payolla, B. L., Tosdal, R. M., 2010. The Rondonian-San Ignacio Province in the SW Amazonian Craton: An Overview. Jounal of South American Earth Sciences, 29: 28-46.

Boger S.D., Raetz M., Giles D., Etchart E., Fanning C.M. 2005. U-Pb Age data from the Sunsas Region of eastern Bolivia, evidence for the allochthonous origin of the Paragua Block. *Precambrian Research*, 139:121-146.

Brito Neves, B. B., 1995. A tafrogênese estateriana nos blocos paleoproterozoicos da América do Sul e processos subsequentes. Geonomos, Belo Horizonte. 3(2):1-21.

Brito Neves, B. B. 2011. The Paleoproterozoic in the South-American continent: Diversity in the geologic time: Journal of South American Earth Sciences, 32: 270-286.

Brito Neves, B.B., Fuck, R.A., 2014. The basement of the South American platform: half Laurentian (N–NW) + half Gondwanan (E–SE) domains. Precambrian Research 244, 75–86.

Brittes, A.F.N., Sousa M.Z.A., Ruiz A.S., Batata E.F., Lafon J.M., Plens D.P., 2013. Geology, petrology and geochronology (Pb-Pb) of the Serra da Bocaina Formation: evidence of an Orosirian Amoguijá Magmatic Arc in the Rio Apa Terrane, south of the Amazonian Craton. Brazilian Journal of Geology, 43(1): 48-69.

Brittes, A.F.N., Sousa M.Z.A., Ruiz A.S., Batata E.F., Lafon J.M., (em prep..). Petrologia e Geocronologia (U-Pb/SHRIMP e Sm-Nd) Da Formação Serra Da Bocaina: Implicações Sobre A Evolução Do Arco Magmático Amoguijá No Bloco Rio Apa – Sul Do Craton Amazônico

Bühn, B., Pimentel, M. M., Matteini, M., Dantas, E. L., 2009. High spatial resolution analysis of Pb and U isotopes for geochronology by laser ablation multi-collector inductively coupled plasma mass spectrometry (LA-MC-ICP-MS). Anais da Academia Brasileira de Ciências, 81: 1-16.

Casquet, C., Rapela, C.W., Pankhurst, R.J., Baldo, E.G, Galindo C., Fanning C.M., Dahlquist, J.A. Saavedra, J. 2012. A history of Proterozoic terranes in southern South America: From Rodinia to Gondwana. Geoscience Frontiers, 3(2):137- 145 p.

Cordani, U, G., Teixeira, W., Tassinari, C. C. G., Ruiz, A. S., 2010. The Rio Apa Craton in Mato Grosso do Sul (Brazil) and Northern Paraguay: geochronological evolution, correlations and tectonic implications for Rodinia and Gondwana. American Journal of Science, 310, 1-43.

Corrêa, J.A., Corrêa Filho, F.C.L., Scislewski, G., Cavallon, L.A., Cerqueira, N.L.S., Nogueira, V.L., 1976. Projeto Bodoquena - Relatório Final, MME/DNPM, Convênio DNPM/CPRM, Superintendência Regional de Goiânia.

De Paolo, D.J., 1981. A neodymium and strontium isotopic study of the Mesozoic calc-alkaline granitic batholiths of the Sierra Nevada and Peninsular Ranges, California. Jounal Geophysical Research 86: 10470-10488.

Del'Arco, J.O., Silva R.H., Tarapanoff I., Freire F.A., Pereira L.G.M., Souza S.L., Luz J.S., Palmeira R.C.B., Tassinari, C.C.G., 1982. Folha SE.21. Corumbá e Parte da Folha SE 20. Ministério das Minas e Energia, Projeto Radam Brasil - Geologia, Rio de Janeiro. 27, 25-160.

Faleiros, F. M., Pavan, M., Remédio, M., Rodrigues, J.B., Almeida, V.V., Caltabeloti,V.V., Caltabeloti, F.P., Pinto, L., Oliveira, A. A., Pinto de Azevedo, E. J., Costa,V.S., 2015. Zircon U-Pb ages of rocks from the Rio Apa Crátonic Terrene (Mato Grosso do Sul, Brazil): New insights for its connection with the Amazonian Craton in pre-Gondwana times. Gondwana Research, 34: 187 – 204.

Gioia, S.M. & Pimentel, M.M., 2000. The Sm-Nd isotopic method in the Geochronology Laboratory of the University of Brasília. Anais da Academia Brasileira de Ciências, 72(2), 219-254.

Glazner, A.F., Bartley, J.M., Coleman, D.S., Gray,W., Taylor, Z., 2004. Are plutons assembled over millions of years by amalgamation from small magma chambers? GSA today 14 (4/5), 4–11.

Godoi, H.O., Martins, E.G., Mello, C.R., Scislewski, G., 1999. Geologia MME/SG. Projeto Radam Brasil. Programa Levantamentos Geológicos Básicos do Brasil. Folhas Corumbá (SE. 21-Y-D), Aldeia Tomázia, (SF. 21-V-B) e Porto Murtinho (SF. 21-V-D), Mato Grosso do Sul, escala 1: 250.000.

Godoy, A.M., Manzano, J.C., Araújo, L.M.B., Silva, J.A., 2009. Contexto Geológico e Estrutural do Maciço Rio Apa, sul do Cráton Amazônico – MS. Revista Brasileira de Geociências, 28: 485-499.

Lacerda Filho, J.V., Brito, R.S.C., Silva, M.G., Oliveira, C.C. De., Moreton, L.C., Martins, E.G., Lopes, R.C., Lima, T.M., Larizzatti, J.H., Valente, C.R., 2006. Geologia e Recursos Minerais do Estado de Mato Grosso do Sul. Programa integração, atualização e difusão de dados de geologia do Brasil. Convênio CPRM/SICME - MS, MME. 10 - 28.

Lacerda Filho, J. V. 2015. Bloco Rio Apa: Origem e evolução tectônica. PhD Dissertation. Institute of Geology. Brasília University, 181 p.

Lacerda Filho, J.V., Fuck, R. A., Ruiz, A. S., Dantas, E. L., Scandolara, J. E., Rodrigues, J. B., Nascimento, N. D. C., 2016. Palaeoproterozoic tectonic evolution of the Alto Tererê Group, southernmost Amazonian Craton, based on field mapping, zircon dating and rock geochemistry. Journal of South American Earth Science. 65, 122 – 141.

Litherland, M., Annells, R.N., Appleton, J.D., Berrangé, J.P., Bloomfield, K., Burton, C.C.J., Darbyshire, D.P.F., Fletcher, C.J.N., Hawkins, M.P., Klinck, B.A., Lanos, A., Mithcell, W.I., O Connor, E.A., Pitfield, P.E.J., Power, G. E Webb, B.C. 1986. The Geology and Mineral Resources of the Bolivian Precambrian Shield. British Geological Survey. Overseas Memoir 9. London, Her Majesty's Stationery Office. 140 p.

Ludwig, K.R., 2003. Isoplot 3.00 - a geochronological toolkit for Microsoft Excel. Berkeley 1240 Geochronology Center, Special, Publication No 4.

Matteini, M., Dantas, E.L., Pimentel, M.M., Buhn, B., 2010. Combined U-Pb and Lu-Hf isotope analyses by laser ablation MC-ICP-MS: methodology and applications. Anais da Academia Brasileira de Ciências, 82, 479-491.

Matzel, J.E.P., Bowring, S.A., Miller, R.B., 2006. Time scales of pluton construction at differing crustal levels; examples from the Mount Stuart and Tenpeak intrusions, north Cascades. Washington. Geol. Soc. America Bull. 118, 1412–1430.

Michel, J., Baumgartner, L., Putlitz, B., Schaltegger, U., Ovtcharova, M., 2008. Incremental growth of the Patagonian Torres del Paine laccolith over 90 ky, Patagonia. Geology 36, 459–462.

Nogueira, S.F., Sousa, M.Z.A., Ruiz, A.S., Batata, M.E.F., Cabrera, R.F., Costa, J.T. 2013. Granito Aquidabã - Suíte Intrusiva Alumiador - Sul do Cráton Amazônico Geologia, Petrografia e Geoquímica. *In*: 13º Simpósio de Geologia da Amazônia, Belém.

Pavan, M., Faleiros, F.M., 2014. Geologia da borda W do Terreno Rio Apa, SE do Craton Amazônico, SW do Mato Grosso do Sul. In: Anais do 47° Congresso Brasileiro de Geologia, Salvador, p. 1668.

Petford, N., Cruden, A.R., McCaffrey, K.J.W., Vigneresse, J.L., 2000. Granite magma formation, transport and emplacement in the Earth's crust. Nature 408, 669–673.

Plens, D.P., Ruiz, A.S., Sousa, M.Z.A., Batata, E.F., Lafon, J.M., Brittes, A.F.N., 2013. Cerro Porã Batholith: post-orogenic A-type granite from the Amoguijá Magmatic Arc – Rio Apa Terrane – South of the Amazonian Craton. Brazilian Journal of Geology, 43 (3): 515-534.

Plens, D.P., Pimentel, M. M., Ruiz, A.S., Fuck, R. A. Lithostructural framework of the eastern terrane of the Rio Apa Block - Southern Amazonian Craton. Brazilian Journal of Geology – Submitted a.

Ramos, V. A; Vujovick, G I. 1993. Alternativas de la evolución del borde occidental de America del Sur durante el Proterozoico. Revista Brasileira de Geociências, 23(3): 94-200.

Ramos, V.A., Vujovich, G., Martino, R., Otamendi, J. 2010. Pampia: a large Cratonic block missing in the Rodinia supercontinent. Journal of Geodynamics, 50, 243-255.

Redes, L. A., Sousa, M. Z. A., Ruiz, A. S., Lafon, J. M., 2015. Petrogeneses and U-Pb and Sm-Nd geochronology of the Taquaral granite: record of an Orosirian continental magmatic arc in the region of Corumbá – MS. Brazilian Journal of Geology. 45(3), 431 – 451.

Redes, L. A., Pimentel, M. M., Ruiz, A. S., Matos, G. R. S., 2016. Granito Correreca - um registro magmático orosiriano no oriente boliviano: implicações tectônicas e estratigráficas. In: Anais do 48 Congresso Brasileiro de Geologia – Porto Alegre – Brazil.

Remédio, M.J., Costa, V.S., Almeida, V.V., Pinto-Azevedo, E.J.H.C.B., Ferrari, V.C., Brumatti, M., Pinto, L.G.R., Caltabeloti, F.P., Faleiros, F.M., 2013. Programa Geologia do Brasil – PGB. Fazenda Margarida. Folha SF.21-X-C-IV. Estado de Mato Grosso do Sul. Carta Geológica. São Paulo: CPRM, 2013, 1 mapa colorido, 95 x 70 cm. Escala 1:100.000.

Ruiz, A. S., 2005. Evolução geológica do sudoeste do Cráton Amazônico região limítrofe Brasil-Bolívia – Mato Grosso. PhD Dissertation. Institute of Geosciences and Exact Sciences - Rio Claro Campus, Universidade Estadual Paulista. 245 p.

Ruiz, A. S., Sousa, M. Z. A., Lima, G. A., D'agrella Filho, M. S. (2014). Ar-Ar step heating ages for milonitic low angle shear zones rocks in the Rio Apa Terrane, South of the Amazonian Craton. 9th South American Symposium on Isotope Geology. São Paulo: CPGEO.

Santos, J. O. S., Hartmann, L. A., Gaudette, H. E., Groves, D. I., Mcnaughton, N. J., Fletcher, I. R., 2000. A new understanding of the Amazon Craton Provinces based on integration of field mapping and U-Pb and Sm-Nd Geochronology Gondwana Research, 3, 453-488.

Santos, J.O.S., Rizzotto, G.J., Potter, P.E., Mcnaughton, N.J., Matos, R.S., Hartmann, L.A., Chemale Jr, F. & Quadros, M.E.S., 2008. Age and Autochthonous Evolution of The Sunsás Orogen in the West Amazon Craton based on mapping and U-Pb Greochronology. Precambrian Research, 165, 120-152.

Santos, G. 2016. Granito Coimbra: Porção norte da Suíte Intrusiva Alumiador na região de Corumbá – MS – Terreno Rio Apa. Dissertação de mestrado, Instituto de Ciências Exatas e da Terra, Universidade Federal de Mato Grosso, 71p.

Schaltegger, U., Brack, P., Ovtcharova, M., Peytcheva, I., Schoene, B., Stracke, A., Marocchi, M., Bargossi, G.M., 2009. Zircon and titanite recording 1.5 million years of magma accretion, crystallization and initial cooling in a composite pluton (southern Adamello batholith, northern Italy). Earth Planet. Sci. Lett. 286, 208–218.

Tassinari, C.C.G., & Macambira, M.J.B., 1999. Geochronological provinces of the Amazonian Craton. Episodes. 38, 174-182.

Tassinari, C.C.G., Bettencourt, J.S., Geraldes, M.C., Macambira, M.J.B. & Lafon, J.M., 2000. The Amazonian Craton. In: Cordani, U.G., Milani, E.J., Thomaz-Filho, A. & Campos, D.A. (eds.). Tectonic Evolution Of South America, Rio de Janeiro. p. 41- 95.

Tassinari, C.G.C., Macambira, M.J.B., 2004. A Evolução Tectônica do Cráton Amazônico. In: Neto-Mantesso, V., Bartorelli, A, Carneiro, C. D. R., Brito-Neves, B.B. (eds). Geologia do Continente Sul-Americano: Evolução da Obra de Fernando Flávio Marques de Almeida. p. 471-486.

Teixeira, W., Geraldes, M.C., Matos, R., Ruiz, A.S., Saes, G., Vargas-Matos, G., 2010. A review of the tectonic evolution of the Sunsas belt, A review of the tectonic evolution on the Sunsas belt, SW portion of the Amazonian Craton. J. S. Am. Earth Sci. 29, 47 - 60.

Teixeira, W., Hamilton, M. A., Girardi, V. A. V., Faleiros, F. M. 2016. Key dolerite dyke swarms of Amazonia: U-Pb constraints on supercontinent cycles and geodynamic connections with global LIP events through time. *Acta Geologica Sinica (English Edition)*, 90 (supp. 1), 84-85, DOI: 10.1111/1755-6724.12902.

Trompette R., Alvarenga C. J. S., Walde D., 1998. Geological evolution of the Neoproterozoic Corumbá graben system (Brazil). Depositional context of the stratified Fe and Mn ores of the Jacadigo Group. Journal of South American Earth Sciences, 11, 587-597.

Ubrich H. H.G.J., Vlach S. R. F., Janasi V. A., 2001. O Mapeamento faciológico de rochas plutônicas. Revista Brasileira de Geociências, 31(2): 163-172.

Vavra, G., Gebauer, D., Schim, R., Compston, W., 1996. Multiple zircon growth and recrystallization during polyphase Late Carboniferous to Triassic metamorphism in granulites of the Ivrea Zone (Southern Alps): and ion microprobe (SHRIMP) study. Contributions to Mineralogy and Petrology, 122: 337-358.

Vargas-Mattos G.L. 2010. Caracterização geocronológica e geoquímica dos granitos proterozoicos: implicação para a evolução crustal da borda SW do Cráton Amazônico na Bolívia. Faculdade de Geologia, Universidade do Estado do Rio de Janeiro, Tese de Doutoramento, 164 p

Wernick, E. 2004. Conceitos fundamentais e classificação modal, química, termodinâmica e tectônica. Editoral Unesp. 665 p.

Wiedenbeck, M., Allé, P., Corfu, F., Griffin, W.L., Meier, M., Oberli, F., Von Quadt, A., Roddick, J.C., Spiegel, W. 1995. Three natural zircon standards for U-Th-Pb, Lu-Hf, trace element and REE Analyses. Geostandards Newsletter, 19:1-23.

Wiens, F.M.S. 1986. Zur lithostratigraphischen, petrographischen und strukturellen Entwicklung des Rio-Apa Hochlandes, Nordost Paraguay: Clausthal, Geologisches Institut der Technischen Universitat Clausthal, Clausthaler Geowissenschaftliche, Ph. D. dissertation, 19, 280 p.

Capítlo 4 - CONSIDERAÇÕES FINAIS E CONCLUSÕES

A abordagem multidisciplinar desenvolvida neste trabalho envolveu mapeamento geológico e estrutural, análises petrográficas, geocronológicas pelo método U-Pb (LA-ICP-MS) em cristais de zircão, isotópicas, Lu-Hf (LA-ICP-MS) em zircão e Sm-Nd em rocha total. Os resultados adiquiridos e discutidos a seguir, são uma complementação aos dados apresentados na literatura a fim da melhor compreensão sobre o quadro geocronológico, tectônico e estrutural do terreno oriental, bem como do Bloco Rio Apa como um todo.

4.1. CONTEXTOS PETROLÓGICO E GEOCRONOLÓGICO

O quadro litogeocronológico do terreno oriental é representado nesse trabalho pelo Ortognaisse Lau de Já, as rochas granito-gnaissicas da Suíte Caracol, as metavulcano-sedimentares do Grupo Alto Tererê, bem como a Província Paso Bravo (que aflora em território paraguaio) e o magmatismo final, Suíte intrusiva Rio Perdido. Na área objeto não aflora a Província Passo Bravo; a Suíte Rio Perdido não é detalhada por se tratar de um episódio posterior ao evento de justaposição dos blocos oriental sobre o ocidental e ocorrer em todo o Bloco Rio Apa.

O Ortognaisse Lau de Já aflora na porção NNE da área como estreito xenólito (aproximadamente 3 km) assimilado pela fácies predominante da Suíte Caracol, constituindo uma faixa de afloramentos descontínuos e restritos. Apresenta a idade mais antiga da área (1822 ± 6 Ma) e εNd positivo (0,69) sugerindo alguma participação de crosta antiga em sua formação, com idade modelo Sm-Nd TDM de 2.03 Ga.

A Suíte Caracol é constituída rochas graníticas com deformação intensa, que muitas vezes as caracterizam como granito-gnaisses, que abrange a grande maioria das rochas aflorantes no terreno oriental. Expõe-se segundo a direção N-S, com aproximadamente 190 km de comprimento e 50 km de largura em território brasileiro, prolongando-se por cerca de 65 km para o Paraguai, com largura entre 80 e 30 km, diminuindo a sul. Com base nos atributos de campo e nas características petrográficas, foram individualizadas seis fácies petrográficas: (i) granito-gnaisse hololeucocrático rosa; (ii) biotita granito-gnaisse rosa; (iii) granito-gnaisse porfirítico rosa; (iv) anfibólio granito-gnaisse rosa; (v) anfibólio biotita granito-gnaisse cinza; (vi) anfibólio tonalito cinza. A primeira é o termo predominante e perfaz cerca de 80% da suíte e as demais são

observadas como lentes orientadas segundo a direção preferencial NW na porção sul da suíte e, na parte norte, onde a deformação mostra-se mais intesa, as lentes seguem o padrão deformacional imposto, gerando dobras regionais. A idade de cristalização obtida para as rochas plutônicas da Suíte Caracol no presente trabalho é de 1776±13 e 1748±19 Ma (LA-ICPMS U-Pb data); Os dados de εNd apresentaram-se positivos a levemente negativos, entre 3.25 a -1.75 e os de εHf, negativos a positivos, oscilando entre -4.64 e 5.32, o que sugerem assimilação de crosta mais antiga pelo magma mantélico parental. Mostram idades modelos TDM Lu-Hf entre 1.92 e 2.30 Ga, e Sm-Nd entre 1.82 e 2.25 Ga.

Foram identificadas rochas vulcânicas na porção sudeste da área. Apesar do alto grau de alteração, foi possível caracterizá-las como lavas dacíticas de textura amigdaloidal. Os resultados de εNd positivos, entre 0,11 e 3,29, indicam pouca ou nenhuma contaminação crustal e TDM entre 1.82 e 2.16 Ga. A área de afloramento restrita e a falta de análises petrográficas, geocronológicas e isotópicas para estas rochas efusivas não nos permite correlacioná-las com alguma porção mapeada até então do terreno oriental, o que distingue os dados obtidos até então como preliminares e sugere a necessidade de novas análises.

O Grupo Alto Tererê é aqui proposto como uma bacia de *back-arc* preenchida por sedimentos provenientes das rochas do terreno oriental, anterior à sultura dos dois blocos. Embora trata-se de uma análise preliminar, arriscamos utilizar como um dos indicadores de tal premissa, os dados geocronológicos U-Pb em amostra da porção metassedimentar que mostram gráfico de probabilidade com pico destacado, interpretado como idade máxima de sedimentação em 1777 Ma. Ademais, os trabalhos publicados até então têm mostrado que terreno ocidental apresenta rochas com dados de cristalização entre 1.8 e 1.9 Ga (Lacerda Filho *et al.*, 2006, 2016; Cordani *et al.*, 2010; Brittes *et al.*, 2013; Plens *et al.*, 2013; Redes *et al.*, 2015; Faleiros *et al.*, 2015; Nogueira, 2015; Santos *et al.*, 2016; Souza *et al.*, 2017). Tais idades não são destacadas nos resultados da amostra analisada do Grupo Alto Tererê. Finalmente, o Grupo Alto Tererê aflora restritamente no terreno oriental do Bloco Rio Apa, o que reforça a sugestão de que os dois blocos não estavam unidos durante a sedimentação do Grupo Alto Tererê. As rochas sedimentares apresentaram valores de εNd positivos entre 1.03 e 2.00, o que sugere não participação de crosta mais antiga pelo magma mantélico parental. Mostram idades modelos T_{DM} Sm-Nd entre 1.90 e 2.01 Ga, coerentes com as rochas do terreno oriental.

4.2. CONTEXTO TECTÔNICO E ESTRUTURAL

Quanto ao contexto tectônico-estrutural do terreno em questão, os dados coletados em mapeamento geológico revelaram estruturas agrupadas em três principais fases deformacionais compressivas, F_1, F_2 e F_3, além de uma fase extensional.

A primeira fase deformacional inicialmente ocorre restrita ao embasamento e é responsável pela foliação de bandamento composicional metamórfico. Posteriormente, em processo de deformação progressiva, as rochas gnáissicas são dobradas, gerando foliação espaçada de clivagem de crenulação. Na Suíte Caracol a fase deformacional F_1 é responsável por foliação penetrativa do tipo xistosidade.

Subsequentemente, na Suíte Caracol, F_2 é responsável pelo dobramento da foliação S_1, gerando dobras, foliação do tipo clivagem de crenulação e xistosidade (S_2). A xistosidade é observada também nas rochas metassedimentares (Grupo Alto Tererê). Os processos de deformação progressiva também são identificados nesta fase de deformação, uma vez que a xistosidade, comumente orientada para NW com mergulhos em ângulos baixos, nas porções norte e extremo oeste assumem alterações em suas trajetórias. Em consequência, foram sugeridos três domínios estruturais para esta fase deformacional F_2: (i) domínio estrutural 1- porção central a sul com orientação predominante SE-NW, e ângulos de mergulho subhorizontalizados; (ii) domínio estrutural 2 - extremo oeste do terreno oriental, com estruturas preferencialmente orientadas para N-S; (iii) domínio estrutural 3 - porção norte da área com a deformação compressiva mais intensa.

A segunda deformação possivelmente esteja relacionada ao metamorfismo de aproximadamente 1300 Ma descrito na literatura (Cordani *et al.,* 2010; Ruiz *et al.,* 2014; Faleiros *et al.,* 2015; Lacerda Filho *et al.,* 2016) e relacionada com a justaposição dos terrenos oriental e ocidental, via cavalgamento de topo para NW e mergulhos de baixo ângulo. Para melhor apresentar e discutir tal premissa, o intuito inicial era realizar a análise de três amostras da Suíte Caracol pelo método LA-ICP-MS em cristais de titanita para a possível obtenção de informações sobre o evento metamórfico. Porém, por problemas instrumentais, não foi possível estabelecer tais dados.

Sugere-se que durante a atuação da fase F_2 as condições de temperaturas prevaleceram entre 300 e 400 ^{o}C em todo o terreno, principalmente nas porções dos domínios estrutural 1 e 2, em que a deformação é menos proeminente. Na porção norte da área, especialmente nas regiões

de rochas cisalhadas, muitas vezes milonitizadas e até xistosas, onde ocorre maior quantidade de zonas de cisalhamento, as temperaturas podem ter sido superiores a 600 ºC.

O evento deformacional F_3 é dúctil-rúptil em toda a extensão do Bloco Rio Apa; as estruturas observadas em meso- e microescala são dobras D_3, foliação de clivagem de crenulação S_3 e lineação L_3 de intersecção entre as foliações S_1 e S_2.

Quanto à abrangência geotectônica, com base na história geológica retratada pelos resultados geocronológicos e isotópicos, as rochas da Suíte Caracol podem tentativamente ser correlacionadas às rochas graníticas e gnáissicas aflorantes no Complexo Chiquitania do Terreno Paraguá no sudoeste do Cráton Amazônico. Boger *et al.* (2005) apresentam para estas rochas idades de cristalização de 1764 ± 12 Ma, e 1333 ± 6 Ma (U-Pb, SHRIMP, zircão). As últimas são interpretadas como pico de metamorfismo.

Seguindo a mesma concepção, autores como Redes *et al.* (2015, 2016) e Faleiros *et al*. (2015) correlacionam o Granito Correreca, na região entre Rincon del Tigre e Santo Corazon no oriente boliviano, com as rochas plutônicas da Suíte Intrusiva Alumiador, de idade ~1.8 Ga, no Terreno Ocidental. Vargas-Mattos *et al.* (2010) e Redes *et al.* (2016) apresentam idades U-Pb em zircão de 1894±13 (Pb-Pb, Evaporação, zircão)e 1855±5 Ma (U-Pb, SHRIMP, zircão), respectivamente, para o Granito Correreca.

Ruiz (2005) e Cordani *et al.* (2010) propõem ainda que idades em torno de 1300 Ma, registradas em toda a extensão do Bloco Rio Apa refletem aquecimento metamórfico, temporalmente correlato à Orogenia San Ignácio (Litherland *et al.*, 1986; Bettencourt *et al.*, 2010) no Terreno Paraguá.

Assim sendo, as análises geocronológicas obtidas pelo método U-Pb (LA-ICP MS em zircão) somadas aos dados isotópicos (Sm-Nd e Lu-Hf), às análises petrográficas, bem como a todo o mapeamento de campo estabelecido também no presente trabalho nos leva a concentir com a proposta de que o terreno oriental e, consequentemente o Bloco Rio Apa como um todo seja uma extensão a sul do Cráton Amazônico, conforme propoem também diversos autores na literatura recente (Ruiz, 2005; Lacerda Filho *et al*.,2006, 2016; Cordani *et* al.,2010; Faleiros *et* al., 2015).

O terreno oriental do Bloco Rio Apa então, como correlacionável com as rochas do Chiquitania Complex in the Paraguá Terrane, no sudoeste do Cráton Amazônico. Tendo a Orogenia San Ignácio que afeta a porção sudoeste do Cráton em aproximadamente 1.3 Ga, sido percursora também da justaposição dos terrenos oriental sobre o occidental.

Capítlo 5 - RECOMENDAÇÕES PARA TRABALHOS POSTERIORES

Uma abordagem exclusiva a respeito das rochas do embasamento beneficiaria a discussão sobre o significado tectônico do Ortognaisse Lau de Já. Trabalho de mapeamento geológico para melhor delimitação da área aflorante, acompanhado de análises laboratorias (petrográficas, geoquímicas, geocronológicas e isotópicas) com destaque para os xenólitos de anfibolitos incorporados às rochas gnáissicas, seria uma chave para o entendimento do ambiente tectônico em que o protólito destes gnaisses foi formado.

Por não terem sido descritas na literatura até então, as rochas vulcânicas também são um alvo potencial para futuros estudos. A delimitação da área de afloramento, além das mesmas análises sugeridas para os gnaisses do embasamento, seriam interessantes, principalmente as geocronológicas para assim sugerir uma possível correlação com alguma das rochas mapeadas até então no terreno oriental do Bloco Rio Apa.

Estudos envolvendo o Grupo Alto Tererê também seriam pertinentes, abrangendo tanto as rochas metassedimentares, quando as rochas básicas. No caso das rochas metassedimentares, novamente sugere-se aqui mapeamento de campo para a investigação de possíveis outras rochas constituintes desta porção, além dos silimanita-quartzo xistos. Maior quantidade de análises petrográficas, geoquímicas e geocronológicas nestas rochas ajudariam a compreender seu contexto tectônico e a esclarecer os debates recentes sobre sua proveniência e deposição. Análises envolvendo a porção metabásica do Grupo Alto Tererê seriam interessantes, uma vez que acrescentariam e enfatizariam os dados de Lacerda Filho *et al.* (2016).

Outro ponto fundamental para se aplicar o mapeamento geológico de detalhe, juntamente com todas as ferramentas que o antecedem, como a análise de imagens de satélite e aerolevantamentos geofísicos, é a porção leste do terreno estudado. Como parte do modelo estrutural proposto, tentativamente foi sugerida mudança na trajetória da foliação principal neste ponto da área. Conforme citado nos textos dos dois artigos, autores de trabalhos recentes (Faleiros *et al.*, 2015; Lacerda Filho, 2015) propõem a existência de um terceiro terreno acoplado ao Bloco Rio Apa. Uma hipótese não anula a outra, o que torna interessante investigação desta área com todas as análises propostas até o momento.

Por fim, seria de extrema importância um artigo publicado em periódicos de circulação internacional, abrangendo os terrenos ocidental e oriental. As discussões realizadas na presente

tese, agregadas aos melhoramentos citados acima, já seriam interessante contribuição relacionada ao contexto tectônico do Bloco Rio Apa. Uma vez descritas juntamente com informações de mesmo teor do terreno ocidental, ajudariam na compreensão do contexto tectônico do Bloco Rio Apa e agregariam dados aos trabalhos já publicados.

REFERENCIAS BIBLIOGRÁFICAS

Almeida, F.F.M., 1965. Geologia da Serra da Bodoquena (Mato Grosso), Brasil. Boletim de Geologia e Mineralogia, Departamento Nacional de Produção Mineral-DNPM, Rio de Janeiro. 219, 1-96.

Almeida, F. F. M., 1967. Origem e evolução da plataforma brasileira Rio de Janeiro, Boletim da Divisão de Geologia e Mineralogia. Boletim 241, 01-36.

Alvarenga, C.J.S., & Saes, G. S., 1992. Estratigrafia e sedimentologia do Proterozóico Médio e Superior da região sudeste do Cráton Amazônico. Revista Brasileira de Geologia, 22: 493-499.

Araújo, H.J.T., Montalvão, P.E.N., 1980. Geologia da Folha SF.21 e parte das Folhas SF.21-V-D e SF.21-X-C, sudoeste do Estado de Mato Grosso do Sul: operação 578/80 - DIGEO. Projeto Radam Brasil, Relatório Interno, Goiânia, 15 p.

Barros, A. M., Silva, R. H. da., Cardoso, O.R.F.A., Freire, F.A., Souza Jr., J.J., Rivetti, M., Luz, D.S., Palmeira, R.C., Tassinari, C.C.G., 1982. Geologia. In: Ministério das Minas e Energia. Projecto RADAMBRASIL, Folha SD. 21, Cuiabá. Rio de Janeiro: RadamBrasil, p. 25-192. (Levantamentos de Recursos Naturais, 26).

Bettencourt, J. S., Leite Jr., W. B., Ruiz, A. S., Matos, R., Payolla, B. L., Tosdal, R. M., 2010. The Rondonian-San Ignacio Province in the SW Amazonian Craton: An Overview. Jounal of South American Earth Sciences, 29: 28-46.

Boger S.D., Raetz M., Giles D., Etchart E., Fanning C.M. 2005. U-Pb Age data from the Sunsas Region of eastern Bolivia, evidence for the allochthonous origin of the Paragua Block. *Precambrian Research*, 139:121-146.

Brito Neves, B. B., 1995. A tafrogênese estateriana nos blocos paleoproterozoicos da América do Sul e processos subsequentes. Geonomos, Belo Horizonte. 3(2):1-21.

Brito Neves, B. B. 2011. The Paleoproterozoic in the South-American continent: Diversity in the geologic time: Journal of South American Earth Sciences, 32: 270-286.

Brittes, A.F.N., Sousa M.Z.A., Ruiz A.S., Batata E.F., Lafon J.M., Plens D.P., 2013. Geology, petrology and geochronology (Pb-Pb) of the Serra da Bocaina Formation: evidence of an Orosirian Amoguijá Magmatic Arc in the Rio Apa Terrane, south of the Amazonian Craton. Brazilian Journal of Geology, 43(1): 48-69.

Brittes, A.F.N., Sousa M.Z.A., Ruiz A.S., Batata E.F., Lafon J.M., (em prep..). Petrologia e Geocronologia (U-Pb/SHRIMP e Sm-Nd) Da Formação Serra Da Bocaina: Implicações Sobre A Evolução Do Arco Magmático Amoguijá No Bloco Rio Apa – Sul Do Craton Amazônico

Bühn, B., Pimentel, M. M., Matteini, M., Dantas, E. L., 2009. High spatial resolution analysis of Pb and U isotopes for geochronology by laser ablation multi-collector inductively coupled plasma mass spectrometry (LA-MC-ICP-MS). Anais da Academia Brasileira de Ciências, 81: 1-16.

Casquet, C., Rapela, C.W., Pankhurst, R.J., Baldo, E.G, Galindo C., Fanning C.M., Dahlquist, J.A. Saavedra, J. 2012. A history of Proterozoic terranes in southern South America: From Rodinia to Gondwana. Geoscience Frontiers, 3(2):137- 145 p.

Cordani, U, G., Teixeira, W., Tassinari, C. C. G., Ruiz, A. S., 2010. The Rio Apa Craton in Mato Grosso do Sul (Brazil) and Northern Paraguay: geochronological evolution, correlations and tectonic implications for Rodinia and Gondwana. American Journal of Science, 310, 1-43.

Corrêa, J.A., Corrêa Filho, F.C.L., Scislewski, G., Cavallon, L.A., Cerqueira, N.L.S., Nogueira, V.L., 1976. Projeto Bodoquena - Relatório Final, MME/DNPM, Convênio DNPM/CPRM, Superintendência Regional de Goiânia.

De Paolo, D.J., 1981. A neodymium and strontium isotopic study of the Mesozoic calc-alkaline granitic batholiths of the Sierra Nevada and Peninsular Ranges, California. Jounal Geophysical Research 86: 10470-10488.

Del'Arco, J.O., Silva R.H., Tarapanoff I., Freire F.A., Pereira L.G.M., Souza S.L., Luz J.S., Palmeira R.C.B., Tassinari, C.C.G., 1982. Folha SE.21. Corumbá e Parte da Folha SE 20. Ministério das Minas e Energia, Projeto Radam Brasil - Geologia, Rio de Janeiro. 27, 25-160.

Faleiros, F. M., Pavan, M., Remédio, M., Rodrigues, J.B., Almeida, V.V., Caltabeloti,V.V., Caltabeloti, F.P., Pinto, L., Oliveira, A. A., Pinto de Azevedo, E. J., Costa,V.S., 2015. Zircon U-Pb ages of rocks from the Rio Apa Crátonic Terrene (Mato Grosso do Sul, Brazil): New insights for its connection with the Amazonian Craton in pre-Gondwana times. Gondwana Research, 34: 187 – 204.

Fossen H. 2012. *Geologia Estrutural*. Trad. de Fabio R.D. de Andrade. São Paulo: Oficina de Texto, 584 p.

Fossen, H., Calavlcante, G. C. G., Pinheiro, R. V. L., Archanjo, C. J., *Article in Press*. Deformation– Progressive or multiphase? Journal of Structural Geology.

Fúlfaro, V.J., 1996. Geology of Eastern Paraguay. In: Comin-Chiaramonti, P., Gómes C.B., (Eds.) Alkaline Magmatism in Central and Eastern Paraguay: Relationship with Coeval Magmatism in Brazil. Fapesp, 17–29, Sao Paulo.

Gioia, S.M. & Pimentel, M.M., 2000. The Sm-Nd isotopic method in the Geochronology Laboratory of the University of Brasília. Anais da Academia Brasileira de Ciências, 72(2), 219-254.

Godoi, H.O., Martins, E.G., Mello, C.R., Scislewski, G., 1999. Geologia MME/SG. Projeto Radam Brasil. Programa Levantamentos Geológicos Básicos do Brasil. Folhas Corumbá (SE. 21-Y-D), Aldeia Tomázia, (SF. 21-V-B) e Porto Murtinho (SF. 21-V-D), Mato Grosso do Sul, escala 1: 250.000.

Godoy, A.M., Manzano, J.C., Araújo, L.M.B., Silva, J.A., 2009. Contexto Geológico e Estrutural do Maciço Rio Apa, sul do Cráton Amazônico – MS. Revista Brasileira de Geosciências, 28: 485-499.

Lacerda Filho, J.V., Brito, R.S.C., Silva, M.G., Oliveira, C.C. De., Moreton, L.C., Martins, E.G., Lopes, R.C., Lima, T.M., Larizzatti, J.H., Valente, C.R., 2006. Geologia e Recursos Minerais do Estado de Mato Grosso do Sul. Programa integração, atualização e difusão de dados de geologia do Brasil. Convênio CPRM/SICME - MS, MME. 10 - 28.

Lacerda Filho, J. V. 2015. Bloco Rio Apa: Origem e evolução tectônica. Tese de Doutorado, Instituto de Geologia. Universidade de Brasília, 181 p.

Lacerda Filho, J.V., Fuck, R. A., Ruiz, A. S., Dantas, E. L., Scandolara, J. E., Rodrigues, J. B., Nascimento, N. D. C., 2016. Palaeoproterozoic tectonic evolution of the Alto Tererê Group, southernmost Amazonian Craton, based on field mapping, zircon dating and rock geochemistry. Journal of South American Earth Science. 65, 122 – 141.

Lima, G. A., Macambira, M. J. B., Sousa, M. Z. A., Ruiz, A. S., submetido. Suíte Intrusiva Rio Perdido: magmatismo intraplaca no sul do Cráton Amazônico – Terreno Rio Apa. Revista de Geologia da USP – Série Científica.

Litherland, M., Annells, R.N., Appleton, J.D., Berrangé, J.P., Bloomfield, K., Burton, C.C.J., Darbyshire, D.P.F., Fletcher, C.J.N., Hawkins, M.P., Klinck, B.A., Lanos, A., Mithcell, W.I., O Connor, E.A., Pitfield, P.E.J., Power, G. E Webb, B.C. 1986. The Geology and Mineral Resources of the Bolivian Precambrian Shield. British Geological Survey. Overseas Memoir 9. London, Her Majesty's Stationery Office. 140 p.

Ludwig, K.R., 2003. Isoplot 3.00 - a geochronological toolkit for Microsoft Excel. Berkeley 1240 Geochronology Center, Special, Publication No 4.

Matteini, M., Dantas, E.L., Pimentel, M.M., Buhn, B., 2010. Combined U-Pb and Lu-Hf isotope analyses by laser ablation MC-ICP-MS: methodology and applications. Anais da Academia Brasileira de Ciências, 82, 479-491.

Memeti, V., Paterson, S., Matzel, J., Mundil, R., Okaya, D., 2010. Magmatic lobes as "snapshots" of magma chamber growth and evolution in large, composite batholithes: An example from the Toulumne intrusion, Sierra Nevada, California. Geological Society of America Bulletin. 122 (11/12), 1912 – 1931.

Nogueira, S.F., Sousa, M.Z.A., Ruiz, A.S., Batata, M.E.F., Cabrera, R.F., Costa, J.T. 2013. Granito Aquidabã - Suíte Intrusiva Alumiador - Sul do Cráton Amazônico Geologia, Petrografia e Geoquímica. *In*: 13º Simpósio de Geologia da Amazônia, Belém.

Paschier C.W., Trouw R.A.J. 2005. *Microtectonics*. (2 Ed). Berlin: Springer, 353 p.

Pavan, M., Faleiros, F.M., 2014. Geologia da borda W do Terreno Rio Apa, SE do Craton Amazônico, SW do Mato Grosso do Sul. In: Anais do 47° Congresso Brasileiro de Geologia, Salvador, p. 1668.

Petford, N., Cruden, A.R., McCaffrey, K.J.W., Vigneresse, J.L., 2000. Granite magma formation, transport and emplacement in the Earth's crust. Nature 408, 669–673.

Plens, D.P., Ruiz, A.S., Sousa, M.Z.A., Batata, E.F., Lafon, J.M., Brittes, A.F.N., 2013. Cerro Porã Batholith: post-orogenic A-type granite from the Amoguijá Magmatic Arc – Rio Apa Terrane – South of the Amazonian Craton. Brazilian Journal of Geology, 43 (3): 515-534.

Plens, D.P., Pimentel, M. M., Ruiz, A.S., Fuck, R. A. Lithostructural framework of the eastern terrane of the Rio Apa Block - Southern Amazonian Craton. Brazilian Journal of Geology – Submitted a.

Plens, D.P., Pimentel, M. M., Ruiz, A.S., Fuck, R. A., Sousa, M. Z. A., Nascimento, N. D. C. Geology and geochronology (U-Pb, Sm-Nd And Lu-Hf) of the Caracol Suite and country rocks: implications to evolution magmatic and tectonics of Rio Apa Block - south of Amazonian Craton. Journal of South American Earth Science – Submitted b.

Ramos, V. A; Vujovick, G I. 1993. Alternativas de la evolución del borde occidental de America del Sur durante el Proterozoico. Revista Brasileira de Geociências, 23(3): 94-200.

Ramos, V.A., Vujovich, G., Martino, R., Otamendi, J. 2010. Pampia: a large Cratonic block missing in the Rodinia supercontinent. Journal of Geodynamics, 50, 243-255.

Ramsay J.G. 1967. Folding and Fracturing of Rocks. New York, McGrawHill.

Redes, L. A., Sousa, M. Z. A., Ruiz, A. S., Lafon, J. M., 2015. Petrogeneses and U-Pb and Sm-Nd geochronology of the Taquaral granite: record of an Orosirian continental magmatic arc in the region of Corumbá – MS. Brazilian Journal of Geology. 45(3), 431 – 451.

Redes, L. A., Pimentel, M. M., Ruiz, A. S., Matos, G. R. S., 2016. Granito Correreca - um registro magmático orosiriano no oriente boliviano: implicações tectônicas e estratigráficas. In: Anais do 48 Congresso Brasileiro de Geologia – Porto Alegre – Brazil.

Remédio, M.J., Costa, V.S., Almeida, V.V., Pinto-Azevedo, E.J.H.C.B., Ferrari, V.C., Brumatti, M., Pinto, L.G.R., Caltabeloti, F.P., Faleiros, F.M., 2013. Programa Geologia do Brasil –

PGB. Fazenda Margarida. Folha SF.21-X-C-IV. Estado de Mato Grosso do Sul. Carta Geológica. São Paulo: CPRM, 2013, 1 mapa colorido, 95 x 70 cm. Escala 1:100.000.

Ruiz, A. S., 2005. Evolução geológica do sudoeste do Cráton Amazônico região limítrofe Brasil-Bolívia – Mato Grosso. Tese de Doutorado, Instituto de Geociências e Ciências Exatas, Universidade Estadual Paulista, 14-245p.

Ruiz, A. S., Sousa, M. Z. A., Lima, G. A., D'agrella Filho, M. S. (2014). Ar-Ar step heating ages for milonitic low angle shear zones rocks in the Rio Apa Terrane, South of the Amazonian Craton. *9th South American Symposium on Isotope Geology*. São Paulo: CPGEO.

Santos, J. O. S., Hartmann, L. A., Gaudette, H. E., Groves, D. I., Mcnaughton, N. J., Fletcher, I. R., 2000. A new understanding of the Amazon Craton Provinces based on integration of field mapping and U-Pb and Sm-Nd Geochronology Gondwana Research, 3, 453-488.

Santos, J.O.S., Rizzotto, G.J., Potter, P.E., Mcnaughton, N.J., Matos, R.S., Hartmann, L.A., Chemale Jr, F. & Quadros, M.E.S., 2008. Age and Autochthonous Evolution of The Sunsás Orogen in the West Amazon Craton based on mapping and U-Pb Greochronology. Precambrian Research, 165, 120-152.

Santos, G. 2016. Granito Coimbra: Porção norte da Suíte Intrusiva Alumiador na região de Corumbá – MS – Terreno Rio Apa. Dissertação de mestrado, Instituto de Ciências Exatas e da Terra, Universidade Federal de Mato Grosso, 71p.

Sato, k., Basei M. A. S., Siga O. J., 2008. Novas técnicas aplicadas ao método U-Pb no CPGeo - IGc/USP: avanços na digestão química, espectrometria de massa (TIMS) e exemplos de aplicação integrada com SHRIMP. *In:* Geol. USP Série Científica, 8: 77-99.

Schobbenhaus, C. & Neves B. B. B., 2003. A Geologia do Brasil no Contexto da Plataforma Sul-Americana. In: Brasil L. A. Bizzi, C. Schobbenhaus, R. M. Vidotti e J. H. Gonçalves (eds.) Geologia, Tectônica e Recursos Minerais do CPRM, Brasília, 2003. 64 p.

Tassinari, C.C.G., & Macambira, M.J.B., 1999. Geochronological provinces of the Amazonian Craton. Episodes. 38, 174-182.

Tassinari, C.C.G., Bettencourt, J.S., Geraldes, M.C., Macambira, M.J.B. & Lafon, J.M., 2000. The Amazonian Craton. In: Cordani, U.G., Milani, E.J., Thomaz-Filho, A. & Campos, D.A. (eds.). Tectonic Evolution Of South America, Rio de Janeiro. p. 41- 95.

Tassinari, C.G.C., Macambira, M.J.B., 2004. A Evolução Tectônica do Cráton Amazônico. In: Neto-Mantesso, V., Bartorelli, A, Carneiro, C. D. R., Brito-Neves, B.B. (eds). Geologia do Continente Sul-Americano: Evolução da Obra de Fernando Flávio Marques de Almeida. p. 471-486.

Teixeira, W., Geraldes, M.C., Matos, R., Ruiz, A.S., Saes, G., Vargas-Matos, G., 2010. A review of the tectonic evolution of the Sunsas belt, A review of the tectonic evolution on the Sunsas belt, SW portion of the Amazonian Craton. J. S. Am. Earth Sci. 29, 47 - 60.

Teixeira, W., Hamilton, M. A., Girardi, V. A. V., Faleiros, F. M., 2016. Key dolerite dyke swarms of Amazonia: U-Pb constraints on supercontinent cycles and geodynamic connections with global LIP events through time. *Acta Geologica Sinica (English Edition)*, 90 (supp. 1), 84-85, DOI: 10.1111/1755-6724.12902.

Trompette R., Alvarenga C. J. S., Walde D., 1998. Geological evolution of the Neoproterozoic Corumbá graben system (Brazil). Depositional context of the stratified Fe and Mn ores of the Jacadigo Group. Journal of South American Earth Sciences, 11, 587-597.

Ubrich H. H.G.J., Vlach S. R. F., Janasi V. A., 2001. O Mapeamento faciológico de rochas plutônicas. Revista Brasileira de Geociências, 31(2): 163-172.

Vavra, G., Gebauer, D., Schim, R., Compston, W., 1996. Multiple zircon growth and recrystallization during polyphase Late Carboniferous to Triassic metamorphism in granulites of the Ivrea Zone (Southern Alps): and ion microprobe (SHRIMP) study. Contributions to Mineralogy and Petrology, 122: 337-358.

Vargas-Mattos G.L. 2010. Caracterização geocronológica e geoquímica dos granitos proterozoicos: implicação para a evolução crustal da borda SW do Cráton Amazônico na Bolívia. Faculdade de Geologia, Universidade do Estado do Rio de Janeiro, Tese de Doutoramento, 164 p

Wiedenbeck, M., Allé, P., Corfu, F., Griffin, W.L., Meier, M., Oberli, F., Von Quadt, A., Roddick, J.C., Spiegel, W. 1995. Three natural zircon standards for U-Th-Pb, Lu-Hf, trace element and REE Analyses. Geostandards Newsletter, 19:1-23.

Wiens, F.M.S. 1986. Zur lithostratigraphischen, petrographischen und strukturellen Entwicklung des Rio-Apa Hochlandes, Nordost Paraguay: Clausthal, Geologisches Institut der Technischen Universitat Clausthal, Clausthaler Geowissenschaftliche, Ph. D. dissertation, 19, 280 p.